Denise Bednorz

From lysimeter to field scale – Examining the transferability of lysimeter measurements to predict nitrogen lea-ching from tile drained arable fields and evaluating the reliability of measurement results from different lysimeter types

11|2017

HELMHOLTZ
CENTRE FOR
ENVIRONMENTAL
RESEARCH – UFZ

- From lysimeter to field scale -
Examining the transferability of lysimeter measurements to predict nitrogen leaching from tile drained arable fields and evaluating the reliability of measurement results from different lysimeter types

Dissertation

zur Erlangung des

Doktorgrades der Naturwissenschaften (Dr. rer. nat.)

Der

Naturwissenschaftlichen Fakultät III

Agrar- und Ernährungswissenschaften,

Geowissenschaften und Informatik

der Martin-Luther-Universität

Halle-Wittenberg,

vorgelegt

von Frau Denise Bednorz

geb. am 24.06.1986 in Wolfen

Gutachter

Prof. Dr. Ralph Meißner

       Martin-Luther-Universität Halle-Wittenberg

       Naturwissenschaftliche Fakultät III

       Agrar- und Ernährungswissenschaften, Geowissenschaften und Informatik

       Helmholtz-Zentrum für Umweltforschung – UFZ

       Department Bodensystemforschung

Prof. Dr. Konrad Miegel

       Universität Rostock

       Agrar- und Umweltwissenschaftliche Fakultät

       Hydrologie/ Meteorologie

Disputation

Datum und Ort der Verteidigung: 19.10. 2017, Halle

                                (Martin-Luther-Universität Halle-Wittenberg)

Kurzfassung

Die landwirtschaftliche Nutzung und die damit einhergehende Verwendung stickstoffhaltiger Düngemittel ist eine der Hauptquellen für diffuse Nitrat-Einträge in Oberflächen- und Grundwasser. Stickstoff liegt vorrangig organisch-gebunden im Boden vor und wird unter feuchtwarmen, aeroben Bedingungen sehr schnell über Ammonium zu Nitrat umgewandelt. Dabei ist Nitrat von den verschiedenen Stickstoffspezies die mobilste, da es aufgrund seiner negativen Schichtladung generell gelöst vorliegt. Somit wird die Nitratdynamik im Wesentlichen durch das lokale Fließregime gesteuert, wodurch es zwingend erforderlich ist, die hydrologischen Bedingungen im Feldmaßstab zu ermitteln. Es ist aber praktisch nicht umsetzbar, für jede landwirtschaftliche Nutzfläche einzelne Fallstudien durchzuführen. Um den Gebietswasserhaushalt als wichtigsten Einflussfaktor auf die Nitrat-Dynamik, zu beschreiben, sind daher Lysimeter seit Jahrzehnten das Mittel der Wahl. Dabei wird die Übertragbarkeit von Messergebnissen, die mit einfachen nicht-wägbaren Gravitationslysimetern (NWGL) gewonnen werden, als kritisch bewertet und gemäß Literatur sollen technisch besser ausgerüstete und zusätzlich tensionsgesteuerte Lysimeter zuverlässigere Ergebnisse liefern. Im Gegensatz zu diesen besitzen NWGL aber den Vorteil, dass sie nicht nur kostengünstiger und wartungsextensiver sind, sondern dass sie an vielen europäischen Standorten vorhanden sind und somit ein breites Spektrum klimatischer, bodenkundlicher sowie nutzungsspezifischer Bedingungen abdecken. In dieser Arbeit wurden aufbauend auf Lysimeter- und Feldexperimenten sowie numerischen Simulationen Antworten auf folgende Fragen gegeben:

(i) Können NWGL-Messergebnisse und darauf aufbauende Simulationen direkt zur Beschreibung des Wasserhaushaltes auf Feldebene übertragen werden und worin bestehen ihre Limitierungen?

(ii) Wie beeinflussen unterschiedliche Standortverhältnisse den Wasserhaushalt und die Stickstoffkinetik und wie kann dies aufbauend auf NWGL-Messungen numerisch nachvollzogen werden?

(iii) Wie wird das Abflussverhalten von Lysimetern durch die untere Randbedingung beeinflusst und kann durch eine Tensionssteuerung die Zuverlässigkeit von Lysimeterergebnissen erhöht werden?

Zur Beantwortung der Fragestellungen (i) und (ii) wurden Lysimeterexperimente und Feldversuche auf zwei benachbarten gedränten Versuchsschlägen (nördliche Altmark, Sachsen-Anhalt, Deutschland) angelegt. Zwischen den NWGL und beiden Versuchsschlägen wurde die landwirtschaftliche Bewirtschaftung in den Versuchsjahren 2013, 2014 und

2015 angeglichen (Mais-Mais-Winterweizen). An den Lysimetern wurden nicht nur die monatlichen Sickerwassermengen und ausgetragenen Nitrat-Frachten, sondern auch Pflanzenentwicklung und meteorologische Parameter bestimmt. Auf den Schlägen wurden sowohl Bodenfeuchte und Nitrat-Konzentration in verschiedenen Tiefen als auch flächen- und schlagspezifische Dränabflussrate und Nitrat-Austragsfracht ermittelt. Aufgrund der quartärgeologischen Situation im Gebiet ist der Untergrund und damit auch die Hydrologie zwischen beiden Schlägen zu unterscheiden (*Schlag BW* - Pseudogley-Parabraunerde-stauwasserbeeinflusst; *Schlag GW* - Gley-Pseudogley-Parabraunerde-Regosol - gespannte Grundwasserverhältnisse).

Zusätzlich zu den Versuchen wurden numerische Simulationen mit der Software HYDRUS zur Beschreibung des Wasserhaushaltes der NWGL und darauf aufbauend der Versuchsschläge durchgeführt. Die Untersuchungen zeigten, dass unter der Voraussetzung vergleichbarer pedo-hydrologischer Bedingungen zwischen NWGL und Versuchsschlag, monatliche Abflussmengen auf beiden Skalen mit einander korrelieren. Das Fließregime von Schlag BW wurde im Wesentlichen durch die Messergebnisse der NWGL und darauf aufbauenden Simulationen beschrieben. Der Wasserhaushalt von Schlag GW entsprach aufgrund der Heterogenität des Untergrundes weder dem von Schlag BW noch dem der NWGL. Bezogen auf Dränabflussmenge und Nitrat-Austragsfrachten über Dränagen wies Schlag GW aufgrund gering durchlässiger Schichten im Oberboden und einer damit einhergehenden Akkumulation von nitrathaltigem Sickerwasser nur ein Zehntel gegenüber Schlag BW auf. Der Dränabfluss wurde im Wesentlichen durch den Grundwasserspiegel bestimmt, während Sickerwasser mit erhöhten Nitratkonzentrationen nur nach Starkregenereignissen bis zu den Dränagen perkolierte. Auf Schlag BW wurde der Dränabfluss nur durch nitrathaltiges Sickerwasser (vergleichbar zu den NWGL) charakterisiert, welches rasch über Dränagen abgeführt wurde. Diese unterschiedlichen hydrologischen Gegebenheiten wurden adäquat innerhalb numerischer Simulationen, bei welchen beide Schläge innerhalb eines Modells zusammengefasst wurden, beschrieben. Diese Simulationen basierten nur auf den an den NWGL erhobenen Daten und konnten durch die Implementierung der bodenphysikalischen Eigenschaften der beiden Versuchsschläge validiert werden. Als Resultat wurde festgestellt, dass NWGL und darauf aufbauende Simulationen eine effiziente Möglichkeit darstellen, um den Wasserhaushalt der Versuchsschläge trotz der verschiedenen Untergrundverhältnisse zu bilanzieren. Die Vergleichbarkeit des Austragsverhaltens zwischen NWGL und Versuchsschlägen basierte aber nur auf der Übereinstimmung monatlicher Sickerwasser- und Dränabflussraten. Diese zeitliche Auflösung ist hin-

sichtlich der Abschätzung des Gefährdungspotentials für Grund- und Oberflächenwasser und somit zur Beantwortung praxisorientierter, hydrologischer Fragestellungen ausreichend, während zur Bewertung wissenschaftlicher Forschungsansätze häufig tägliche oder sogar stündliche Daten verglichen werden müssen. In diesem Zusammenhang wird der Einfluss der unteren Randbedingung von Gravitationslysimetern als kritisch hervorgehoben, da deren Abflussverhalten von den tatsächlichen bodenhydrologischen Bedingungen abweichen soll. Zur Testung dieser These wurde ein weiterer Versuch mit wägbaren Lysimetern angelegt. Hierzu wurden die Messergebnisse (Bodenfeuchte in verschiedenen Tiefen, Matrixpotential am unteren Lysimeterrand, tägliche Abflussraten) eines wägbaren Gravitationslysimeters (GL) mit denen eines wägbaren, tensionsgesteuerten Lysimeters (TL) verglichen. Die Tension am unteren Rand von TL wurde in Abhängigkeit vom registrierten Matrixpotential eines ungestörten Bodenprofils geregelt. Die Ergebnisse zeigten, dass trotz des höheren technischen Aufwands keine Vorteile bei der Verwendung von TL gegenüber GL bestehen. Zwar wurde der, wie in der Literatur hervorgehobene, Einfluss der gesteuerten unteren Randbedingung nachgewiesen, jedoch ist nicht nur die Tensions-Registrierung, sondern vor allem die Steuertechnik extrem störanfällig. Da bei monatlichen Sickerwassermengen keine Beeinflussung des Abflussverhaltens durch den unteren Lysimeterrand nachgewiesen wurde, können bei dieser zeitlichen Auflösung weiterhin Gravitationslysimeter verwendet werden. Zudem besteht gegenwärtig ein erhöhter Forschungsbedarf hinsichtlich einer verbesserten Lösung zur Tensionsregulierung bei gesteuerten Lysimetern.

Summary

Agricultural land use and the related application of fertilizers are the main sources for diffuse nitrate inputs into surface- and groundwater. In the soil, predominantly sorbed organic nitrogen occurs which is transformed very fast over ammonia to nitrate under temperate, aerobe conditions. Because in the environment nitrate occurs as the negatively charged nitrate-ion, it is generally solved, being the most mobile N-species. As a result, it is absolutely required to determine the local flow regime due to the impact of the water balance on the nitrate-dynamic. Because it is not realizable to perform separate case studies for every site-specific problem, since decades lysimeters are a scientifically accepted tool to estimate the water balance, as a major N-leaching control factor, on field scale. But the transferability of data from simple constructed non-weighable gravitation lysimeters (NWGL) is questioned and the reliability of data from more technical ambitious devices with tension controlled boundaries is emphasized in literature. But NWGL obtain the advantages to be more cost effective, having lower maintenance requirements and being available at many lysimeter stations in Europe. They are still working, covering a broad spectrum of climatologically, soil and use-specific conditions. Based on lysimeter measurements, field experiments and numerical simulations the following questions were answered:

(i) Could NWGL –measurements and further numerical simulations be directly transferred to predict the water regime on field scale and what are their limitations?

(ii) To which extend does soil heterogeneity influence water flow and nitrogen kinetic and could the NWGL-measurements and -simulations be used to evaluate the impact?

(iii) Does the lower boundary condition influence the water balance of lysimeters and would the implementation of a tension controlled lower boundary optimize the reliability of lysimeter measurements?

For the objectives (i) and (ii), lysimeter experiments (NWGL) and field trials at two neighboring tile-drained, arable fields (northern Altmark, Saxony-Anhalt, Germany) were realized. Agricultural management of the NWGL and the fields was adjusted for the observation period 2013-2015 (maize, maize, winter wheat). At the NWGL, despite monthly seepage rates and discharged nitrate-loads, also plant development and daily meteorological parameters were registered. At the field site, depth depending soil moisture and nitrate concentration in soil solution as well as daily outflow rates and discharged nitrate-loads via drains were determined. Furthermore, detailed soil analysis provided different soil physical and hydrological situations (*field BW* – homogeneous distributed Stagnic Gleysol Luvisol,

backwater influenced; *field GW* – Gleysol, Stagnic Gleysol Luvisol, Regosol, confined groundwater).

In addition to the experiments, numerical simulations with the HYDRUS software package were performed to describe water flow of the NWGL and based on these the water balance of both fields. The results showed that monthly measured and modelled discharge rates of the NWGL and field BW correlate with each other because of similar pedo-hydrological conditions. Water balance of field GW did neither correspond to field BW nor to the NWGL because of the heterogeneous subsurface and the confined groundwater conditions. For the whole observation period, the amount of drained water and discharged nitrate-loads was only 1/10 at field GW as compared to field BW because of impermeable layers in the top soil of field GW. Thus, drained water was mainly characterized by groundwater, whereby nitrate-enriched seepage water only percolates to the tile-drains after heavy rain events. In contrast to that at field BW, water infiltrated very fast, whereby drained water was mainly characterized by nitrate-enriched percolating seepage water, being comparable to the NWGL. These different hydrological situations were described adequately by numerical simulations, combining both fields within one modeling domain. These simulations based on the information obtained at the NWGL, and the implemented soil physical properties of both fields. It can be stated, that the NWGL-measurements and further numerical simulations are an efficient approach to predict the soil water balance of both fields although their different pedo-hydrological properties. But the comparability of the discharge behavior of the NWGL and the fields based only on the similarity of monthly measured and simulated discharge rates. This temporal resolution is sufficient for answering more practical, hydrological questions like evaluating the potential risk for ground- and surface waters, whereas for scientific approaches, daily or hourly values have to be compared.

In this context, the impact of the lower boundary of gravitation lysimeters is assessed as critical, influencing water flow in an inadequate manner as compared to field conditions. To evaluate this thesis, another experiment with weighable lysimeters was performed. Therefore, measuring results (depth depending soil moisture, matric potential at the lower boundary, daily outflow rates), of a weighable gravitation lysimeter (GL) were compared to the results of a neighboring weighable tension-controlled lysimeter (TL). Tension was adjusted according to registered tension of a surrounding, undisturbed soil profile.

The results provided no advantages of TL as compared to GL although the additional technical effort. The impact of a controlled lower boundary as emphasized in literature was

reproduced. But not only tension registration, also regulation is extremely prone to errors. Because the monthly discharge behavior was not influenced by the lower lysimeter boundary, for those temporal resolutions, gravitation lysimeters can be used. Moreover, recently there is a need for further research to optimize the control technology for tension regulation.

Table of content

Figures

Tables

Abbreviations

BMELV – Bundesministerium für Ernährung, Landwirtschaft und Verbraucherschutz

BMU – Bundesministerium für Umwelt

DWD – Deutscher Wetterdienst

EU – European Union

FE – Finite Element

Field BW – backwater influenced field

Field GW – groundwater influenced field

GL – gravitation lysimeter (weighable)

HY – hydrological year, time frame from the 1st November until 31st October in the following year

HHY – hydrological half year, hydrological summer from 1st November until 30th April; hydrological winter from 1st May until 31st October

LAGB – Landesamt für Geologie und Bergbau Sachsen-Anhalt

LAWA – Bund/ Länder-Arbeitsgemeinschaft Wasser

N - nitrogen

N_t – total nitrogen

N_{org} organic nitrogen

N_{min} mineral, inorganic nitrogen

NH_4-N – ammnoia-nitrogen

NH_4^+ - ammonia ion

NO_2-N – nitrite-nitrogen

NO_2^- - nitrite ion

NO_3-N – nitrate-nitrogen

NO_3^- - nitrate ion

NWGL – non-weighable gravitation lysimeter

P – precipitation

TL - tension-controlled lysimeter (weighable)

UFZ – Helmholtz-Zentrum für Umweltforschung GmbH

UGT – Umwelt-Geräte-Technik GmbH

1. **Introduction**

1.1 Nitrate in the focus of the European water protection policy

Nitrogen (N) and its reactive components are not only important nutrients for crop and plant growth but also harmful contaminants because of their extensive application as fertilizers at agricultural used areas (Follett, 2004). Because Nitrate (NO_3-N) is generally solved, it is the most mobile N-species, being since decades in the focus of the European water protection policy. Total nitrogen (N_t) in soil consists generally of organic N (N_{org}). N_{org} is either naturally in the soil organic matter fraction or it is added to the soil system after manure application, biological N fixation or by plant residue after harvest (Follett, 2004). During mineralization, bacteria decomposite organic matter, whereby ammonia (NH_4-N) is released. The microbial activity directly depends on temperature and soil moisture. NH_4-N could not only be sorbed by plants but also by minerals, mainly negatively charged clay minerals in the soil, because it generally occurs as the positive charged ion NH_4^+. Thus, it is accumulated in the subsurface not being translocated into greater depth being a stable depot for plant nutrition (Follett, 2004). But under warm, moist and aerobe conditions, during nitrification NH_4-N is transformed very fast over nitrite (NO_2-N) to the also plant available nitrate (NO_3-N). Because of the negative surface charge of the nitrate ion NO_3^- in the environment, it is not attracted by soil particles or organic matter, being soluble (Follett, 2004). Under anaerobe conditions, bacteria use NO_3-N for metabolic processes, whereby nitrate is denitrified to gaseous N. But this process is only of concern in temporary saturated soils and works as a natural N-sink (Robertson and Groffman, 2007).

According to Follett (2004) NO_3-N is the major N-component in waters. In this context, agricultural land use is recognized since decades as one of the main sources for diffuse NO_3-N-inputs into surface- and groundwater (Randall and Goss, 2008). Because in human organisms' nitrate is transformed to carcinogenic nitrosamines, in the regulation concerning drinking water, a limit value of 50 mg l^{-1} NO_3^- (= 11.3 mg NO_3-N l^{-1}) was introduced. To minimize NO_3-N-losses and to reverse NO_3-N-pollution trends, the European Union adapted standardized rules whereby one of the first directives of the EU-environmental protection policy was adapted in 1991 (91/676/EWG, 1991). This nitrate directive was implemented with the German fertilizer ordinance in 1996, which was novelled in 2012 implying several restrictions. Despite an agricultural management according to good management practices to minimize nitrogen surpluses and inputs into agricultural systems, other official instructions like the operation of monitoring wells as well as reporting obligations within a 4-year rhythm were stated. Furthermore, to establish a framework for com-

munity action in the field of water policy, in 2000 the European Water framework directive was adopted (2000/60/EG, 2000). Beside the general aim to reverse trends in environmental pollution, the main objectives indicated in this directive are to fulfill a good ecological and chemical status for surface waters and a good quantitative and chemical status for groundwater until 2015. In 2006, a separate directive for the compartment groundwater was adopted (2006/118/EG, 2006).

Since the German fertilizer ordinance was implemented a decreasing trend regarding N-surpluses in agriculture is reproduced. According to BMU and BMELV (2012) between 1990 and 2010 in Germany the N-surplus is reduced from 111 $kgN\ ha^{-1}$ to 68 $kgN\ ha^{-1}$. But the Working Group on Water issues of the Federal States (LAWA) contributes that in 2010 still 37 % of the groundwater bodies in Germany are in a bad chemical status. With 27 % of these, this is primary caused by exceeding NO_3-N-concentrations, resulting from agriculture. Regarding surface water NO_3-N-contamination, since decades drainages are known as the major entry phase for NO_3-N loads because the main part of NO_3-N passing the root zone is intercepted by the drains (David et al., 1997; Hatfield et al., 1999; Blann et al., 2009; Warsta et al., 2013). Because of generally high discharge rates during winter, short hydraulic residence times and resulting from this negligible denitrification it is assumed that for the hydro-climatically conditions of Germany approximately 22 % of the diffuse N-inputs into surface waters are induced by tile drains (Kahle and Mehl, 2014). But subsurface drainage is often needed at fields to lower the water table and to prevent water logged zones as a requirement for the efficient agricultural use in dependence of soil physical properties and meteorological conditions (Schepper et al., 2015).

Beside the impact of land use, groundwater contamination directly depends on the local hydraulic conditions, which could be either confined or unconfined. Whereby confined groundwater is protected by a flow-impeding layer, unconfined groundwater is directly connected to the atmosphere and the upper soil (Follett, 2004). As a result, in accordance with studies of Refsgaard et al. (2014) there are robust and vulnerable areas which have to be considered. Furthermore, NO_3-N-leaching to the groundwater bodies directly depends on the water holding capacity of the soil, whereby leaching is more intensive at permeable sandy soils as compared to heavy soils (Pärn et al., 2012).

There is still a discrepancy in agriculture between optimizing crop yield production and minimizing the use of fertilizers to reduce N-losses. There are many studies examining management effects including soil tillage, manure application or nitrification inhibitors on the N-dynamic to improve the N-efficiency of agricultural practice with regard to reduce

N-losses into the environment (Goss et al., 1993; Randall and Iragavarapu, 1995; Weed and Kanwar., 1996; Randall et al., 1997; Randall and Mulla, 2001; Dinnes et al., 2002; Nakamura et al., 2007; Burkart and Stoner, 2008; Randall and Goss, 2008; Übelhör et al., 2014; Salem et al., 2015). But recent studies show that the impact of soil physical properties in combination with water table effects covers the influence of agricultural management on N-leaching (Bednorz et al., 2016). In this context, not only NO_3-N-leaching but also nitrogen transformation should be considered, whereby for both processes, according to Rubol et al. (2012) hydrological conditions are major control parameters. The main nitrogen transformation processes in the soil-plant-water-atmosphere system are mineralization from N_{org} to NH_4-N, nitrification from NH_4-N to NO_3-N and denitrification from NO_3-N to gaseous N. The transport of the resulting N-species is described by partial differential equations that govern dispersive-advective transport, which are part of a sequential first-order decay chain describing the N-transformations according to Simunek et al. (2012):

$$\frac{\partial \theta \cdot c_{Norg}}{\partial t} + \frac{\partial \rho \cdot s_{Norg}}{\partial t} = \frac{\partial}{\partial x_i}(\theta \cdot D_{ij\ Norg}^W \cdot \frac{\partial c_{Norg}}{\partial x_j}) - \frac{\partial q c_{Norg}}{\partial x_i} - k_{min} \cdot \theta \cdot c_{Norg} - k_{min} \cdot \rho \cdot s_{Norg} \tag{1}$$

$$\frac{\partial \theta \cdot c_{NH4-N}}{\partial t} + \frac{\partial \rho \cdot s_{NH4-N}}{\partial t} = \frac{\partial}{\partial x_i}(\theta \cdot D_{ij\ NH4-N}^W \cdot \frac{\partial c_{NH4-N}}{\partial x_j}) - \frac{\partial q c_{NH4-N}}{\partial x_i} + k_{min} \cdot \theta \cdot c_{Norg} + k_{min} \cdot \rho \cdot s_{Norg}$$
$$- k_{nit} \cdot \theta \cdot c_{NH4-N} - k_{nit} \cdot \rho \cdot s_{NH4-N} - Sc_{root NH4-N} \tag{2}$$

$$\frac{\partial \theta \cdot c_{NO3-N}}{\partial t} = \frac{\partial}{\partial x_i}(\theta \cdot D_{ij\ NO3-N}^W \cdot \frac{\partial c_{NO3-N}}{\partial x_j}) - \frac{\partial q c_{NO3-N}}{\partial x_i} + K_{nit} \cdot \theta \cdot c_{NH4-N} + K_{nit} \cdot \rho \cdot s_{NH4-N}$$
$$- K_{den} \cdot \theta \cdot c_{NO3-N} - Sc_{root,NH4-N} \tag{3}$$

with θ water content ($L^3 L^{-3}$), $c_{Norg,NH4-N,NO3-N}$ the solute concentration of N_{org}, NH_4-N and NO_3-N in the liquid phase ($M L^{-3}$), $s_{Norg,NH4-N}$ the solute concentration of N_{org} and NH_4-N in the solid phase ($M M^{-1}$), ρ the soil bulk density ($M L^{-3}$), D the dispersion coefficient tensor ($L^2 T^{-1}$), $k_{min,nit,den}$ the first-order rate constant for mineralization, nitrification and denitrification (T^{-1}), q the volumetric flux ($L T^{-1}$), S the sink term and c_{root} the solute concentration of the sink term ($M L^{-3}$).

According to Gusman and Marino (1999), mineralization and nitrification mainly occur in the upper root zone, whereby from 30 cm depth, denitrification is the predominant N-transformation process. The temporal course of NO_3-N in the soil profile and thus NO_3-N-leaching and the N transformation rates mineralization, nitrification or denitrification directly depend on the soil texture (Kersebaum and Richter, 1991; Marchetti et al., 1997; Adamchuk et al., 2004; Heumann et al., 2011a; Heumann et al., 2011b) and further water

table effects, caused by precipitation or subsurface drainage (Jury and Nielson, 1989; Pärn et al., 2012; Filipovic et al., 2014). Thus, a combination of several parameters like agricultural management, weather conditions and soil properties should be taken into account when validating the potential risk of NO_3-N-losses, whereby it is not expedient only focusing on the agricultural use (Vos, 2001; Silva et al., 2005; Gooday et al., 2008; Schepper et al., 2015). The subsurface of Germany is shaped by quaternary deposits, accompanied by several surface degradations due to ice ages and warm periods. Geological maps of the LAGB (1999) provide small scale soil heterogeneity in these areas. It is not realizable to carry out separate case studies for every site-specific problem. Thus, the recent challenge is to find the right balance between simplifying and specifying measurements and simulations to predict water flow and nitrogen transport on field scale. In this context, areas should be classified into robust and vulnerable according to Refsgaard et al. (2014) when evaluating the potential risk of NO_3-N-losses. Based on this classification, Bednorz et al. (2016) provides that simple constructed lysimeters can be used as point information to describe the water balance as the key process determining N-leaching on field scale. In the following chapter, the role and recent developments of different lysimeter devices for answering hydrological and nitrogen transport questions is discussed.

1.2 The role of lysimeters to answer hydrological and nitrogen transport questions

To exactly determine solute transfer for answering both scientific and practical questions regarding environmental protection and sustainable agricultural management, quantifying the soil water balance in the unsaturated zone is absolutely required (Meissner et al., 2014). In this context, since decades lysimeters are mostly used for describing the soil water regime for larger scales because of their advantage to deliver information at a scale between laboratory and field scale (Allen et al., 2011). Lanthaler and Fank (2005) conclude, that most of the lysimeters in Europe are used predominantly for answering agricultural questions and for monitoring specific nutrient losses into the environment.

According to the German Industrial Standard (DIN-4049-3, 1994) a lysimeter is defined as a device which is filled with soil substrates, and equipped with a method to collect seepage water to calculate mass and solute balances with regard to soil type, vegetation, local climate or other site conditions. There are various types of lysimeters used in seepage research which can be classified according to Bergström (1990) or DWA (2012) to their size, filling procedure, weighability or the method for collecting seepage water. Each of these criteria substantially influences the reliable reproducibility of the results (Hagenau et al.,

2015). In general, lysimeters deliver only small-scale information. Thus, they should be evaluated critically whereby certain criteria should be fulfilled to optimize the reliability of lysimeter measurements (Allen et al., 1991; Allen et al., 2011).

Regarding the size of lysimeters an increasing surface would be an advantage because this would at least encompass small scale natural soil and crop variability according to Hagenau et al. (2015). In addition to that they should be sufficient deep not to hinder root growth and to overcome the natural zero flux plane in dependence on local climate and other site conditions (Meissner et al., 2007). Furthermore, to avoid edge and oasis effects the cultivated and the surrounding vegetation should be the same (Bavel et al., 1963). Regarding the filling procedure of lysimeters, they can be filled disturbed (backfilled) or monolithic. Johnson et al. (1995) or Troxler et al. (1998) conclude that backfilled lysimeters do not represent field conditions due to their changed subsurface texture. As a result, a monolithic undisturbed lysimeter filling should be preferred. But as compared to a disturbed lysimeter filling, this procedure is more expensive also obtaining several disadvantages in dependence of the technology of extracting the soil monoliths (Meissner et al., 2007).

Regarding their technical features, a weighing mechanism would be advantageous because weighable lysimeters will provide the most accurate data for short time periods. In contrast to non-weighable devices, via the measured mass changes the water mass balance and in this context actual evapotranspiration could be directly determined (Allen et al., 2011). But the accuracy of the data not only depends on the accuracy of the weighing mechanism but also on a well lysimeter management. According to Meissner et al. (2014) a large weighing lysimeter would be the best option to answer hydrological questions. But this will not only increase maintenance requirements but also the costs for lysimeter installation. The advantages of simplified lysimeters in general as a low cost alternative could also be reproduced by Lanthaler and Fank (2005), stating that the majority of the lysimeters in Europe (82.4 %) are non-weighable because of low costs and maintenance requirements. Two third of them are backfilled.

According to Weihermüller et al. (2007) by the drainage behavior and thus by the lower boundary condition two different lysimeter systems can be distinguished - gravitational and tension controlled lysimeters. The review of actual literature provides that this lower boundary is the most controversially discussed aspect in literature. According to the results of Abdou and Flury (2004), Peters and Durner (2009) or Barkle et al. (2014), it describes the major drawback of gravitation lysimeters. Their lower boundary at the seepage face is

exposed to atmospheric pressure. Thus, resulting in a disruption of the naturally occurring hydraulic gradient, a water saturated layer at the bottom has to be formed before water can drain out of the lysimeter. As a result the leachate flux occurs at different times and also underestimated as compared to the field condition or tension-controlled devices (Gee et al., 2009). To prevent this waterlogged zone above the drain face, tension-controlled lysimeters with fixed or variable tension (Greco, 2006; Zacharias et al., 2011) at the drain face were developed. Studies by Vereecken and Dust (1998) or Zhu et al. (2002) show, that these lysimeters perform better than gravitation lysimeters, whereas Meissner et al. (2010) conclude that there are no significant differences between both types for larger observation periods. A dynamic tension control of lysimeters obtains the advantage that water fluxes of these devices are close to field conditions because the pressure head at their lower boundary is adjusted to measured tension at the same depth in the surrounding field soil (Groh et al., 2016). But the reliability of these lysimeter data could only be guaranteed when the lysimeters are installed close to their sampling site as not only soil physical properties but also the location of the water table at the surrounding soil should be comparable to the lysimeter excavation site. Otherwise, according to Groh et al. (2016) registered tension in the soil could affect water balance of the lysimeters in an inadequate manner. Moreover, the implementation of a tension controlled lower boundary to mimic field conditions is not only expensive but technically ambitious, increasing the maintenance requirements (Weihermüller et al., 2007; Hagenau et al., 2015).

Simplified non-weighable gravitation lysimeters are located at several research stations in Europe. The first ones in Germany were installed in the 1920ies and they are still working (Lanthaler and Fank, 2005). In the last years, a huge number of technical ambitious devices were developed. A critical overview, given in Weihermüller et al. (2007) lead to the conclusion, that the applied measuring facility depends on the one hand on the scientific question and additionally on the financial budget. The review of actual literature provides that the reliability of simple constructed gravitation lysimeters is generally questioned. For practical hydrological questions, Bednorz et al. (2016) concludes, that gravitation lysimeters would be applicable, whereas for the evaluation of data with a daily or even smaller measuring rhythm, technically ambitious devices should be used. Because lysimeters deliver only small scale information, independently of their technical construction, information gathered from them should be handled as temporal information, only describing the sample location, not being spatially representing another point (Weihermüller et al., 2007). Thus, further numerical simulations are required to transfer lysimeter results to describe

water flow on field scale. The scaling problem when describing hydrological and solute transport processes as well as the numerical implementation of lysimeter data to describe water flow for larger scales is described in the following chapter.

1.3 Numerical simulations to mind the gap between lysimeter and field scale

To mind the gap between lysimeter and field scale, further numerical simulations are absolutely required to describe water and solute balances (Weihermüller et al., 2007). In this context, in vadose zone research upscaling hydrological processes is of major concern. According to Vereecken et al. (2007) there is a huge discrepancy between small scales like lysimeter or local scale, where hydraulic properties and soil fluxes are generally measured, and larger scales like the field or the catchment scale, where models are used to predict the flow regime and where management decisions are made. Thus, the models are constructed at scales, being much larger as compared to the scale, where the properties are determined. Within this thesis, upscaling from lysimeter to field scale is observed. Thus, upscaling of soil hydraulic properties and resulting from this the influence of the spatial heterogeneity seems to be of major concern.

Smith (1999) highlights in this context, that methods are required, which accommodate the increased spatial variability. Upscaling in general means the use of so called "upscaling schemes" to predict the spatial heterogeneity of soil hydraulic properties which are determined from small scale data. A critical overview of several schemes is given in Zhu et al. (2007). Within this thesis, not a stochastic or geostatistical upscaling approach of unsaturated hydraulic properties is considered, but a simplified adaption of lysimeter results to predict and to describe the flow regime on field scale is evaluated. Within this thesis it is proven, if measurements derived from lysimeters, at least delivering point information are applicable to calibrate and validate numerical models describing soil water balance and solute transport for larger scales, already highlighted by Wriedt (2004).

Regarding numerical simulations,Vereecken et al. (2016) gave a critical review on recent developments when modeling soil processes. Although a large number of analytical and numerical modeling tools are available, state of the art to describe water and solute fluxes in the unsaturated zone seems to be, according to Ramos et al. (2012), the HYDRUS software package, which was developed by Simunek et al. (2012). HYDRUS numerically solves the Richards`equation for saturated-unsaturated water flow and the convection-dispersion equation for heat and solute transport using Galerkin-type linear finite element schemes. Not only regarding water flow but mainly regarding solute kinetic, simplified

approaches as well as detailed extensions can be implemented within the HYDRUS simulations. The actual literature provides that there is a discrepancy between simplifying and detailing these numerical simulations. As highlighted by Refsgaard et al. (2014), water flow and solute transport at catchment scale models should obtain the predictive capability on small spatial scales in order to provide support for agricultural management decisions. This is in line with studies of Warsta et al. (2013), stating that the local scale and especially local tile-drain network has a key impact on groundwater and surface water flow. As a result, each case is unique. Schepper et al. (2015) summarize possible generalizations and simplifications in numerical simulations with regard to the impact of small scale soil-heterogeneity on tile-drains. They also conclude that the temporal resolution of the input parameters as well as the mesh size in the modeling domain and the chosen boundary conditions directly influence the modeling results. But the more specified and detailed the numerical simulations are, the longer the simulation times will be. Furthermore, regarding nitrogen transport and transformation, HYDRUS provides simplified and detailed simulation approaches. N-kinetic and transport in HYDRUS is simulated based on equations (1), (2) and (3). Thus, dispersive-advective transport in combination with sequential first-order-decay chains describe not only N-transport, but also N-transformations. But the more specified solute transport is simulated, the more input data, which are often not all monitored in the field are required to describe the solute behavior adequately. Thus, it would be more expedient to break down general transformation or transport processes to the key determinants. It is out of question that hydrology controls NO_3-N leaching. Thus, based on validated water flow models, an efficient evaluation of the potential risk for NO_3-N losses in dependence of the subsurface conditions should be possible. But the recent question is to which extend could simulations be simplified still having the predictive capability to evaluate N-losses.

1.4. Objectives

The review of actual literature provides that agricultural management is seen as the main source for diffuse N-inputs into the environment. But there are a few actual studies stating, that not only agricultural management but mainly soil heterogeneity on field scale has to be considered because of the impact of the local flow regime and thus of heterogeneous soil properties on the NO_3-N-dynamic. In this context, it is hard to find the right balance between simplifying and specifying not only facilities like lysimeters to obtain measurement results, but also numerical simulations to predict N-losses at agricultural used areas with

different pedo-hydrological properties. The specification level in general depends on the scientific task. Within this thesis, the main objectives are:

(i) Could measurement data from simple constructed non-weighable gravitation lysimeters (NWGL) be transferred to describe the water flow on field scale?

(ii) To which extend do different soil properties influence the water balance and the resulting N-dynamic at drained arable fields and could NWGL-measurements be used as point information for further field scale simulations?

(iii) Does the development of technically ambitious lysimeter techniques optimize the reliability of lysimeter data to predict water flow on field scale?

To answer these questions, two separate case studies were performed, summarized in the following flow chart in Figure 1.1.

1. Coupled lysimeter experiments and field trials in Saxony-Anhalt

| Evaluating the transferability from lysimeter to field scale |

comparable meteorological conditions
equalized agricultural management

| **Lysimeter experiments** | | **Field experiments at two tile-drained arable fields** |

three non-weighable gravitation lysimeters (NWGL)

comparable pedo-hydrological conditions

homogeneous backwater influenced field BW

different pedo-hydrological conditions — **Impact of soil heterogeneity**

different pedo-hydrological conditions

heterogeneous groundwater influenced field GW

Comparability between measured and modelled monthly discharge rates of NWGL and field BW?
Impact of soil heterogeneity on drain rates and N-leaching of field BW and field GW?
Using NWGL-measurements to simulate water balance of field BW and GW?

2. Lysimeter experiments in Brandenburg

| Determining the impact of the lower boundary condition on the flow regime |

comparable meteorological conditions, pedo-hydrological conditions and vegetation

| **soil measuring station** | **weighable tension-controlled lysimeter (TL)** | **weighable gravitation lysimeter (GL)** |

tension registration — **regulation** → tension regulation ← **comparison** → no tension regulation

Does the lower boundary condition influence the depth depending course of soil moisture?
Does the lower boundary condition influence the temporal course and amount of discharged water?
Does a dynamic tension-controll optimize the reliability of lysimeter measurements?

Figure 1.1: Flowchart summarizing the coupled lysimeter and field experiment to evaluate the transferability from lysimeter to field scale, and further lysimeter experiments to determine the influence of the lower boundary condition on the daily discharge behavior.

Coupled lysimeter experiments and field trials in Saxony-Anhalt were performed to determine the transferability of data registered at lysimeter scale to predict the flow regime on field scale. Agricultural management is equalized and meteorological conditions are comparable at the lysimeter and the field site. Because of an impermeable clay in the subsurface, one of the investigated drained fields shows backwater influenced pedo-hydrological conditions (field BW) corresponding to the flow regime of the NWGL. It was proven, if the measured outflow rates at the NWGL could describe the drain rate of field BW. The other field site is heterogeneous, showing confined groundwater conditions (field GW). Based on detailed measurements regarding hydrological data (soil moisture, ground-/ backwater head, and drain rate) as well as N-transport data (N_{min} in soil; NO_3-N-concentration in soil solution, groundwater, backwater and drained water at field BW and GW), the impact of heterogeneous soil properties on water flow and N-transport was determined. Furthermore, it was proven if the NWGL data are applicable as point information to predict water flow of both fields - BW and GW within numerical simulations.

Because the investigated NWGL are mainly used to answer practical questions regarding water protection, the similarity of the discharge behavior between the NWGL and the investigated fields BW and GW based on monthly discharge rates. The in literature highlighted impact of the lower boundary on the daily discharge behavior of lysimeters is proven in a second lysimeter experiment in Brandenburg (cf. Figure 1.1). Daily depth depending soil moisture and matric potential as well as outflow rates from a weighable gravitation lysimeter (GL) were directly compared to measured values of a weighable lysimeter with variable-controlled tension (TL). Tension was adjusted according to registered tension of a surrounding soil measuring station in an undisturbed soil profile (cf. Figure 1.1). Within this second lysimeter experiment, not only the impact of the lower boundary, but also the practical feasibility of those technical ambitious devices was examined.

Actual literature emphasized to develop more technically complex lysimeters. Within this thesis, it is examined if the development of modern and technical ambitious lysimeter devices delivers more reliable data and to which extend simple constructed lysimeters could still be used to predict the flow regime on field scale. Furthermore, the possibility to numerically simulate water flow of fields with heterogeneous pedo-hydrological properties based on measuring results of simple constructed gravitation lysimeters describing the water balance and thus stand precipitation, evapotranspiration or groundwater recharge under the prevailing conditions was evaluated.

2. **Material and Methods**

2.1 Experimental studies to examine the transferability from lysimeter to field scale

2.1.1 Study area of the lysimeter experiments and the field trial in Saxony-Anhalt

The lysimeter experiments and the field trial were established in August 2012 in the northern part of the federal state Saxony-Anhalt in Germany (Figure 2.1).
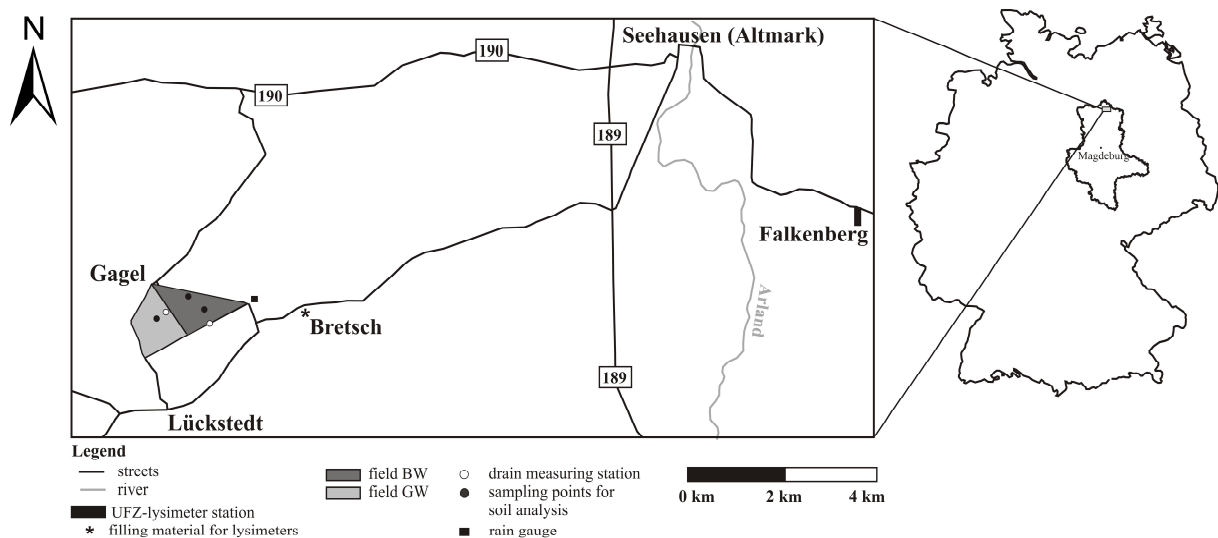
Figure 2.1: Lysimeter experiments and field trial in the northern Altmark region, Saxony-Anhalt, Germany.

For the lysimeter experiments, three non-weighable gravitation lysimeters (NWGL) were used, which are located at the lysimeter station of the Helmholtz Centre for Environmental Research - UFZ in Falkenberg (easting: 4487464, northing: 5858543). The field trial was established 20 km in the west of the lysimeter station near the village Lückstedt. For the investigations, two tile-drained arable fields were provided by the agricultural cooperative "Altmärkische Höhe" e.G in Lückstedt. The western field has an extension of 52 ha, the eastern field has a size of 81 ha. Climatically, the testing sites belong to the temperate zone of Central Europe within the transition zone from maritime to continental climate (average annual precipitation: 524.5 mm (1968-2007; Falkenberg); annual mean temperature: 9.2 °C (1994-2007; Falkenberg)). In Figure 2.2, the monthly long-term precipitation registered at the UFZ - station as compared to the actual monthly precipitation, measured at the UFZ - station for the whole observation period of three hydrological years (HY) 2013, 2014 and 2015 are summarized. Each HY begins at the 1st November and ends at 31st October in the following year.
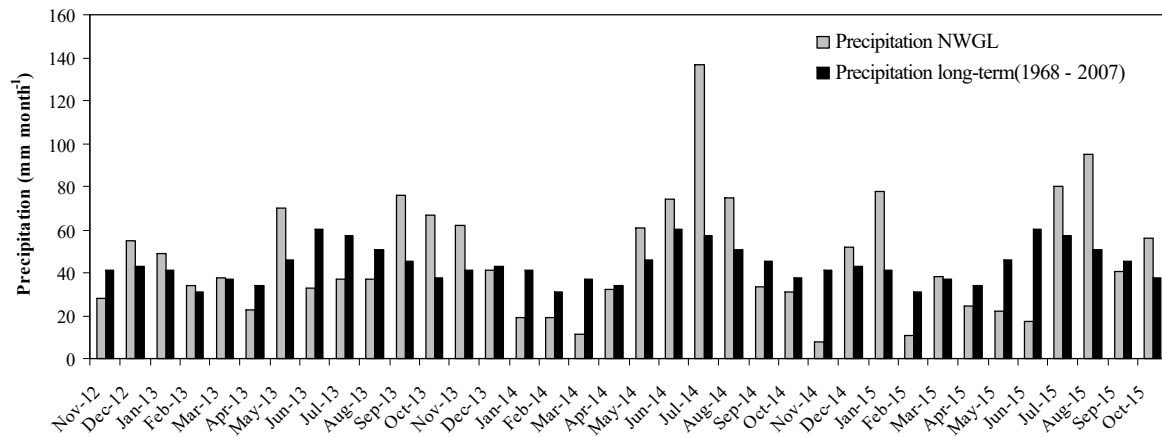
Figure 2.2: Monthly long-term precipitation registered at the NWGL as compared to recent monthly precipitation at the NWGL.

The annual rainfall in the HY 2013 (546.2 mm) and 2015 (521.9 mm) was comparable to the long-term average with 524.5 mm, whereby the HY 2014 was too wet with 595.6 mm. Despite the common course of the year regarding rainfall, the precipitation surplus in the HY 2014 resulted from exceeding rainfall in the hydrological summer. Thus, in July and August 2014, compared to the long-term precipitation, registered amount of rain at the NWGL showed a surplus of 79.8 mm and 23.9 mm, respectively. The HY 2015 was the driest year within the observation period, resulting from rain deficits at the beginning of this HY in November 2014, and during the vegetation period. The difference between actual registered precipitation and the long-term average were - 33.9 mm in November 2014, -24.0 mm in May 2015, and - 42.9 mm in June 2015, whereby a surplus was registered in July and August 2015 with 22.0 mm and 44.0 mm, respectively (Figure 2.2).

The subterranean layer of the northern Altmark region is characterized by quaternary deposits, whereas mainly the younger Saalian deposits shape the landscape (LAGB, 2003). According to the LAGB (1999) typically soil types which also characterize the subsurface of both fields in Lückstedt are Luvisols, Stagnic Gleysol (-Luvisols) as well as Gleysols. The investigation area belongs to the soil region "old moraine areas" which covers 1/3 of Saxony-Anhalt, and as a part of this region to the soils of the "ground moraine plates and the end moraines" (LAGB, 1999). The subsurface of the investigated fields as well as the filling material of the lysimeters are characterized as a Stagnic Gleysol Luvisol, which is a typical soil material of this soil region. Regarding the distribution of the 72 soils in Germany, Stagnic Gleysol Luvisol is on rank seven, covering 3.8 % of the total area of Germany (BGR, 2007). So, the filling substrate of the lysimeters as well as the subsurface of the field trial characterizes a representative soil region in Germany. In the 1970ies, a systema-

tic subsurface drainage network (PVC-pipes with an inner diameter from 63 mm until 110 mm, depth approximately 0.8 to 1.0 m) was installed at the fields due to the low hydraulic conductivity of the soil and to improve the soil fertility. The drainages, being parallel arranged to each other, have a gap distance of 10 m, discharging water to the main drains which end in an open ditch.

2.1.2 Lysimeter design – Non-weighable gravitation lysimeters (NWGL)

The internal structure of the three investigated non-weighable gravitation lysimeters (NWGL) according to Meissner et al. (2010) is illustrated in Figure 2.3.
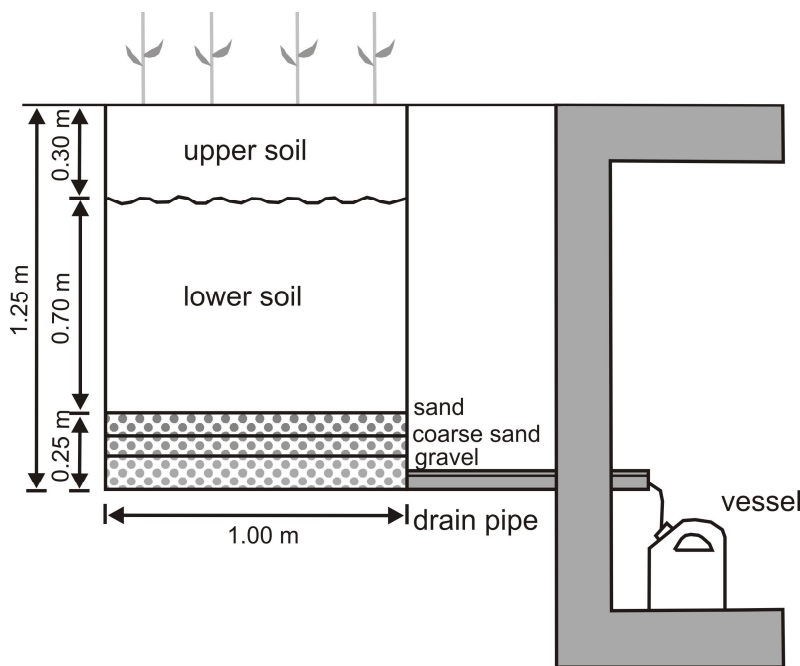
Figure 2.3: Internal structure of the investigated non-weighable gravitation lysimeters (NWGL).

The NWGL consist of a stainless-steel vessel with a quadratic surface area of 1 m^2 and a depth of 1.25 m. At the bottom a drain pipe is located from which the seepage water can discharge freely only following gravitation. This pipe is overlain by a graduated filter-layer consisting of sand, over coarse sand over gravel. Above the filter layer, the lysimeters were filled disturbed, but horizon-wise separated in 1983 (topsoil: 0-30 cm; subsoil: 31-100 cm) with soil substrates from the local region Bretsch (cf. Figure 2.1), 5 km in the east of Lückstedt (Meissner et al., 2010). Analyzed soil physical properties from Godlinski (2005) and Meissner et al. (2010) are summarized in Table 2.1.

Table 2.1: Soil physical parameters of the filling material of the NWGL taken from Godlinski (2005) (determined before filling) and Meissner et al. (2010).

z (cm)	sand (%)	silt (%)	clay (%)	BD (g cm^{-3})	Porosity (-)	$\theta_{pF1.8}$ (m^{3}m^{-3})	$\theta_{pF2.5}$ (m^{3}m^{-3})	$\theta_{pF3.0}$ (m^{3}m^{-3})	$\theta_{pF4.2}$ (m^{3}m^{-3})	K_s (m d^{-1})
0-30	73.6	14.3	12.1	1.5	0.32	0.27	0.15	0.08	0.06	0.75
30-100	75.2	17.4	7.4	1.8	0.32	0.19	0.12	0.07	0.05	0.19
100-125	Drainage layer									

z-depth; BD-bulk density; $\theta_{pF1.8/; 2.5; 3.0; 4.2}$-water content at pF stages 1.8; 2.5; 3.0; 4.2; K_s-saturated hydraulic conductivity.

2.1.3 Field conditions – Backwater influenced (BW) and groundwater influenced (GW)

At the field site, the interpretation of soil maps and geological maps, provided by the LAGB, reveal that the subsurface of both fields differs significantly (Figure 2.4 a). The subsurface of field BW is characterized by homogeneous distributed Stagnic Gleysol Luvisol which developed under backwater influenced conditions from periglacial clayey sand, overlaying glacially clay. The subsurface of field GW is characterized by Regosol, Gleysol as well as Stagnic Gleysol (–Luvisol). For the different soil types, not only the source substrates have to be distinguished, ranging from aeolian sand for the Regosol to sandy and clayey materials for the (Stagnic) Gleysols, but also the respective development conditions are different. Whereas Gleysols generally develop under groundwater influenced conditions, Stagnic Gleysol Luvisols only develop under a backwater influenced flow regime (Figure 2.4 a).
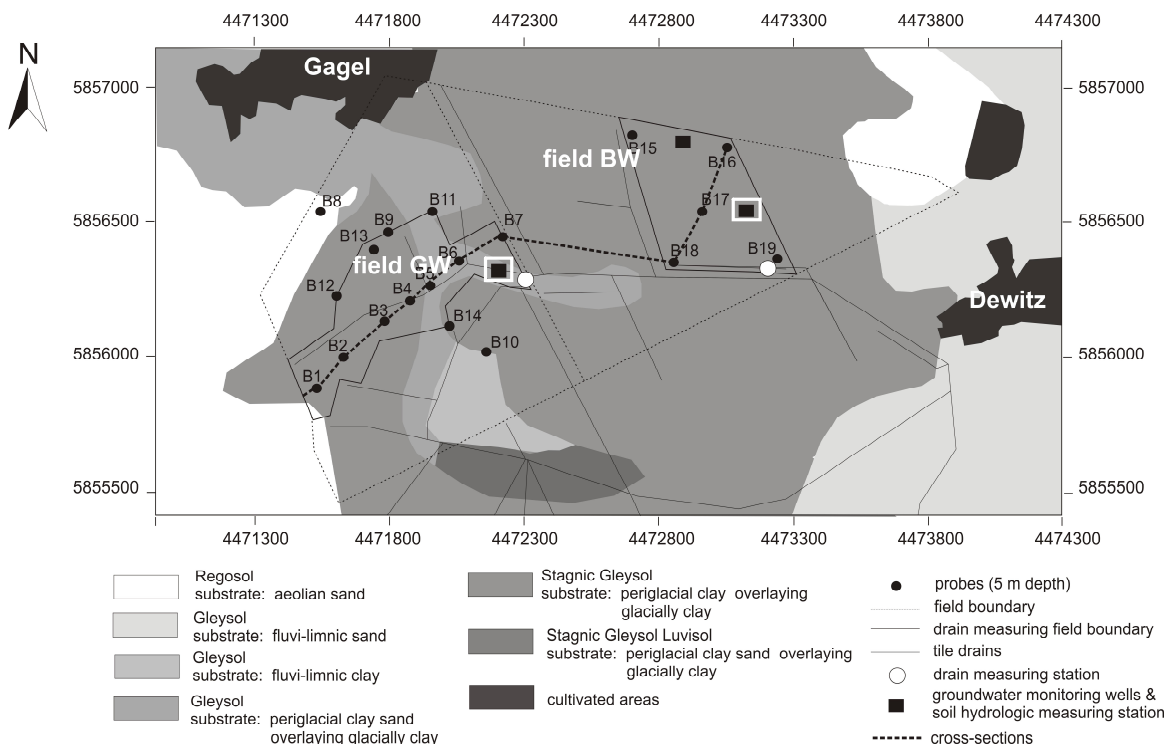
a
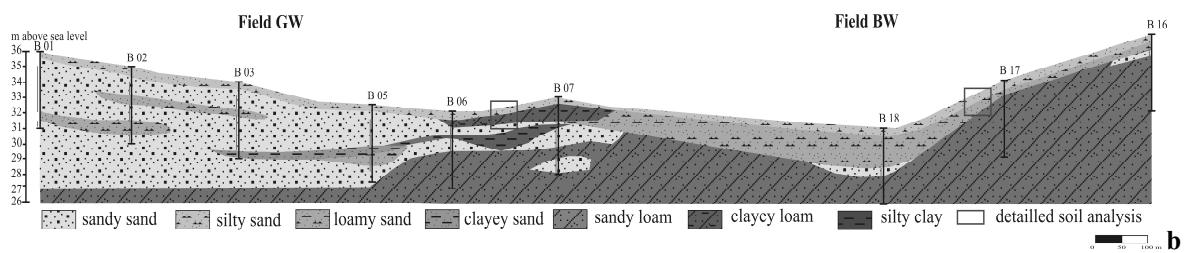
Figure 2.4: a) Maps of the soil types and soil substrates in the subsurface of both fields GW (ground-water influenced) and BW (backwater influenced); b) cross-section between both fields; marked rectangles in figures a) and b) represent the location of detailed soil analysis.

To get an overview of the geological and hydrological situation in the investigation area, 20 drillings with a depth of five meters respectively were performed and used to develop a cross section between both fields (Figure 2.4 a, b). The specific soil horizons were subdivided and described according to the German mapping guideline (Finners et al., 2005). From each horizon, one composite sample was taken and analyzed in the laboratory regarding grain size distribution according to DIN-ISO-11277 (2002). The laboratory analyses lead to the conclusion that boulder clay is lying in alternating strata with sandy layers at the western field GW. These sandy layers are characterized as aquifers here. The groundwater head is about one meter under floor, whereby groundwater is confined because of a flow-impeding clayey material above the sandy layer (Figure 2.4 b). The sandy layers crop out in transition to the other field, whereas here a homogenous distribution of boulder sand, overlaying boulder loam and clay was determined (Figure 2.4 b). Because of the impermeable clayey material, this field is backwater influenced (field BW).

At two locations of field BW and at one representative location of field GW, detailed soil analyses were performed in the top 1.2 m (cf. Figures 2.1, 2.4 a, b). Therefore, in eight different depth (sampling rings, diameter of 10 cm, six replications at each horizon: 0-6 cm, 16-22 cm, 24-30 cm, 32-38 cm, 42-48 cm, 60-68 cm, 80-86 cm, 110-116 cm depth) soil samples were taken and analyzed in the laboratory regarding soil physical parameters and grain size distribution. Grain size distribution was analyzed according to DIN-ISO-11277 (2002), whereby for describing soil physical properties, water content at different pF-stages was determined according to DIN-ISO-11274 (2009). pF value is the decadic logaritm of soil water tension (matric potential). Saturated hydraulic conductivity according to DIN-18130-1 (1998) was analyzed assuming a constant pressure head. Because of similar results for determined soil properties, five different material layers for each field soil were assigned for further evaluation (Table 2.2).

Table 2.2: Soil physical parameters of the field soil determined in the laboratory (six replications) – grain size distribution with sieving and hydrometer analysis according to DIN-ISO-11277 (2002), water content at different pF-values with pressure pot without hysteresis according to DIN-ISO-11274 (2009), saturated hydraulic conductivity K_s with constant pressure head according to DIN-18130-1 (1998).

z (cm)	sand (%)	silt (%)	clay (%)	BD (gcm^{-3})	Porosity (-)	$\theta_{pF1.8}$ (m^{3}m^{-3})	$\theta_{pF2.5}$ (m^{3}m^{-3})	$\theta_{pF3.0}$ (m^{3}m^{-3})	$\theta_{pF4.2}$ (m^{3}m^{-3})	K_s (m d^{-1})
Field BW										
0-25 L1	48.5	45.9	5.6	1.6	0.36	0.26	0.20	0.18	0.06	0.31
25-55 L3	52.9	41.0	6.1	1.7	0.34	0.24	0.18	0.16	0.08	0.16
55-75 L6	54.9	34.5	10.6	1.7	0.34	0.29	0.26	0.25	0.18	0.06
75-100 L6	46.0	39.9	14.1	1.8	0.32	0.28	0.26	0.25	0.25	0.09
100-125 L4	37.8	44.7	17.5	1.8	0.31	0.28	0.25	0.23	0.16	0.05
Field GW										
0-20 L1	47.3	46.4	6.3	1.4	0.47	0.27	0.22	0.19	0.07	0.80
10-30 L2	53.5	39.0	7.5	1.5	0.41	0.26	0.19	0.18	0.06	0.57
30-75 L3	59.0	34.3	6.7	1.7	0.34	0.26	0.20	0.17	0.07	0.16
75-100 L6	48.3	34.7	17.1	1.8	0.33	0.27	0.23	0.21	0.12	0.05
100-125 L5	64.9	30.6	4.5	1.6	0.34	0.34	0.20	0.19	0.04	0.20
Combination of field BW and GW										
Layer 1	47.9	46.2	5.9	1.5	0.41	0.26	0.21	0.18	0.06	0.55
Layer 2	53.5	39	7.5	1.5	0.40	0.26	0.19	0.18	0.06	0.57
Layer 3	55.9	37.7	6.4	1.7	0.34	0.25	0.19	0.17	0.07	0.16
Layer 4	43	39.7	17.3	1.8	0.32	0.28	0.24	0.22	0.14	0.05
Layer 5	64.9	30.6	4.5	1.6	0.34	0.34	0.20	0.19	0.04	0.20
Layer 6	50.4	37.2	12.4	1.8	0.33	0.28	0.26	0.25	0.21	0.07

BW-backwater influenced; GW-groundwater influenced; L-layer; z-depth; BD-bulk density; $\theta_{pF1.8/;\ 2.5;\ 3.0;\ 4.2}$-water content at pF stages 1.8; 2.5; 3.0; 4.2; K_s-saturated hydraulic conductivity.

Although the soil substrates for filling the NWGL were taken only 5 km in the east of Lückstedt, the properties between the field soils and the NWGL material differs. Compared to the NWGL filling material, the field BW soil has higher silt and lower sand contents, showing larger clay contents with greater depth, corresponding to a decreasing saturated hydraulic conductivity (K_s) (cf. Tables 2.1, 2.2). As compared to K_s of 0.19 m d^{-1} in the lower soil of the NWGL, K_s is smaller than 0.10 m d^{-1} from 55 cm depth at field BW, being nearly impermeable in 1.00 m depth with 0.05 m d^{-1}. But although the soil properties differ, the general pedo-hydrological conditions are comparable between NWGL and field BW. At both, the water balance and the amount of discharged water is influenced by backwater conditions.

But these comparable conditions could not be reproduced at field GW. At field GW, it was remarkable that as compared to the material layers above, from 1.00 m to 1.25 m, bulk density and clay content decrease whereby hydraulic conductivity increases from 0.05 md^{-1} to 0.20 m d^{-1}. As already discussed, the material from 1.00 m depth is characterized as the sandy aquifer, cropping out in transition to field BW (cf. Figure 2.4 b).

Based on the 20 drillings with a depth of five meters and the developed 2 D-cross section, it could be achieved that this sandy aquifer is underlain by an impermeable clayey material, which also characterizes the subsurface of field BW. For further analysis and simulations, the fields were not only handled separate from each other, but also were combined according to Figure 2.5. Therefore, the mean values of the soil physical properties of the respective layers were calculated (cf. Table 2.2).
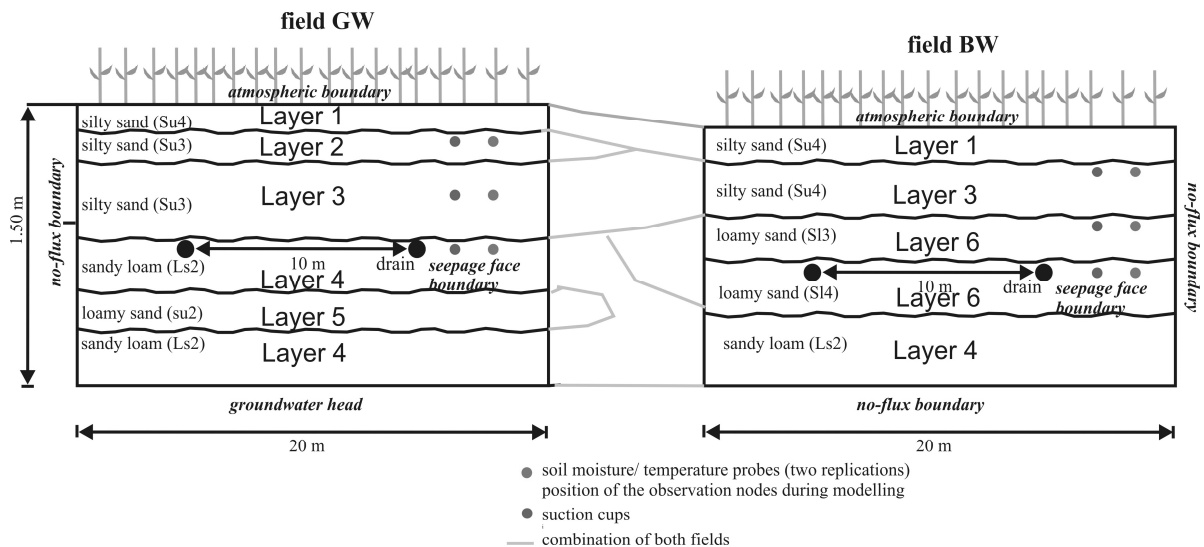
Figure 2.5: Combination of field GW and field BW.

2.1.4 Crop rotation and soil tillage at the lysimeters and the field trial

From August 2012, the crop rotation and the seed rate of the NWGL and field BW was adjusted for the whole observation period (November/1/2012 until October/31/ 2015). The crop rotation of field GW was adjusted from October 2013 (Table 2.3).

Table 2.3: Crop rotation of the NWGL, field BW and GW.

	8/2012-3/2013	4/2013-9/2013	10/2013-3/2014	4/2014-9/2014	10/2014-9/2015
NWGL	CC	M	WCC	M	WW
Field BW	CC	M	WCC	M	WW
Field GW	M	WW	WCC	M	WW

CC- freezes catch crop-field peas; M-maize; seed rate of 80,000 grains ha^{-1}; WCC-winter catch crop (winter rye (75 kg ha^{-1}) and legume grass mixture (25 kg ha^{-1}); WW-winter wheat; seed rate of 200 kg ha^{-1}.

In the first observation year HY 2013, the main crop grown at the NWGL and field BW was maize, followed by winter catch crops. In HY 2014, maize was the main crop grown at the NWGL, field BW and GW. The agricultural management regarding soil tillage, fertilization, and maize seed rate in 2013 was comparable to 2014. Fertilization and reduced soil tillage in both years was performed in the mid of March 2013/ 2014. At the NWGL three liters of cattle slurry (2.7 kg N_{org} m^{-3} organic substance) and 0.3 ml nitrification inhibitor (PIADIN: active ingredient combination 1 H-1,2,4 Triazol + 3-Methylpyrazol, SKWP, Germany) per m^2 was applied manually, whereas at the field trial a disc harrow was used for loosening the upper soil and for a shallow distribution of the liquid slurry (30 m^3 ha^{-1}) and nitrification inhibitor. The maize was sawn in the mid of April 2013/ 2014 with a seed rate of eight plants per m^2. In May 2014, a mineral fertilization (calcium ammonium nitrate-KAS) was applied with an amount of 70 kg N ha^{-1}. After the maize harvest at the end of September 2014, stubble clearing and sowing of the winter wheat (200 kg ha^{-1}) followed. Mineral fertilization with 70 kg N ha^{-1} (ammonium sulfate nitrate - ASS) in March, 57 kg N ha^{-1} (KAS) in April and 57 kg N ha^{-1} (KAS) in May 2015 was applied.

2.1.5 Lysimeter and field measurements

Water balance and NO_3-N-leaching

To evaluate the transferability of the NWGL data to predict the water regime on field scale, the outflow rates of the NWGL were compared to the drain rates of the field trial for an observation period of three hydrological years 2013, 2014 and 2015. In the HY 2013 outflow of the NWGL was collected manually in monthly intervals, whereas in 2014 and 2015, a daily to weekly interval was implemented. Furthermore, discharged water was analyzed regarding NO_3-N-concentration for calculating discharged NO_3-N-loads.

At both fields, BW and GW, in 2012 drain measuring stations were installed to capture the time-depending amount of discharged water via drainages from a specified area (cf. Figure 2.4 a). Therefore, a Venturichannel was installed in the shaft of a collector drain. The fields are morphologically depressions sloping with 1.2 % to the collector drains. The measuring principle based on the registration of the water level (using an ultrasonic sensor -type UNKD 30I6112/S14, Baumer, Frauenfeld, Switzerland) for calculating the flow rate. At the collector drain with the former described Venturichannel, PVC-suction drains ended. They are arranged parallel to each other and drain an area of 26 ha at field BW, and 24 ha at field GW, providing the determination of the area specific drain rate from these drain measuring fields (cf. Figure 2.4 a). In HY 2013 only monthly rates were registered whereas

in HY 2014 and 2015 a daily rhythm was implemented at both, field BW and GW. Additionally, at the drain outlet daily water samples were taken by an auto-sampler for further laboratory analysis regarding NO_3-N-concentration in discharged water. Thus, from drain rate and concentration, daily discharged NO_3-N-loads via drains were calculated. In February 2014, monitoring wells (perforated HDPE-pipe to 5 m depth, inner diameter: 3.81 cm) for registering groundwater- (field GW), backwater head (field BW) and specific NO_3-N-concentration, as well as two soil hydrological measuring facilities were installed (cf. Figure 2.1, 2.4 a). For the measuring facilities, the soil at each field was excavated (length x width x depth= 5 m x 3 m x 2 m). As illustrated in Figure 2.5, TDR-probes (UMP1; measuring accuracy +/- 2 Vol.%, UGT, Müncheberg (Germany)) for registering soil moisture/ temperature (two replications at each horizon) and suction cups for extracting soil solution (three replications at each horizon) were installed at three different depths (35 cm, 60 cm and 85 cm below ground surface). For the whole observation period, at field BW and GW N_{min}- and N_{org}-soil-analysis in 30 cm, 60 cm and 90 cm depth were performed (VDLUFA, 2002). Dry matter maize/ winter wheat yields and N-uptake were determined after harvest (DIN-EN-ISO-16634-1, 2008). Additionally, to characterize the chemical conditions at both fields, sulfate (SO_4), dissolved organic carbon (DOC), pH-value as well as nitrite (NO_2-N) and ammonia (NH_4-N) in soil solution, drained water, ground- and backwater were analyzed (DIN-EN-1484, 1997; DIN-EN-ISO-10304-1, 2009; DIN-EN-ISO-10523, 2012).

Meteorological conditions

Meteorological data like temperature, precipitation (P_{NWGL}), relative humidity, net radiation and wind speed were monitored by the weather station of the UFZ in Falkenberg with a daily rhythm. In addition to that, in August 2014, a rain gauge was installed at the field site.

Comparing P_{NWGL} to registered precipitation at the weather station of the German Meteorological Service ($P_{Seehausen}$, located in the town Seehausen between Falkenberg and Lückstedt) and at the field (P_{field}, installed in April 2014) provided, that deviations between P_{NWGL}, $P_{Seehausen}$ and P_{field} were generally smaller than +/- 10 % for each hydrological half year (HHY 1, 2= HY 2013; HHY 3, 4=HY 2014; HHY 5, 6=HY 2015) (Figure 2.6 a).
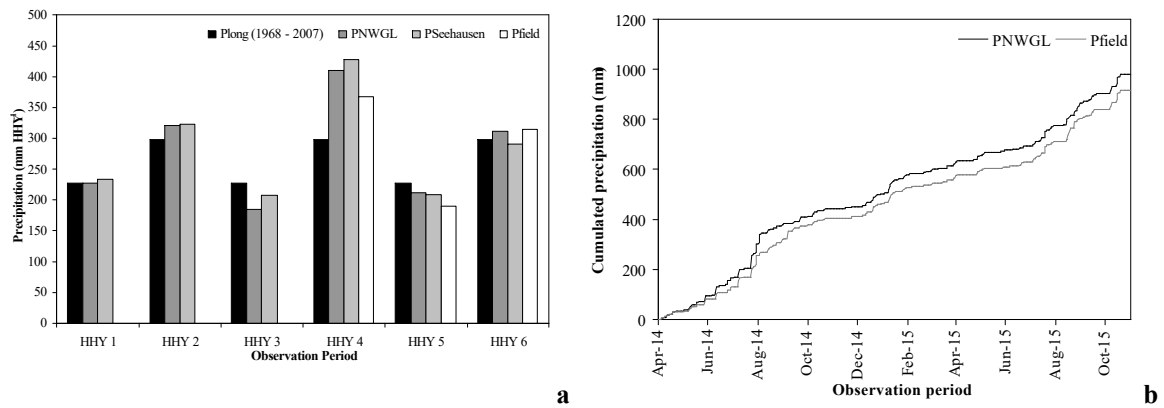
Figure 2.6: a) Precipitation for every hydrological half year (HHY), registered at the UFZ-station (P$_{NWGL}$), the DWD-station (P$_{Seehausen}$) and the weather station at the field trial (P$_{field}$) compared to the long-term average precipitation in Falkenberg (P$_{long}$); b) cumulated precipitation at the lysimeter station and the field trial.

The cumulated daily amounts of P$_{NWGL}$ and P$_{field}$ revealed a similar temporal course of precipitation in Falkenberg and Lückstedt (Figures 2.6 b). This was the precondition for evaluating the transferability from NWGL measurements to predict the flow regime of field BW and GW.

Plant development data

Development stages of the crops grown at the NWGL and thus crop height and surface cover fraction (SCF) were determined with a biweekly rhythm. SCF was determined via photographing the plants perpendicular to the NWGL surface. This is illustrated in Figure 2.7 a) for the cultivated maize in 2014, two months after seeding.
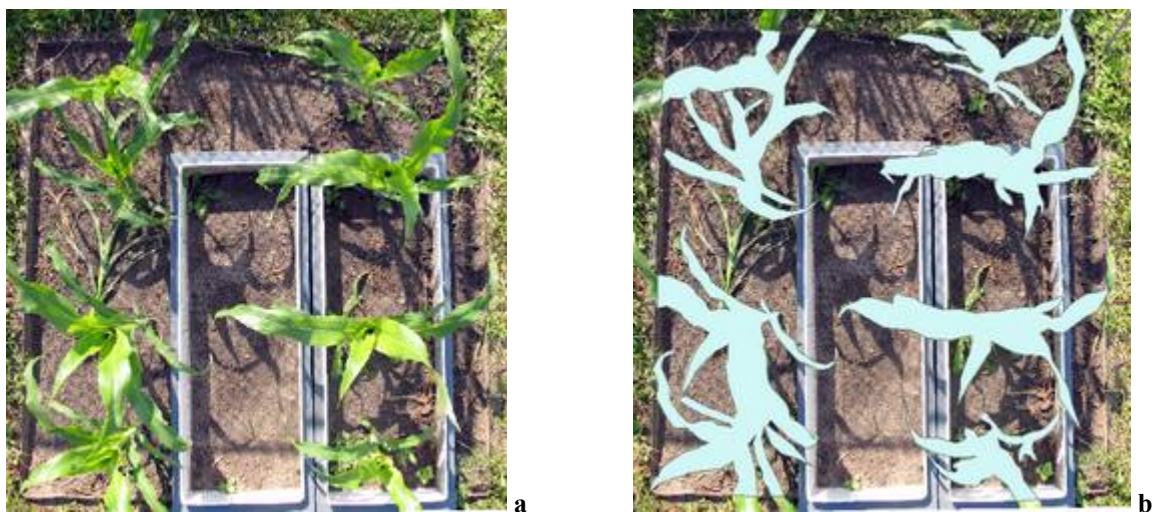
Figure 2.7: a) Perpendicular photographed maize plants in June 2014 at the NWGL; b) polygon-shape drawn in ArcView to digitalize the maize plants for calculating surface cover fraction (SCF).

The photos were imported into the Geoinformation system (GIS) ArcView® of the Company ESRI. For the surface of the NWGL, an area of 1 m^2 was assigned via georeferencing the picture. A polygon-shape was drawn to characterize the maize plants, illustrated in Figure 2.7 b. The respective area of these maize polygons was calculated automatically within the GIS because of the previous georeferencing. The relation of the polygon area to the total area characterizes the SCF. Dry matter maize and winter wheat yields of the NWGL and the field were determined after harvest.

Overview of the measured data

Table 2.4 summarizes the respective parameters, registered at the NWGL and both fields.

Table 2.4: Registered parameters at the NWGL, field BW, and field GW.

	NWGL	Field BW	Field GW
Water balance parameters			
Precipitation	x	x	x
Meteorological parameters to calculate potential evapotranspiration	x		
Depth depending soil moisture		x	x
Outflow rates	x	x	x
Groundwater/ backwater head		x	x
Plant development data			
Plant development (SCF/ LAI)	x		
Root depth	x	x	x
Yield	x	x	x
N-transport parameters			
NO_3-N-uptake by plants	x	x	x
NO_3-N in soil solution		x	x
N_{min} in the soil		x	x
NO_3-N concentration in discharged water	x	x	x
NO_3-N concentration in groundwater/ backwater		x	x

Regarding the water balance and the nitrogen transport, at the NWGL only input and output was registered, whereby the NWGL worked as a kind of black-box-system. In contrast to that at both fields BW and GW, despite in- and output the change in water storage was considered via measuring the depth depending course of soil moisture. Furthermore, regarding nitrogen N_{min} and NO_3-N in several compartments was observed, revealing the transport and transformation behavior of nitrogen at both sites.

2.2 Experimental studies to evaluate the impact of the lower boundary on lysimeter measurements

2.2.1 Study area of the lysimeter experiments in Brandenburg

To evaluate the impact of the lower boundary condition on the water balance of lysimeters, experiments were established in May 2014 at the research station of the company Umwelt-Geräte-Technik (UGT) GmbH at Müncheberg (Federal State Brandenburg) in Germany, 50 km in the east of Berlin. Climatically, the testing site belongs to the temperate zone of Central Europe with continental climate conditions (average annual precipitation: 531 mm; average annual temperature: 8.4 °C – weather station of the German Meteorological Service DWD in Strausberg, 15 km in the east of Müncheberg). For the whole observation period from June 2014 until October 2015, meteorological data were registered at the UGT-weather station directly neighboring to the investigated lysimeters. Regarding the whole observation period, compared to the long term-precipitation of 873.0 mm for 17 months (DWD-Station Strausberg-1981-2010), 600.6 mm were registered in Müncheberg. Figure 2.8 illustrates monthly precipitation registered in Müncheberg, compared to the long-term monthly average precipitation of the DWD-station in Strausberg (Figure 2.8).
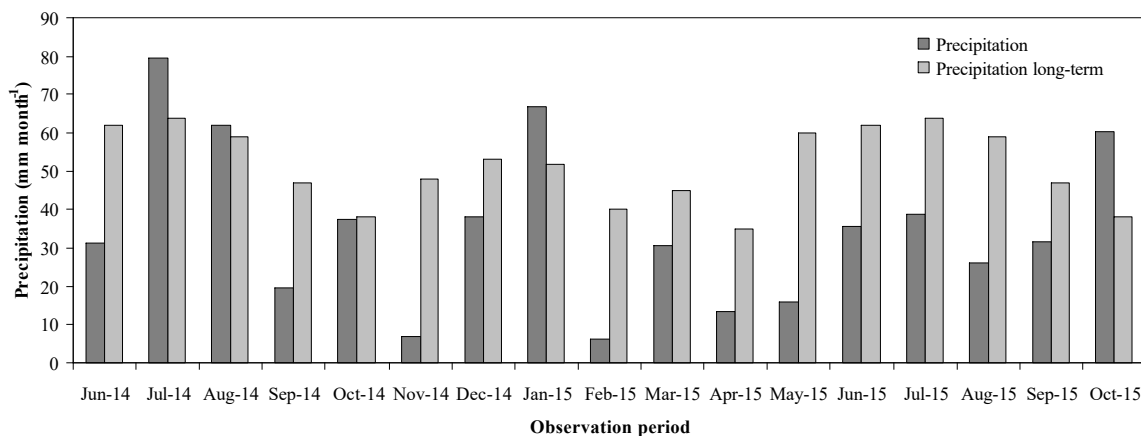
Figure 2.8: Actual monthly precipitation at the weather station Müncheberg as compared to monthly long-term average precipitation of the DWD-station in Strausberg (15 km in the east of Müncheberg).

Maximum precipitation, exceeding the long-term average was observed in July 2014 (79.5 mm), August 2014 (62 mm) and January 2015 (67.0 mm). Following this, the registered precipitation from February 2015 until the end of the observation period was generally low.

2.2.2 Experimental setup – Tension-controlled lysimeter (TL) – Gravitation lysimeter (GL) – Soil measuring station

The design of both investigated lysimeters as well as the implemented measuring technology in the lysimeters and in the surrounding undisturbed, natural soil is illustrated in Figure 2.9
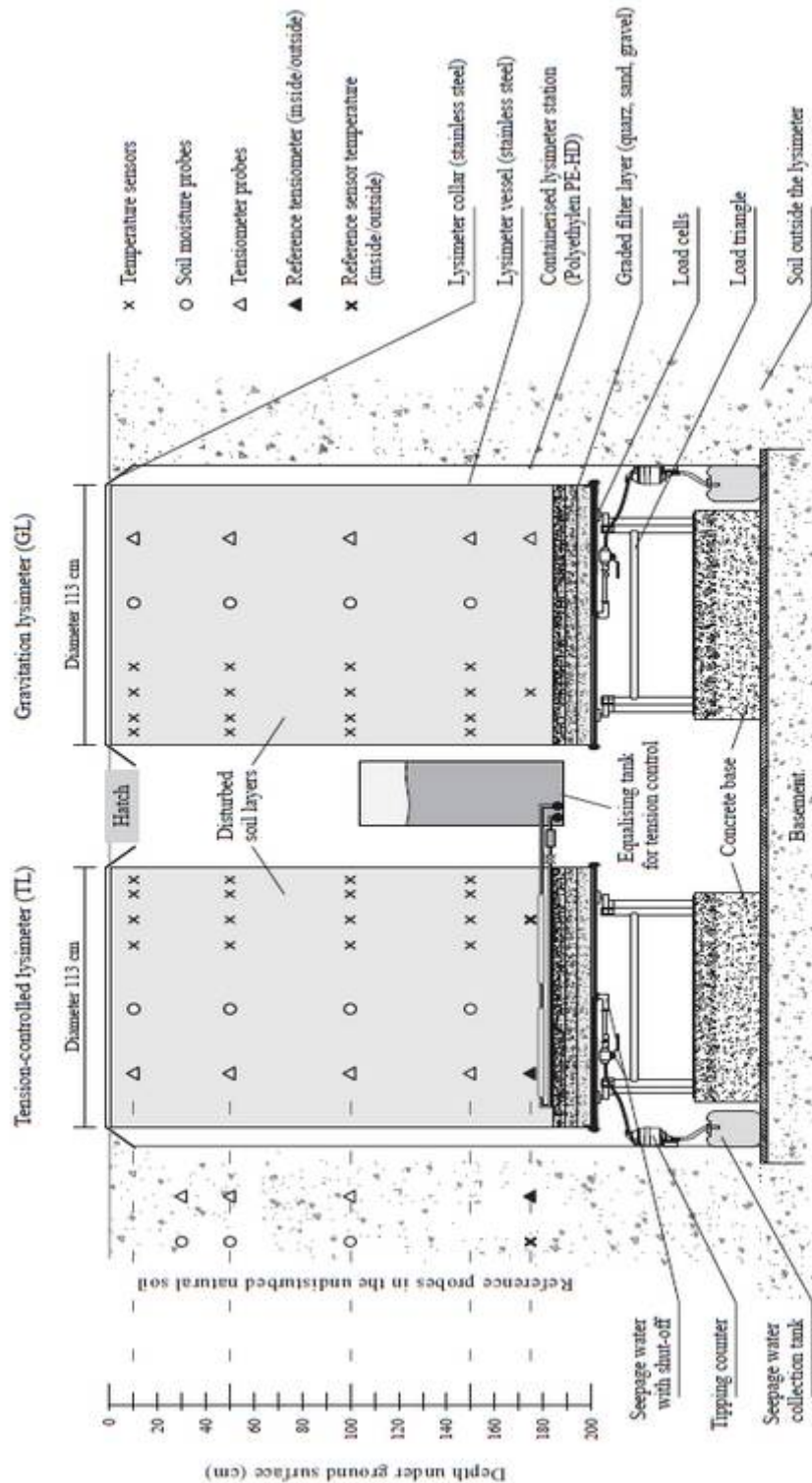
Figure 2.9: Experimental setup of the tension-controlled (TL) and the gravitation lysimeter (GL) in Müncheberg (Brandenburg).

The tension-controlled lysimeter TL and the gravitation lysimeter GL, both being weighable (high resolution load cells mounted on a load triangle in combination with an UGT weighing monitor), consist of a stainless-steel vessel with a surface area of 1.0 m^2 and a depth of 2.0 meters. At the bottom of both lysimeters a filter layer with a thickness of 15 cm consisting of quartz sand over coarse sand over gravel is implemented. Above the filter layer, the lysimeters were filled disturbed but horizon wise with sandy loam in May 2014. The lysimeter vessels were filled manually to ensure the comparability between the unsaturated soil hydraulic properties of the TL and the GL. In lysimeter literature it is well known that monolithically extracted lysimeter vessels from the same soil site and with the same land management could show different water and solute fluxes due to spatial heterogeneity in soil properties (Haferkorn, 2000; Knoblauch, 2009; Gebler et al., 2015). Because this experiment focused on the impact of the lower boundary condition, the unsaturated soil hydraulic properties should be as similar as possible. At four different depths, soil samples of the filling material were analyzed in the laboratory regarding dry density, porosity, water content at saturation as well as water content at different pF-values according to DIN-ISO-11274 (2009), listed in Table 2.5.

Table 2.5: Laboratory results of the lysimeter filling material of the TL and the GL.

	soil type	BD (gcm^3)	Porosity (-)	$\theta_{pF1.8}$ (m^{3}m^{-3})	$\theta_{pF2.5}$ (m^3 m^{-3})	$\theta_{pF3.0}$ (m^3 m^{-3})
TL						
10 cm	sL	1.41	0.47	0.23	0.19	0.15
50 cm	sL	1.63	0.39	0.23	0.18	0.14
100 cm	sL	1.79	0.33	0.21	0.16	0.14
150 cm	sL	1.75	0.34	0.22	0.16	0.11
GL						
10 cm	sL	1.41	0.47	0.22	0.15	0.10
50 cm	sL	1.68	0.37	0.21	0.15	0.09
100 cm	sL	1.56	0.41	0.20	0.15	0.12
150 cm	sL	1.71	0.36	0.24	0.18	0.09

sL: sandy loam; BD: bulk density; $\theta_{pF1.8/; 2.5; 3.0}$-water content at pF stages 1.8; 2.5; 3.0.

In 10 cm depth, soil physical properties of both lysimeters are comparable whereas in 50 cm, bulk density at the TL is slightly smaller and porosity greater as compared to the GL. In 100 and 150 cm depth, the filling material of TL reveals a higher compaction with a bulk density of 1.79 and 1.75 g cm^{-3} as compared to GL with 1.56 and 1.71 g cm^{-3}.

The lysimeters as well as the surrounding area were covered with clipped grass for the whole observation period. In 10 cm, 50 cm, 100 cm and 150 cm depth the TL and the GL were equipped with probes for registering soil moisture (UMP1; measuring accuracy +/- 2

Vol.%, UGT, Müncheberg (Germany)) and pressure head (Tensio 100; measuring accuracy +/- 1 kPa; suction pressure range: 0-85 kPa, UGT, Müncheberg (Germany)). Additionally, at the undisturbed soil and inside the lysimeter vessels, a tensiometer in 175 cm depth was installed above the drain face to account for the effect of the lower boundary (cf. Figure 2.9). The registered tension at the GL (tension probe) was compared to the controlled variable tension of the TL in this depth. The tension of the TL was controlled via a water filled equalizing tank in the lysimeter shaft to mimic registered tension of the undisturbed soil profile outside (cf. Figure 2.9). The tank (volume of five liters) has two pipe connections. The first one is at the bottom of the tank (permanently water filled) and it is connected via a pipe to ceramic tubes inside the TL. These tubes (nine) were installed above the filter layer in 180 cm depth and arranged radially. Respectively three of them were connected with each other to a pressure cycle. If one of the tubes was defect, one pressure cycle could be switched off (via a tap system) whereas the other two could still work. Via a tap system the cycles were combined with each other to one pipe, which was connected to the equalizing tank. The second pipe connection at the equalizing tank was installed at its top (air volume without water) and yielded in a pumping system. Via recirculating air flow, a negative or positive pressure could be regulated inside the tank. Via pressure control, in dependence of the registered pressure head in the undisturbed soil (reference tensiometer outside in 175 cm depth), water was pumped into the TL or removed via ceramic tubes from the lysimeter to regulate the water content of the TL in transition to the filter layer (above the filter layer). In addition to that, further sensors (UMP/ TDR and tensiometer) in 30 cm, 50 cm and 100 cm depth were installed in the surrounding undisturbed natural soil (loamy sand) for continuously measuring soil moisture and tension (cf. Figure 2.9). But soil moisture probe in 30 cm depth was defect at the natural soil outside. The amount of discharged water of both lysimeters was registered by a tipping counter (cf. Figure 2.9). Soil moisture, water tension, seepage rate, mass change and meteorological parameters were registered with a ten-minute resolution. For data evaluation, daily values were calculated.

2.3 Numerical simulations with HYDRUS 1D/ 2D

2.3.1 Governing equations describing water flow and simplified solute transport

The water regime of the NWGL, field BW and GW as well as the TL and the GL was simulated using the software package HYDRUS. Furthermore, a simplified solute transport model was adapted for the combined field BW-GW model. The software package HYDRUS solves the Richards´ equation numerically for describing the spatial distribution of the soil moisture

1D for the NWGL:

$$\frac{\partial \theta}{\partial t} = \frac{\partial}{\partial z}\left[K\left(\frac{\partial h}{\partial z}+1\right)\right] - S \tag{4}$$

2D for the field models, the TL and the GL:

$$\frac{\partial \theta}{\partial t} = \frac{\partial}{\partial x_i}\left[K\left(K_{ij}^A \frac{\partial h}{\partial x_j}+K_{iz}^A\right)\right] - S \tag{5}$$

Where θ is the volumetric water content ($m^3\ m^{-3}$), h is the pressure head (m), S is the sink term (d^{-1}), z is the depth (m), x_i (i=1, 2) are the spatial coordinates (m), t is the time (d), K_{iz}^A are the components of the dimensionless anisotropy tensor K^A, and K is the unsaturated hydraulic conductivity ($m\ d^{-1}$).

The sink term S in equation (4) and (5) represents the root water uptake (RWU), which is calculated according to Feddes et al. (1978) as a potential and depth dependent sink term:

$$S(h) = a(h)S_P, \tag{6}$$

Where a(h), the root water uptake stress response function is a dimensionless function of the pressure head h, ranging from $0 \leq a \leq 1$, and S_P is the potential root water uptake rate (d^{-1}).

The root water uptake stress response function is described as:

$$a(h) = \frac{h-h_4}{h_3-h_4} \text{ for } h_4 < h \leq h_3$$

$$a(h) = 1 \text{ for } h_3 < h \leq h_2$$

$$a(h) = \frac{h-h_1}{h_2-h_1} \text{ for } h_2 < h \leq h_1$$

$$a(h) = 0 \text{ for } h \leq h_4 \text{ and } h > h_1 \tag{7}$$

Where h_1, h_2, h_3 and h_4 are crop-specific threshold values (Simunek et al., 2008). These values were taken from the integrated HYDRUS data base (**maize/ wheat**: h_1= 0.1 m/ 0 m; h_2= -0.3 m/ 0.01 m; h_3= -3.25 m/ -5 m/ h_4= -80 m/ -160 m; **grass**: h_1= -0.1 m, h_2= -0.25 m, h_3= -3 m, h_4= -80 m).

The spatial distribution of S_P is described as:

$$S_P = b(x, y, z)S_T T_P \tag{8}$$

Where b is the normalized root distribution (m^{-1}), T_P is the potential transpiration rate (m d^{-1}) and S_T is the width of the model surface associated with transpiration (for 1D simulation S_T omitted).

Measurements at the end of the vegetation period provided a maximum rooting depth of 0.70 m, with maximum root density in 0.30 m for **maize** in the HY 2013 and 2014 and **wheat** in the HY 2015, and a maximum depth of 0.15 m for the **catch crops**.

For the experiments in Müncheberg, a maximum rooting depth of 0.10 m was assumed for **grass**, with maximum root density in 0.05 m depth.

The unsaturated soil hydraulic properties $\theta(h)$ and K(h) are highly non-linear functions of the pressure head. In HYDRUS, there are five different analytical models to describe the hydraulic properties. Within this thesis the parameters were described according to van Genuchten-Mualem (Van Genuchten, 1980):

$$\theta(h) = \theta_r + \frac{\theta_s - \theta_r}{\left[1 + |\alpha h|^n\right]^m} \quad h < 0; \qquad \theta(h) = \theta_s \quad h \geq 0 \tag{9}$$

$$K(h) = K_s S_e^l \left[1 - \left(1 - S_e^{1/m}\right)^m\right]^2 \tag{10}$$

Where θ_s is the saturated water content (m^3 m^{-3}), θ_r is the residual water content (m^3 m^{-3}), m, n, l are empirical parameters (-), S_e the effective water content (m^3 m^{-3}) and K_S the saturated hydraulic conductivity (m d^{-1}).

Only for the combined field BW-GW-model, a simplified solute transport model was implemented with a non-reactive component. Solute transport was described by the convection dispersion equation within HYDRUS:

$$\frac{\partial \theta \cdot c}{\partial t} = \frac{\partial}{\partial x_i}\left(\theta \cdot D_{ij} \cdot \frac{\partial c}{\partial x_j}\right) - \frac{\partial qc}{\partial x_i} - Sc_{root} \tag{11}$$

With c the solute concentration (in our case %), q_i the ith component of the volumetric flux density (m d^{-1}), D_{ij} the dispersion coefficient tensor (m^2 d^{-1}), S the root solute uptake (% d^{-1}) and c_{root} the maximum possible concentration for root solute uptake.

Based on equations (1), (2), (3) and (11), it was assumed that the N-transport was mainly driven by the flow regime. To focus only on the impact of soil heterogeneity and hydrology on the N-kinetic it was a precondition, that the first-order rate constants describing mineralization, nitrification, and denitrification k_{min}, k_{nit} and k_{den} at field BW and GW are comparable.

These constants express the amount of N that is mineralized or denitrified within a certain time unit. Thus, if the conversion rate is identical between field BW and GW, the amount of mineralized and denitrified N depends mainly on the water residence times and thus on the flow regime.

Because nitrification is a very fast process (0.20 d^{-1} Jansson and Karlberg, 2001; 0.02-0.5 d^{-1} Lotse et al., 1992; 0.15-0.25 d^{-1} Ling and El-Kadi, 1998) it was assumed that the spatial and temporal variability of N-transformation between both, field BW and GW, is mainly described by k_{min} and k_{den}.

Mineralization rate k_{min} was analytically calculated according to Kersebaum and Richter (1991) and Carbon et al. (1991) with the measured soil moisture and temperature of the hydrological measuring stations at field BW and GW:

$$k_{min} = 5.6E12\exp[-9800/(T+273)]F_{wm} \tag{12}$$

$$F_{wm} = \theta/f_c \quad \text{if } \theta < f_c \qquad F_{wm} = f_c/\theta \quad \text{if } \theta > f_c \tag{13}$$

With T soil temperature (°C), F_{wm} water content factor (m^3 m^{-3}), θ water content (m^3 m^{-3}), f_c water content at field capacity(m^3 m^{-3}).

From 30 cm depth, denitrification k_{den} is the predominant N-transformation process. Soil specific k_{den} was calculated according to Marchetti et al. (1997) with registered soil moisture and temperature in three different depths:

$$k_{den} = k_{15} \cdot F_{wd} \cdot F_t \tag{14}$$

$$F_{wd} = \exp[0.304 + 2.94(\theta_s - \theta) - 47(\theta_s - \theta)^2] \tag{15}$$

$$F_t = 0.67\exp(0.43(T_s - 10)) \quad \text{if } T_s \leq 10°C \quad F_t = \exp(0.08(T_s - 15)) \quad \text{if } T_s > 10°C \tag{16 a \& b}$$

With k_{15} rate coefficient for denitrification at 15 °C (0.01 d^{-1}), F_{wd} water content factor (m^3 m^{-3}), θ water content (m^3 m^{-3}), θ_s water content at saturation (m^3 m^{-3}), T_s soil temperature at saturation (°C).

2.3.2 Initial and boundary conditions

Initial conditions are a precondition to solve the Richards`equation. Therefore, regarding water flow modeling the spatial distribution of soil moisture θ or hydraulic head h, and in the case of solute transport simulations the distribution of the concentration c at the beginning of the modeling period have to be defined:

$$\theta(x,z,t) = \theta_0(x,z) \quad h(x,z,t) = h_0(x,z) \quad c(x,z,t) = c_0(x,z) \quad \text{for t=0} \tag{17}$$

Furthermore, boundary conditions at the borders of the modeling domains have to be defined for each process that is simulated. Regarding water flow modeling, in HYDRUS the

boundary types *no flux, constant pressure head/ flux, variable pressure head/ flux, free* or *deep drainage, seepage face* as well as *atmospheric boundary* are provided (Simunek et al., 2012). These boundary types could be classified as *system-independent* and *system-dependent boundaries*.

System-independent conditions are boundary conditions, where the specified boundary value, e.g. specified head, flux or gradient, does not depend on the status of the soil system. According to Simunek et al. (2012), these types are also described as Dirichlet, Neumann and Cauchy boundary types. In contrast to that, the system-dependent boundary types are directly influenced by external conditions and the resulting flow regime and soil moisture conditions inside the modeling domain and could be for example atmospheric flux or seepage face. Regarding solute transport, according to Simunek et al. (2012) in HYDRUS two different boundary types are specified which are defined as Dirichlet- and Cauchy-type.

In the following, the used boundary conditions to numerically describe water flow (and simplified solute transport) within both studies (Northern Altmark and Müncheberg) are described. Furthermore, the calculation approaches for the respective boundary values are summarized.

NWGL and field trial

For the NWGL, field BW and the combined field BW-GW-models, the **atmospheric flux** characterized the upper boundary condition for flow modeling. The potential atmospheric flux across the upper boundary is expressed by the following equation according to Simunek et al. (2012):

$$\left| K\left(K_{ij}^{A} \frac{\partial h}{\partial x_j} + K_{iz}^{A} \right) n_i \right| \le E \tag{18}$$

$$h_A \le h \le h_S$$

Where E is the maximum rate of potential evaporation or infiltration (m d^{-1}), h is the pressure head at the soil surface (m), and h_a and h_s are minimum and maximum allowed pressure head at the soil surface under the prevailing conditions.

When maximum infiltration rate E is exceeded, surface runoff is calculated within HYDRUS.

In general, atmospheric flux is defined as the difference of stand precipitation and potential evaporation, whereas potential transpiration is used to define root water uptake. The potential evapotranspiration ETp was calculated with the crop-coefficient k_c, listed in Table

2.6 (Dommermuth and Trampf, 1991; DVWK, 1996) and reference-evapotranspiration ET_0 according to Allen et al. (1998):

$$ETp = k_c \bullet ET_0, \text{ with } ET_0 = \frac{0.408 \times \Delta(Rn - G) + \gamma \times \frac{900}{T + 273} \times u_2 \times (e_s - e_a)}{\Delta + \gamma \times (1 + 0.34 \times u_2)} \tag{19}$$

Where Rn is the net-radiation (MJ m^{-2} d^{-1}), G is the soil heat flux (MJ m^{-2} d^{-}), Δ the slope of saturation vapor pressure curve (kPa °C^{-1}), e_s the saturation vapor pressure (kPa), e_a the actual vapor pressure (kPa); u_2 wind velocity in a height of 2 m (m s^{-1}) and γ the psycrometric constant (kPa/°C).

Table 2.6: k_c-values for maize (M) and winter wheat (WW) according to DVWK (1996) and Dommermuth & Trampf (1991) to calculate the respective potential evapotranspiration.

	Jan.	Feb.	Mar.	Apr.	May	Jun.	Jul.	Aug.	Sep.	Oct.	Nov.	Dec.
M	0.65	0.65	0.6	0.45	0.6	0.9	1	1.05	1.05	0.8	0.65	0.65
WW	0.65	0.65	0.9	1.0	1.15	1.45	1.40	0.65	0.65	0.7	0.65	0.65

The specific parameters to calculate ETp according to equation (19) were registered at the weather station of the UFZ in Falkenberg. Due to the biweekly monitoring of the surface cover fraction (SCF) at the NWGL, illustrated in Figure 2.7, the leaf area index (LAI) was calculated according to Simunek et al. (2013), enabling the splitting of ETp into Ep and Tp according to Ritchie (1972):

LAI=-1/a*ln(1-SCF) (20)

$$Ep = ETp \cdot \exp(-a \cdot LAI) \qquad Tp = ETp - Ep \tag{21}$$

Where a is the radiation extinction coefficient (according to Meurer et al. (2013) 0.46 for maize and 0.78 for wheat).

According to von Hoyningen-Hüne (1983) interception was calculated:

$$I = LAI \times b\left(1 - \frac{1}{1 + (SCF * P /(b * LAI))}\right) \tag{22}$$

Where b is the plant specific interception constant (b = 0.5 mm d^{-1} Leterme and Mallants (2011))

As a result, the registered precipitation P_{NWGL} was reduced to the real stand specific precipitation P_{stand} via considering interception by the plants.

The lower boundary of the NWGL were described by a ***seepage face*** boundary as well as the tile drains of the fields in 80 cm depth:

$$q_o(x,z,t) = 0 \text{ for } h(x,z,t) < 0 \text{ at } (x,z)\varepsilon\Gamma_S \tag{23}$$

$$h_o(x,z,t) = 0 \quad \text{for } h(x,z,t) \geq 0 \quad \text{at } (x,z)\varepsilon\Gamma_S \tag{24}$$

Where Γ_s is the segment of the seepage face boundary-type. A seepage face describes that water is discharged out of the modeling domain, when this part of the area is saturated.

The left and right borders of the fields as well as the lower boundary of field BW were described by **no flux boundaries**, which belong to the system-independent boundary conditions, being a Neumann boundary type specified flux:

$$\left| K\left(K_{ij}^A \frac{\partial h}{\partial x_j} + K_{iz}^A \right) n_i \right| \leq E = -\left[K\left(K_{ij}^A \frac{\partial h}{\partial x_j} + K_{iz}^A \right) \right] n_i = \sigma_1(x,z,t) \text{for}$$
$$(x,z) \in \Gamma_N \tag{25}$$

Where Γ_N is the segment of the Neumann boundary-type, σ_1 is a function of x, z and t, n_i are the components of the outward unit vector normal to Γ_N.

The lower boundary of field GW was characterized as a **specified head** because at this site, the measured groundwater head was implemented.

$$h(x,z,t) = \omega(x,z,t), \tag{26}$$

Where ψ is a function of x, z, t, and h is the pressure head (m of water, 1 m = 10 kPa registered tension, negative values-unsaturated, positive-saturated, zero- groundwater head).

Regarding solute transport a **Cauchy type boundary** was used, which can be explained as:

$$-\theta D_{ij} \frac{\partial c}{\partial x_i} n_i + q_i n_i c = q_i n_i c_0 \quad \text{for } (x,z)\varepsilon\Gamma_C \tag{27}$$

Where q_i and n_i represents the outward fluid flux, n_i is the outward unit normal vector, c_o is the concentration of the incoming fluid, and Γ_c is the segment of the Cauchy boundary-type.

GL and TL

For the GL- and the TL-models again the **atmospheric flux** was used as an upper boundary, whereby potential evapotranspiration ETp was calculated according to Allen et al. (1998) from the measured meteorological data of the weather station in Müncheberg. ETp was splitted into Ep and Tp according to Ritchie (1972) and equation (21). For the clipped grass, leaf area index LAI according to Simunek at al. (2008) and Sutanto et al. (2012) was calculated:

LAI =0.24*h$_{grass}$, (28)

Where h$_{grass}$ is the height of the grass (10 cm).

To assume only gravitational flow, a **seepage face** was used as a lower boundary. For the tension controlled water flow the controlled, measured tension was implemented as a **variable head** according to equation (26).

2.3.3 Model setups

2.3.3.1 From lysimeter to field scale – NWGL and field BW-model

As already stated, the pedo-hydrological conditions of the NWGL are comparable to field BW. As a first step, it was proven if the NWGL measurements could predict the flow regime of field BW. The numerical simulations for both models were carried out for three HY from November/1/2012 until October/31/2015. The NWGL were described 1D-vertical (depth=1.25 m) via implementing 125 evenly distributed nodes. Three different material layers according to Table 2.1 or Figure 2.10 were assigned. The modeling domain describing the field was characterized as a rectangle (2D) with a length of 20 m and a depth of 1.25 m (Figure 2.10).
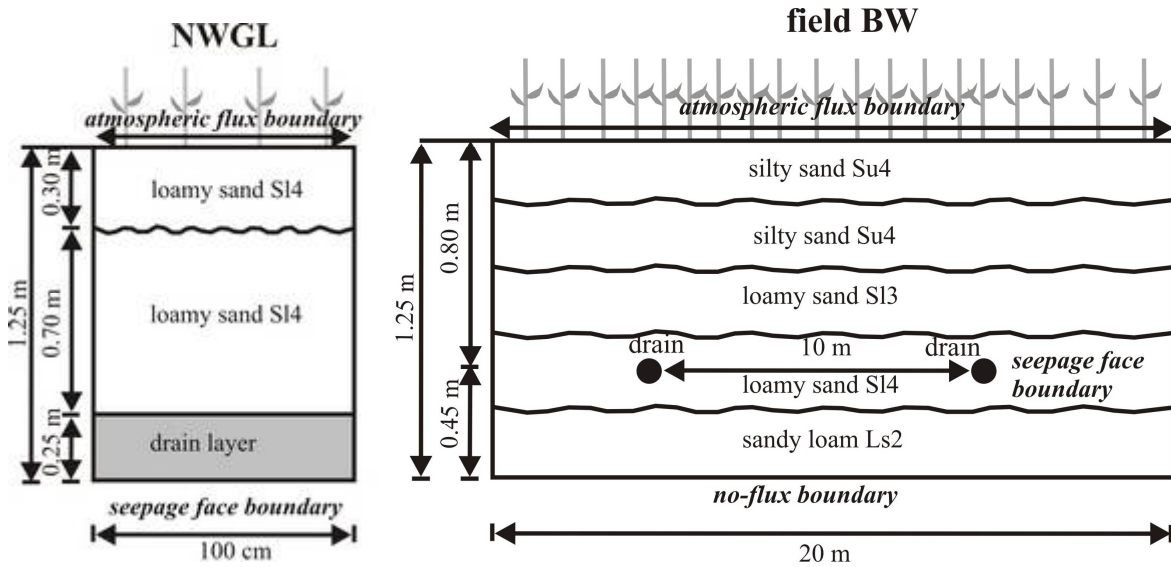
Figure 2.10: Setup for the NWGL-model and the field BW-model.

For spatial discretization, a finite-element (FE)-mesh was used with a general mesh size of 0.1 m and a mesh refinement at the drainages. Five different material layers according to Table 2.2 and Figure 2.10 were assigned. The drainages were implemented as openings in 0.8 m depth and described as seepages faces, corresponding to the lower boundary of the NWGL. The upper boundary, characterized as an atmospheric flux and root water uptake, was equal in both models. As initial condition for the field model a uniform pressure gradient (-1.35 m at the top and -0.1 m at the bottom) was used. For the NWGL model, measured soil moisture of neighboring lysimeters at the lysimeter station, which were equipped

with specific probes, was defined as an initial condition. At the top θ was 0.18 m³ m⁻³, decreasing uniformly to 0.11 m³ m⁻³ from 0.00 m to 1.00 m depth. The initial θ at the top of the filter layer was 0.10 m³ m⁻³, increasing uniformly to 0.15 m³ m⁻³ to 1.25 m depth. The initial unsaturated soil hydraulic properties were calculated with the HYDRUS- integrated Rosetta-Module (Schaap et al., 2001; Simunek et al., 2008). Measured grain size distribution, bulk density and water content at pF 2.5 and 4.2 are used as input values to describe the initial van Genuchten-parameters in HYDRUS. During calibration, saturated hydraulic conductivity (K_s) as well as residual (θ_r) and saturated water content (θ_s) were determined inversely from the initial parameters. Therefore, daily outflow rates from December 2013 until March 2014 measured at the NWGL and the field were used to calibrate these parameters. For determining upper and lower limits for θr, θs and K_s during the calibration process, maximum and minimum registered soil moisture of the hydrological measuring stations, as well as laboratory determined values were implemented (cf. Table 2.2). For model validation monthly outflow rates for the whole observation period were compared.

2.3.3.2 The impact of soil heterogeneity – Combined BW-GW-model

To determine the impact of soil heterogeneity, according to Figure 2.5 both fields were combined within one model. Thus, surface runoff and lateral interactions of field GW and BW could be taken into account because no watershed could be reproduced. Because soil tillage and crop rotation between field BW and GW was adjusted from HY 2014, in contrast to the NWGL and field BW-simulations, the modeling period for the combined model covered only two HY (2014 and 2015).

The modeling domain was characterized by a rectangle with a length of 40 m, combining field BW and GW. The left site had a depth of 1.50 m, decreasing to 1.25 m at the right site (cf. Figure 2.5). The domain was discretizised with a finite element (FE-) mesh (FE-size = 0.1 m; refinement at drains). The drain pipes (four) were again implemented as openings and described as seepage faces. The boundary conditions are illustrated in Figure 2.5. Atmospheric flux was the same as in the NWGL and the separate field BW-model to examine if the NWGL measurements could be used to simulate the flow regime of field GW although different pedo-hydrological conditions were observed. Because the subsurface of field BW is nearly impermeable, a no-flux-boundary was used whereas field GW was described by a variable groundwater head (measured with a biweekly rhythm). Six different material layers according to Figure 2.5 were implemented. The initial water retention properties according to Van Genuchten (1980) were calculated from measured grain size distri-

bution, bulk density and water content at pF 2.5 and 4.2 (summarized in Table 2.2 – Combined model) with the HYDRUS Rosetta-Module (Schaap et al., 2001; Simunek et al., 2008).

Calibration was performed from May 2014 (beginning of soil moisture registration) until September 2015 (from September-soil moisture probes were defect). For the calibration process, daily measured soil moisture data in 35, 60 and 85 cm were compared to modelled data in the same depth via implementing observation notes. During calibration, residual and saturated water content were adjusted according to minima and maxima recorded soil moisture values in the field. As initial condition a uniform hydraulic gradient was assumed (top: -1.1 m; bottom: 0.15 m). The model was validated via comparing real and modelled monthly drain rates for both HY.

2.3.3.3 The impact of the lower boundary condition – TL-and GL-model

Both, TL and GL were modelled separately with a seepage face as well as a controlled lower boundary. For the tension control on the one hand the measured tension of the surrounding soil ("tension soil") was implemented and on the other hand the tension that was registered inside the TL after pressure head regulation ("tension TL") was used. The model setups are illustrated in Figure 2.11.
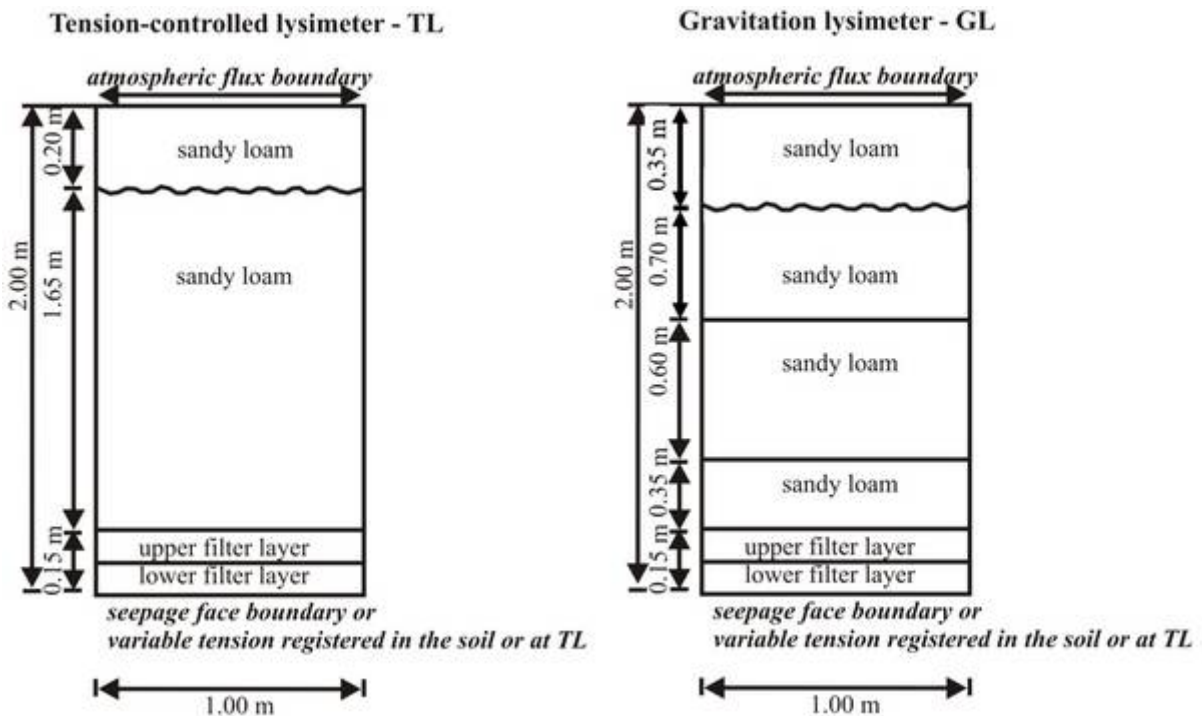
Figure 2.11: Setup of the TL-model and the GL-model.

For the seepage face models, the modeling domain was described by a rectangle with a length of one meter and a depth of two meters. They were discretizised by a finite element (FE) mesh (horizontal discretization 20, vertical discretization 100) with a mesh refinement at the lower boundary. For the tension-controlled approach, the filter layer was excluded whereas the depth of these models was 1.85 m, only consisting of the soil layer. The soil layer of the TL was divided into two sub layers (top soil from 0-0.2 m depth; lower soil from 0.2 - 1.85 m depth). At the GL, despite the top soil layer from 0-0.35 m depth, an additional layer from 0.90 to 1.50 m was implemented in the lower soil layer (0.35-1.85 m depth). The reason for this was the observed inhomogeneous compaction during lysimeter filling, whereas bulk density in this depth is smaller as compared to the density of the material above and below (cf. Table 2.5).

The filter layer was splitted into two sub-layers (filter layer 1 from 1.85 to 1.95 m; filter layer 2 from 1.95 to 2.00 m) for the modeling process. According to laboratory results (listed in Table 2.5) the unsaturated soil hydraulic properties of the TL and the GL were not the same but they were comparable. The values in Table 2.5 were again used to determine initial van Genuchten-parameters for the current models with the HYDRUS Rosetta-Module (Schaap et al., 2001; Simunek et al., 2008). For inversely calibrating these initial values, the registered soil moisture in 10 cm, 50 cm, 100 cm and 150 cm and the registered tension in 175 cm depth from June/15/2014 until September/30/2014 were used. The models were validated from June/15/2014 until October/31/2015 via comparing daily outflow rates.

2.3.4 Goodness of fit criteria

To validate the comparability of measured data series and to describe the calibration quality and model performance of the simulations, regression analyses were performed and examined for specific quality and efficiency criteria, which are already discussed in detail (Legates and McCabe, 1999; Krause et al., 2005; Harmel and Smith, 2007; Moriasi et al., 2007; Ritter and Munoz-Carpena, 2013). Definitions of the various error and efficiency criteria and the used symbols are: NSE – Nash-Sutcliffe efficiency; RMSE – Root mean square error; SD - standard deviation, n_t – times that SD is greater than RMSE. O_i – observed (measured) data; P_i – predicted (modelled) data; $\overline{O}$ – mean of all observed data; $\overline{P}$ – mean of all predicted data

$$RMSE = \sqrt{n^{-1} \sum_{i=1}^{n} (O_i - P_i)^2} \tag{29}$$

$$NSE = 1.0 - \frac{\sum\limits_{i=1}^{n}(O_i - P_i)^2}{\sum\limits_{i=1}^{n}(O_i - \overline{O})^2} = 1 - \left(\frac{RMSE}{SD}\right)^2 \tag{30}$$

NSE is an efficiency criteria that ranges between 1.0 (best fit) to -∞.

$$n_t = \frac{SD}{RMSE} - 1 \tag{31}$$

According to Ritter and Munoz-Carpena (2013), n_t represents the times that spread of observations (SD) is greater than the mean error between both data series. The higher n_t, the better the fit between the data. According to Ritter and Munoz-Carpena (2013) the significance of the relationship between to data series as well as the model performance could be classified as "very good" for NSE > 0.9 and n_t > 2.2, "good" for NSE of 0.8 to 0.9 and n_t of 1.2 to 2.2, "acceptable" for NSE of 0.65 to 0.80 and n_t 0.7 to 1.2 and "unsatisfactory" for NSE < 0.65 and n_t < 0.7.

The correlation coefficient R between two data series is defined as:

$$R = \sqrt{\left(\frac{\sum\limits_{i=1}^{n}(O_i - \overline{O})(P_i - \overline{P})}{\sqrt{\sum\limits_{i=1}^{n}(O_i - \overline{O})^2}\sqrt{\sum\limits_{i=1}^{n}(P_i - \overline{P})^2}}\right)^2} \tag{32}$$

R which was calculated during regression analyses should lie in the range of 0.8 to 1, whereas the gradient of the regression line should tend to 1.0.

3. __Results__

3.1 The transferability from lysimeter to field scale

3.1.1 Measured water balances of the NWGL and the backwater-influenced field BW

Within the conducted study in the northern Altmark region, the comparability of the water balances between NWGL and field BW was examined. A water balance is characterized by the difference of precipitation and outflow. As illustrated in Figure 2.6 a) and the following Figure 3.1 a), registered monthly precipitation at the NWGL and the field trial was not the same, but it was comparable. Furthermore, also the measured monthly outflow from NWGL and field BW showed a similar trend (Figure 3.1 a, b).
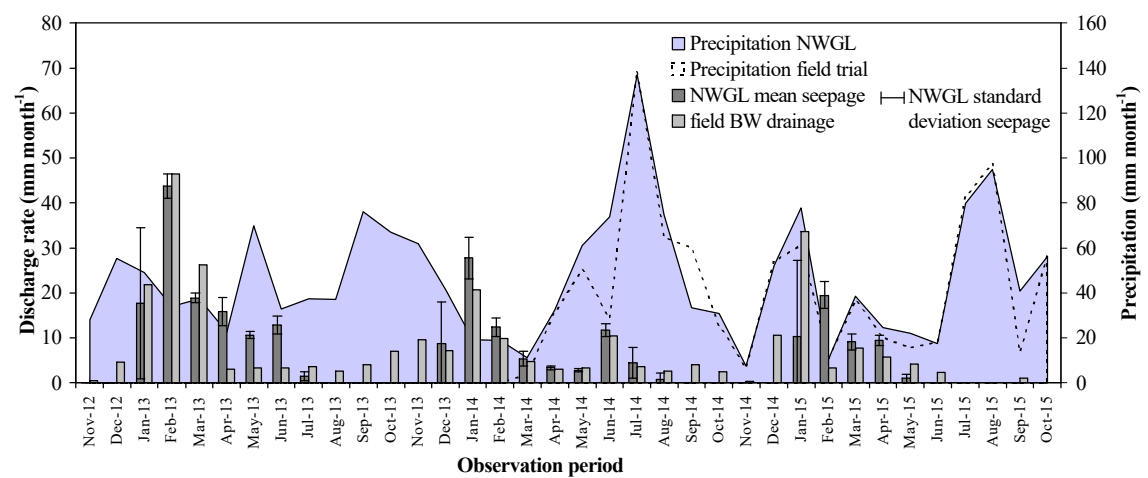
a
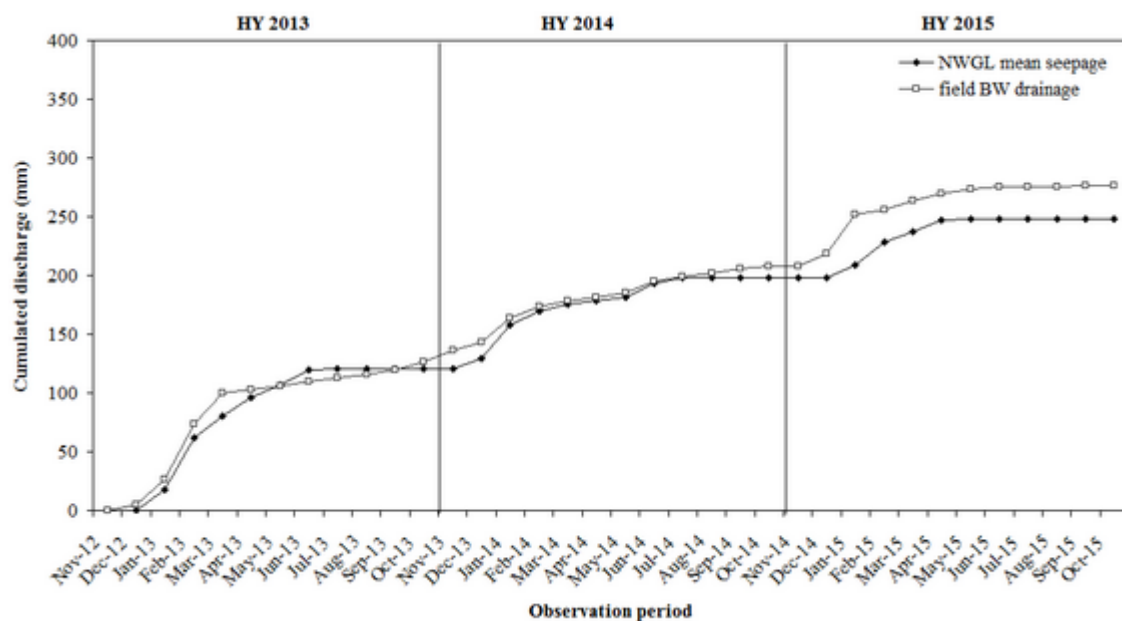
b
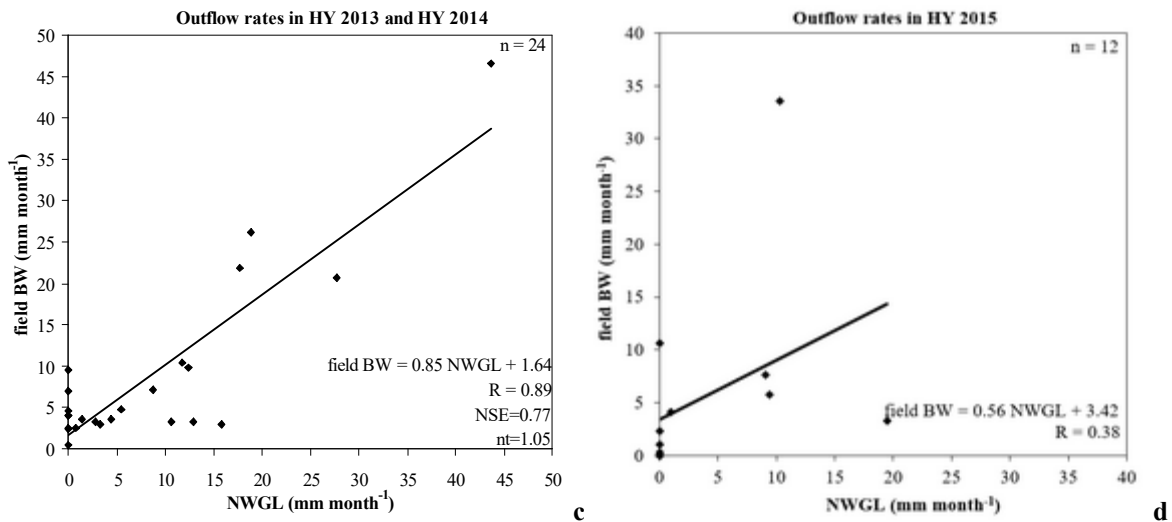
Figure 3.1: a) Measured monthly outflow rates of the NWGL (mean seepage of three NWGL and standard deviation SD) and the drained field BW as compared to registered precipitation; b) Cumulated outflow from the NWGL and the drained field BW for the hydrological years HY 2013, 2014 and 2015; c) Regression analyses between measured monthly outflow rates of NWGL and field BW for HY 2013 and HY 2014; d) Regression analyses between measured monthly outflow rates of NWGL and field BW for HY 2015.

In general, maximum discharge rates at both sites were registered during hydrological winter in the vegetation free period. In HY 2013 in January (NWGL/ field BW: 17.7/ 21.8 mm month^{-1}), February (NWGL/ field BW: 43.7/ 46.6 mm month^{-1}) and March (NWGL/ field BW: 18.8/ 26.2 mm month^{-1}) and in HY 2014 in January (NWGL/ field BW: 28.7/ 20.7 mm month^{-1}) and February (NWGL/ field BW: 12.4/ 9.9 mm month^{-1}). A very significant aspect illustrated in Figure 3.1 a) is the huge amount of precipitation in the hydrological summer 2014 (June, July and August). Mainly in July 2014, at the NWGL 137 mm and at the field trial 138.8 mm rainfall were measured, whereby no significant outflow could be registered at both sites. Thus, in July 2014 outflow was 4.5 mm at the NWGL, 3.6 mm at field BW, and in August 2014 0.8 mm from the NWGL and 2.6 mm from field BW.

In HY 2015, during hydrological winter the deviations in maximum discharge rates between both sites were relatively high with 10.3 mm month^{-1} (NWGL) compared to 33.6 mm month^{-1} (field BW) in January, and 19.3 mm month^{-1} (NWGL) compared to 3.3 mm month^{-1} (field BW) in February.

Furthermore, the NWGL generally fell dry during and after vegetation periods from August to November 2013, September to December 2014 and June to October 2015. In contrast to that water was still discharged from field BW, although the amounts were relatively small as compared to the discharged amount of water during hydrological winters (cf. Fig-

ure 3.1 a). When the NWGL began to discharge water after drying up, the amount of monthly water discharged from the three NWGL differed significantly, revealing a huge standard deviation in these months (cf. Figure 3.1 a). But comparing mean cumulated outflow of the three NWGL and field BW clarified, that the measured discharge on both scales was comparable for HY 2013 and 2014, revealing a mean total outflow in HY 2013 of 121.0 mm from the NWGL and 126.5 mm from the field BW, and in HY 2014 77.4 mm from the NWGL and 81.4 mm from the arable site (Figure 3.1 b). The results of further regression analyses between measured monthly outflow rates of NWGL and field BW for these two HY revealed NSE of 0.77 and n_t of 1.05.

According to the quality criteria of Ritter and Munoz-Carpena (2013) both data series correlate with each other (Figure 3.1 c). In HY 2015 total outflow from the NWGL (49.2 mm) is reduced by 19.5 mm as compared to the outflow of field BW (68.7 mm). Furthermore, the comparison of monthly discharge rates did not show any correlation between NWGL- and field- data series in this year (Figure 3.1 d). In the hydrological winter (HHY 5 11/1/2014 – 4/30/2015), the discharged amount of water from the NWGL (48.2 mm) showed a deficit of 13.0 mm as compared to the drain flow of field BW (61.2 mm), whereas the discharge rates of both testing sites were comparable in the hydrological winters of HY 2013 and 2014 (NWGL/ field: 96.0 / 102.7 mm in HHY 1; 57.7/ 55.0 mm in HHY 3).

3.1.2 Simulated water balances of the NWGL and the backwater-influenced field BW

3.1.2.1 Calibration results and upper boundary for validation

Within the calibration period from December 2013 until March 2014, the best fit between measured and modelled outflow rates from NWGL and field BW (NWGL: NSE=0.75, n_t=0.98; field BW: NSE=0.71, n_t=0.87) was achieved by the calibrated van Genuchten parameters, listed in Table 3.1.

Table 3.1: Calibrated van Genuchten-model for the NWGL filling material and the field BW soil, based on initial residual/ saturated water content and hydraulic conductivity as well as the respective upper and lower limits in brackets.

NWGL						
z in m	θr ($m^3\ m^{-3}$) *	θs ($m^3\ m^{-3}$) *	α (1 m^{-1})	n (-)	Ks (m d^{-1}) *	l (-)
0.00-0.31	0.04 (0.03+/-0.02)	0.40 (0.39+/-0.02)	3.15	1.54	0.70 (0.75+/-0.3)	0.50
0.31-1.00	0.04 (0.02+/-0.02)	0.32 (0.30+/-0.02)	5.26	1.42	0.55 (0.25+/-0.3)	0.50
1.01-1.25	0.04	0.31	14.50	2.68	6.00	0.50

Field BW soil						
z in m	θr (m³ m⁻³) *	θs (m³ m⁻³) *	α (1 m⁻¹)	n (-)	Ks (m d⁻¹) *	l (-)
0.00-0.25	0.07 (0.02+/-0.05)	0.29 (0.32+/-0.05)	1.20	1.39	0.85 (0.55+/-0.3)	0.50
0.25-0.55	0.02 (0.03+/-0.05)	0.40 (0.31+/-0.05)	2.00	1.30	0.20 (0.20+/-0.05)	0.50
0.55-0.75	0.01 (0.04+/-0.05)	0.40 (0.35+/-0.05)	2.80	1.20	0.20 (0.1+/-0.1)	0.50
0.75-1.00	0.01 (0.06+/-0.05)	0.33 (0.31+/-0.05)	4.30	1.60	0.10 (0.05+/-0.05)	0.50
1.00-1.25	0.05 (0.05+/-0.05)	0.40 (0.36+/-0.05)	2.60	1.33	0.03 (0.04+/-0.01)	0.50

z-depth; θr-residual water content (in brackets initial θr and upper and lower limit); θs-saturated water content (in brackets initial θs and upper and lower limit); α, m, n -parameters in the soil water retention function with m=1-1/n; Ks-saturated hydraulic conductivity (in brackets initial Ks and upper and lower limit); l-tortuosity parameter in the conductivity function; * calibrated values.

These values based on the initial parameters and their specific upper and lower limits, also summarized in Table 3.1. Within the calibration period for both, minima and maxima daily discharge rates were reproduced (Figure 3.2 a, b).
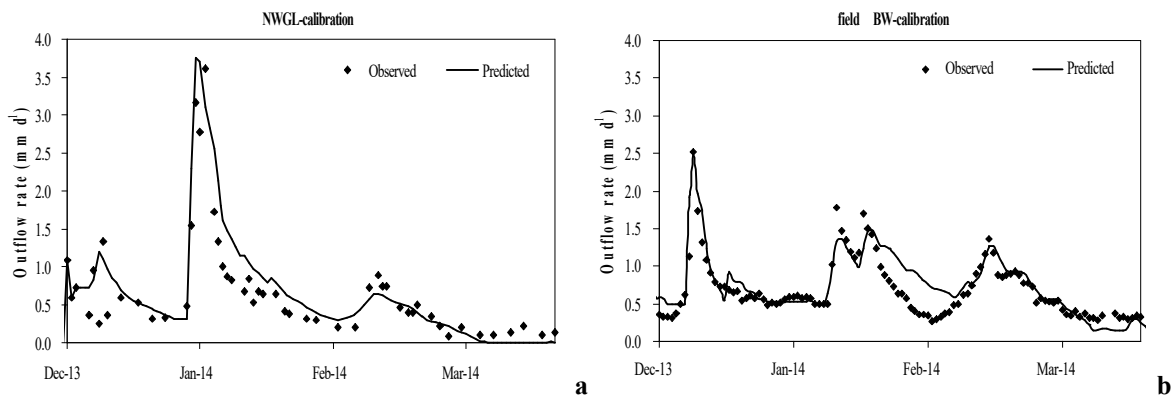
Figure 3.2: Observed and predicted daily outflow rates for a) NWGL and b) field BW for the calibration period from December 2013 until March 2014.

For the whole modeling period from November/1/2012 until October/31/2015, actual atmospheric flux, being equal in both models, (P_{Stand} - surface runoff - Ep) was 913.8 mm, whereas a total root water uptake (RWU) of 627.0 mm was calculated. RWU was determined from the potential transpiration rate. Thus, RWU directly depends on LAI. Maximum LAI for maize was reached in June 2013 and 2014 (LAI =4.9 in HY 2013 and HY 2014), for wheat in May 2015 (LAI = 5.2). Regarding the whole observation period, the difference of actual atmospheric flux and RWU was 286.8 mm. In comparison to that, cu-

mulated measured outflow from field BW was 276.6 mm, and 247.7 mm from the NWGL (Figure 3.3).
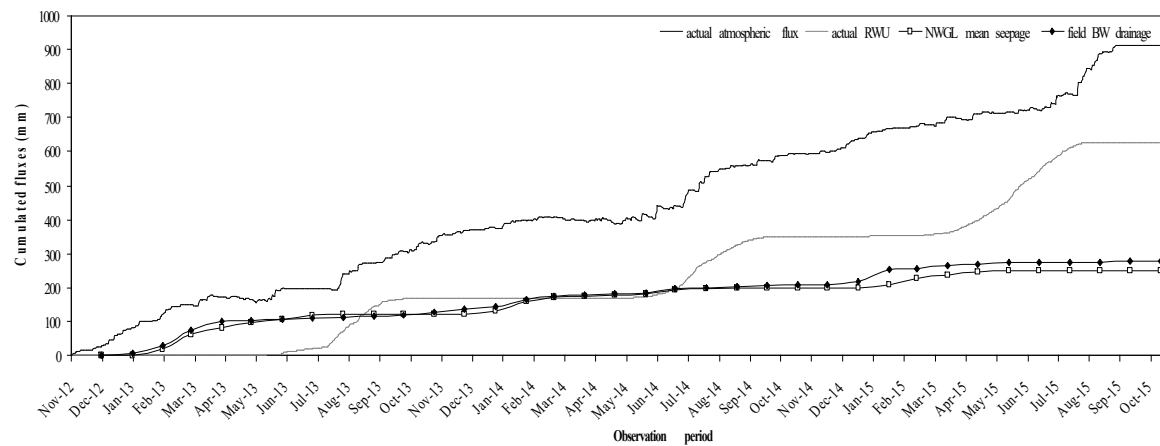
Figure 3.3: Cumulated simulated actual atmospheric flux and root water uptake (RWU) for model validation, compared to cumulated measured mean outflow of the lysimeters (NWGL) and the drained field BW.

3.1.2.2 NWGL-model

The numerical simulations describing the water balance of the investigated NWGL could only reproduce monthly measured outflow rates of the NWGL for the first two HY, but not for the third one (NWGL measured/ modelled: 121.0 / 118.0 mm in HY 2013; 77.4/ 85.9 mm in HY 2014; 49.2 / 89.0 mm in HY 2015) (Figure 3.4 a).
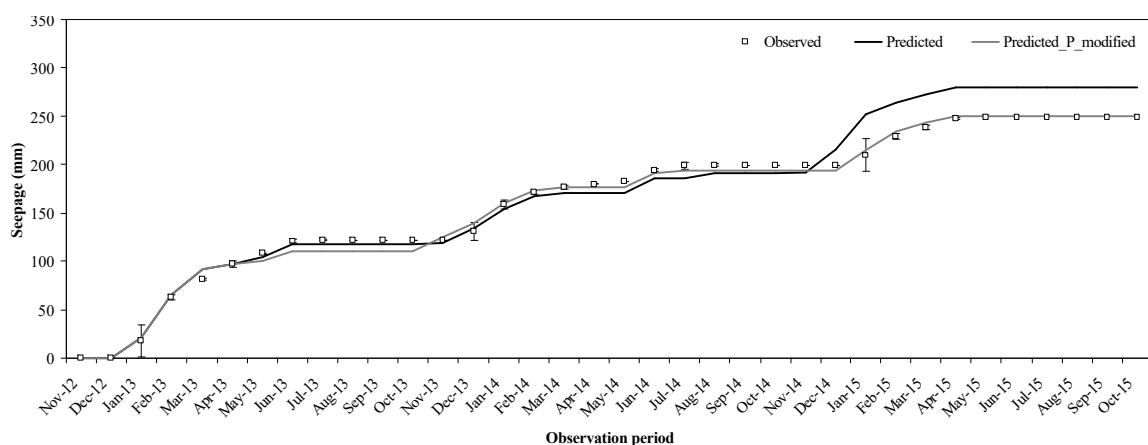
a
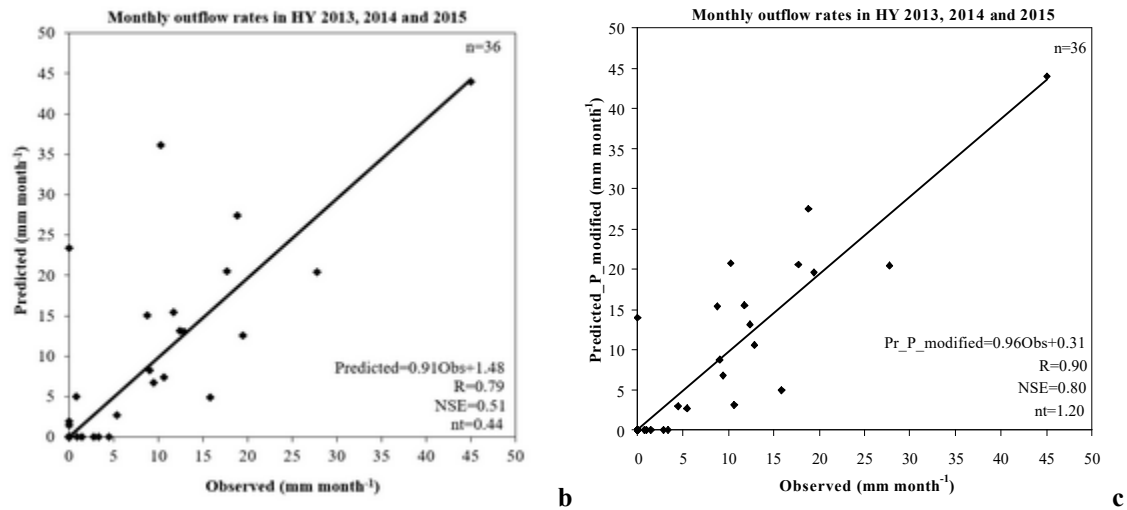
Figure 3.4: a) Cumulated outflow measured (Observed), simulated with the same atmospheric flux as in the field BW-model (Predicted) and simulated excluding heavy rain events in July and August 2014 (Predicted_P_modified); Regression analysis of observed and predicted monthly outflow rates, calculated with b) P and c) $P_{modified}$.

In contrast to the measured outflow for the whole observation period, which was 247.7 mm, the NWGL-model over predicted the amount of discharged water by 38.5 mm. Correlation analyses between measured and modelled monthly outflow rates for HY 2013 and 2014 revealed a gradient of the regression line of 0.95 and R of 0.90, NSE of 0.77 and n_t of 1.09, validating the model performance. But there was no correlation between measured and simulated monthly outflow rates for HY 2015.

3.1.2.3 Field BW-model
Comparing observed and predicted monthly outflow rates for each HY verified the high quality of the field BW-model with the implemented input parameters, derived from the NWGL (Figure 3.5 a).
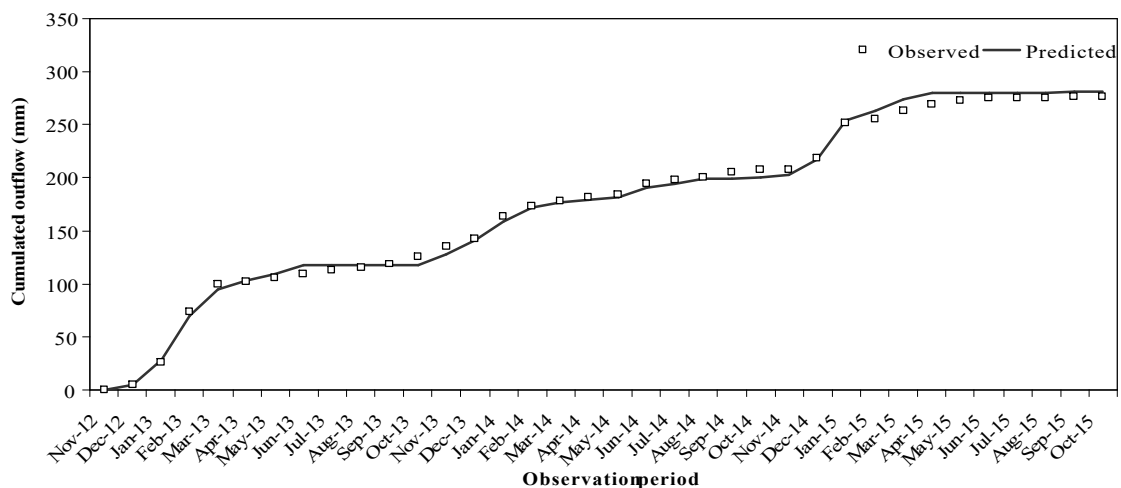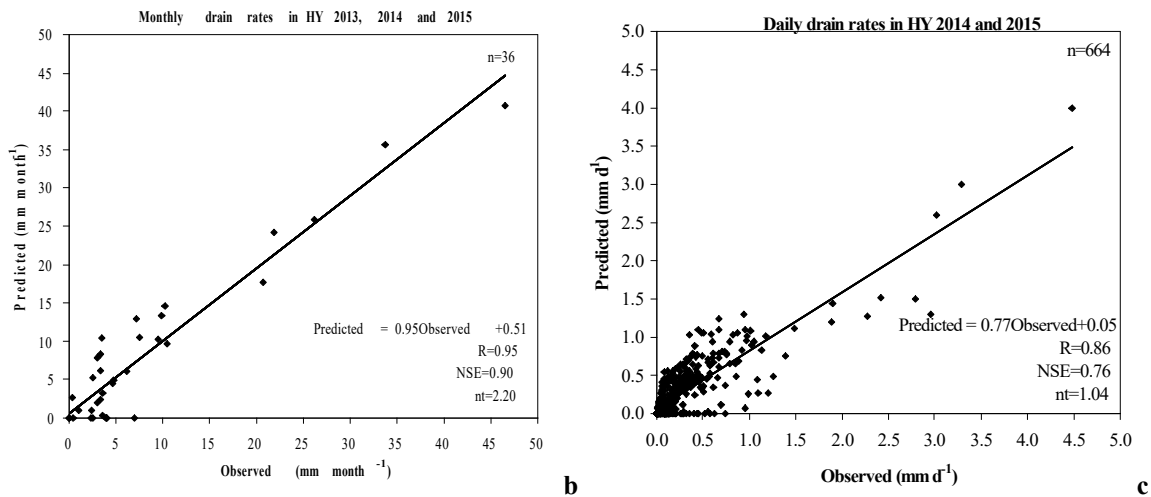
Figure 3.5: a) Cumulated observed and predicted drain flow from field BW for HY 2013, 2014 and 2015; Regression analyses between b) monthly observed and predicted drain rates in HY 2013, 2014 and 2015; c) daily observed and predicted drain rates in HY 2014 and 2015.

The registered total discharge from field BW (276.6 mm) was simulated adequately by the field BW-model with 276.5 mm (Figure 3.5 a). The simulations represented the registered amount of discharged water not only for the HY 2013 and 2014, but also for the HY 2015 (field measured/ modelled: 126.5/ 117.8 mm in HY 2013; 81.4/ 82.5 mm in HY 2014; 68.7 / 76.2 mm in HY 2015). Regression analyses between monthly measured and modelled outflow rates for three HY revealed an R of 0.95, NSE of 0.90 and n_t of 2.20. The gradient of the regression line clarified, with 0.95, the nearly perfect fit between modelled and measured values (Figure 3.5 b). With NSE of 0.76 and n_t of 1.04, the model performance describing daily values was also validated. But the gradient of the regression line was only 0.77, implying a higher uncertainty between modelled and measured daily drain rates (Figure 3.5 c). Comparing simulated and observed soil moisture in 35, 60 and 85 cm depth from May/16/2014 until October/31/2015, illustrated in Figure 3.6 a, b, c, revealed a correlation coefficient R of 0.90 respectively between the data series for each depth.
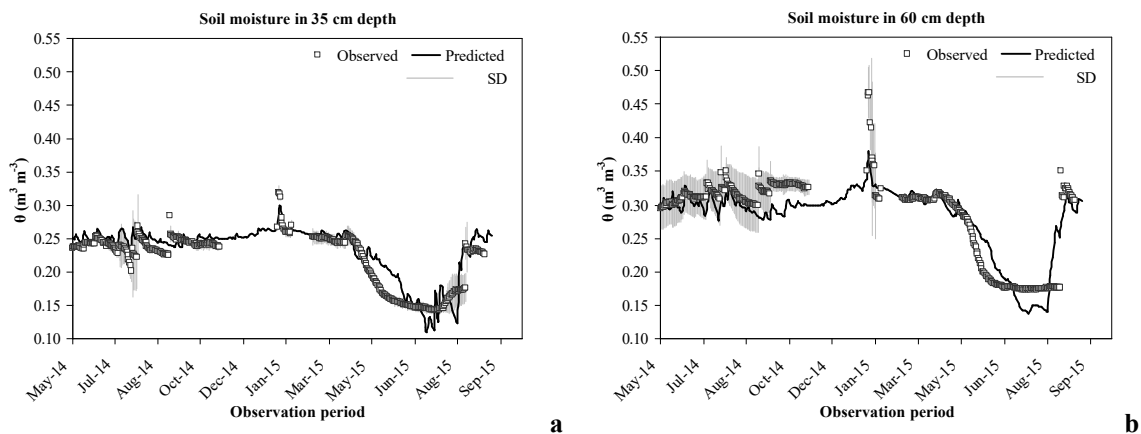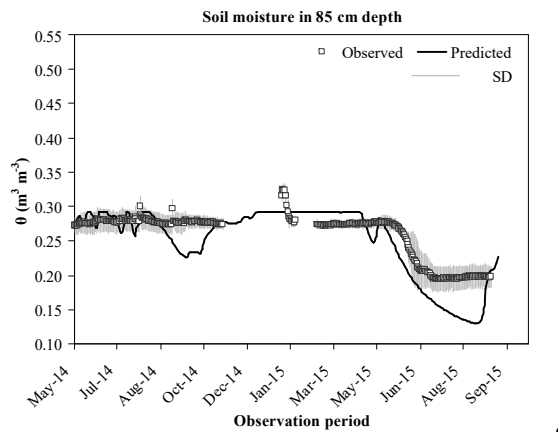
Figure 3.6: Observed (registered mean value of two TDR-probes at each horizon and standard deviation SD) and predicted soil moisture at the field BW soil in a) 35 cm; b) 60 cm, and c) 85 cm depth.

A gradient of the regression line of 0.92 (35 cm depth), 0.82 (60 cm depth) and 1.3 (85 cm depth) could be calculated. Note that measured soil moisture obtained data gaps from November/4/2014 to January /11/2015 and September/15/2015 to October/31/2015 due to a defect data logger. Furthermore, from January/27/2015 to February/26/2015, no soil moisture could be registered by the implemented probes because of ground frost. NSE and n_t in 35 and 60 cm depth (NSE/n_t: 0.80/1.25 in 35 cm; 0.65/ 0.74 in 60 cm) revealed, that the model represents measured soil moisture, whereas these criteria were failed for 85 cm depth (NSE=0.63 and n_t = 0.65). But it should be summarized, that the simulations described the water balance of the investigated field BW adequately, although the parameters for the upper boundary were only determined at NWGL.

3.1.3 Evaluating deviating measured and modelled outflow rates at both scales

Measured and modelled results showed that there was an impact on the NWGL water balance, leading to a deficit as compared to field BW. This impact could not be reproduced for the field site. In the HY 2013 and 2014 not only measured discharge rates of the NWGL and field BW correlated with each other, but also the simulations described the observed discharge behavior of both. But in the HY 2015, the NWGL-model could only reproduce measured outflow for field BW, but not for the NWGL. This was not reproducible because all input parameters for modeling were determined at the NWGL. Various parameters could cause deviations between both sites. To examine the influence of different unsaturated soil hydraulic properties on deviating measured outflow rates in the HY 2015, the calibrated material layers one and two of the NWGL-model from 0 to 30 cm and 31 to 100 cm depth (cf. Table 3.1) were directly transferred to the field BW-model. The calcula-

tions revealed, that measured field BW outflow in the HY 2013 and 2014 was again simulated adequately, whereby modelled outflow in the HY 2015 was too high as compared to measured discharge (measured/ modelled field with NWGL-van Genuchten-parameters: 126.5 / 128.1 mm in HY 2014; 81.4 / 77.1 mm in HY 2014; 68.7/ 87.4 mm in HY 2015). As a result, differences in soil hydraulic properties led of course to deviating flow rates between both scales. But this does not explain lower outflow rates registered at the NWGL in HY 2015. As a next step, deviations between P_{NWGL} and P_{field} as an influencing parameter were assumed. But in HHY 4, the hydrological summer of HY 2014, P_{NWGL} showed a surplus of 43 mm compared to P_{field}, and a surplus of 20 mm in HY 2015 (cf. Figure 2.6 a). Higher outflow rates at the field could not be justified via comparing registered precipitation because P_{field} was smaller as compared to P_{NWGL}. For the whole observation period, there was one significant difference between the three HY, which was also remarkable in Figure 3.1 a). In July and August 2014, registered P_{NWGL} showed a surplus of 79.8 mm and 23.9 mm compared to P_{long}. A detailed evaluation of precipitation data, registered in a ten-minute-interval at the UFZ – station in Falkenberg, revealed that there were heavy rain events at July/24/2014, July/30/2014 and August/4/2014 (Figure 3.7 a, b, c).
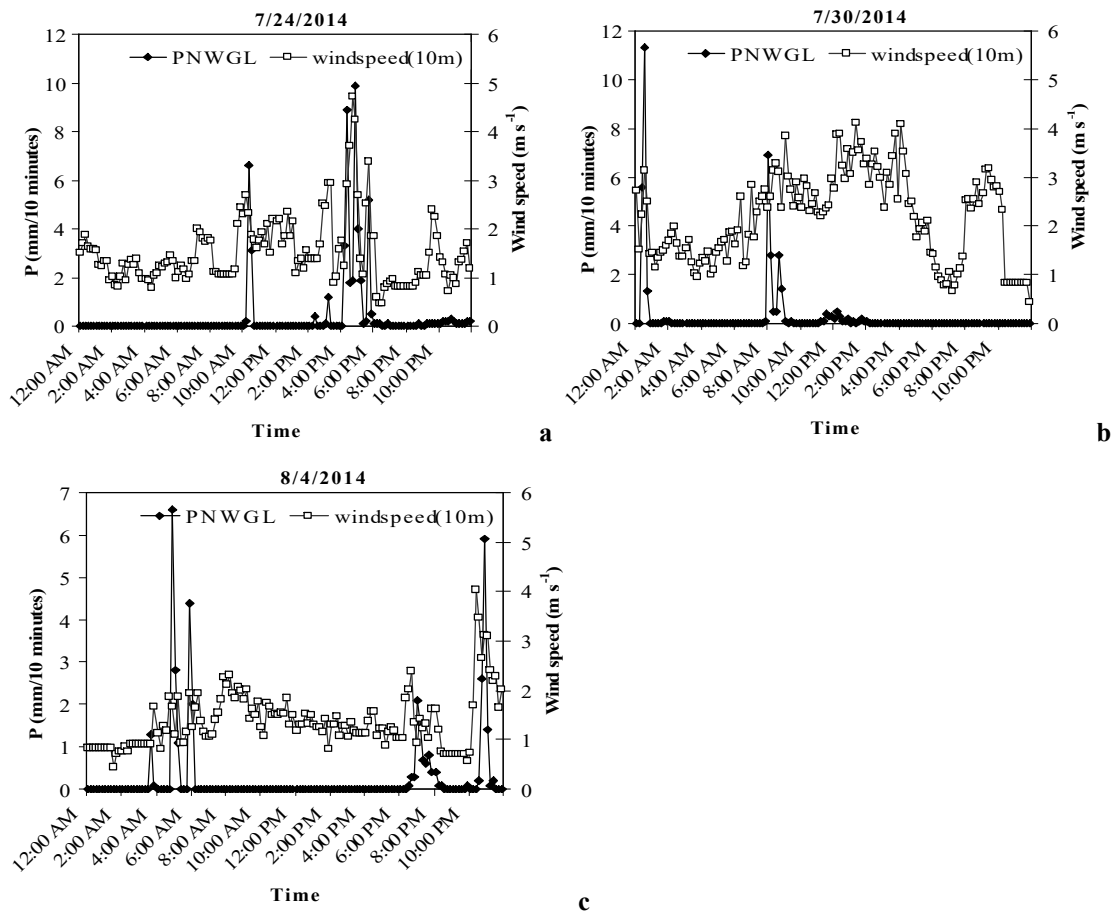
Figure 3.7: Heavy rain in combination with wind, registered in a) and b) July; and c) in August 2015 at Falkenberg.

Especially at the two events in July, it rained more than 10 mm in 10 minutes. P_{stand} for the specific rain events, and that means registered precipitation minus calculated interception by the cultivated maize was, 50.1, 34.6, and 34.0 mm d^{-1} respectively. Furthermore, within HYDRUS, a surface runoff of 27 mm d^{-1} for July/24/2014 and 20 mm d^{-1} for July/30/2014 and August/4/2014, respectively was calculated and implemented for the NWGL- and the field BW-model. As a result, effectively (P_{stand}-surface runoff) at these three dates 23.1 mm, 14.6 mm and 14 mm d^{-1} precipitation should match the NWGL surface. But resulting from these input parameters, modelled outflow for HY 2015 only reproduced measured outflow of the field BW, but not of the NWGL It was assumable that heavy rain in combination with wind, the small surface area of the NWGL and the relatively height of the grown maize (maximum = 2.8 m) led to the fact, that the main amount of precipitation was not matching the surface area of the NWGL. The leaves of the cultivated maize protruded beyond the edge of the NWGL, whereby during heavy rain, precipitation intercepted by the plants dropped off. During these heavy rain events, especially in July, maize had maximum height and LAI. In former development stages of the crop, for example illustrated in Figure 2.7, the leaves won't protrude beyond the NWGL surface.

Thus, for further numerical simulations, P_{stand} (trial and error) was reduced at these three dates ($P_{modified}$ 3 mm d^{-1}). In contrast to the field BW-model, the atmospheric flux at the second NWGL-model was reduced by 42.7 mm, revealing 244.1 mm as a difference between actual atmospheric flux and root water uptake. Using this reduced precipitation ($P_{modified}$) as an upper boundary in the NWGL-model revealed an adequate simulation of the monthly measured discharge rates of the NWGL. With a gradient of the regression line of 0.96, R of 0.90, NSE of 0.80 and n_t of 1.20 the model performance was validated according to Ritter and Munoz-Carpena (2013) (cf. Figure 3.4 c).

Whereas $P_{modified}$ does not influence the modeling results for the HY 2013, deviations between measured and modelled outflow in 2014 and 2015 were minimized in contrast to the original NWGL-model (NWGL measured/ modelled: 77.4/ 75.4 mm in HY 2014; 49.2/ 47.7 mm in HY 2015). As a result, for three years the modified NWGL-model simulated an outflow of 241.2 mm compared to measured 247.7 mm.

3.2 The impact of soil heterogeneity on water flow and NO$_3$-N-leaching

3.2.1 Indicators for describing the chemical milieu of both fields - BW and GW

Field BW and GW differ significantly regarding their pedo-hydrological properties. It was examined, if the chemical conditions are influenced by these differences. To get an overview of the chemical milieu at each field, as a first step mean values (for the whole observation period) of the measured pH, SO$_4$ and DOC as well as of the N species NO$_2$-N, NH$_4$-N and NO$_3$-N in soil solution, drain flow and groundwater/ backwater of both fields were determined (Table 3.2).

Table 3.2: Mean values (mean of the whole observation period) for pH, sulfate (SO$_4$) dissolved organic carbon (DOC), nitrite (NO$_2$-N), ammonia (NH$_4$-N) and nitrate (NO$_3$-N) at each compartment at both fields.

	pH (-)		SO$_4$ (mg l^{-1})		DOC (mg l^{-1})		NO$_2$-N (mg l^{-1})		NH$_4$-N (mg l^{-1})		NO$_3$-N (mg l^{-1})	
Field	GW	BW	GW	BW	GW	BW	GW	BW	GW	BW	GW	BW
soil solution in												
35 cm	8.2	8.0	68.5	60.9	n.d.	n.d.	0.41	0.16	0.14	0.12	31.3	25.2
60 cm	8.2	8.1	37.2	108.0	n.d.	n.d.	0.05	0.34	0.11	0.21	34.3	27.5
85 cm	8.0	8.1	25.4	179.6	n.d.	n.d.	0.04	0.25	0.04	0.15	36.5	44.2
drainage water	8.1	8.0	129.0	110.0	7.2	8.5	0.01	0.16	0.01	0.01	6.6	20.5
groundwater backwater	8.1	7.9	69.8	168.8	4.3	4.4	0.02	0.08	0.03	0.02	1.1	23.2

n.d.: not determined.

The measured pH-values in each compartment of field GW and BW were similar, not showing temporal fluctuations, lying in the range of 7.9 to 8.2. SO$_4$-contents registered in drain flow of field GW and BW (129 mg l^{-1} at field GW and 110.0 mg l^{-1} at field BW) were also comparable. But although a decreasing SO$_4$-concentration with increasing depth (25.4 mg l^{-1} in 85 cm), concentration raised to 69.8 mg l^{-1} in groundwater at field GW. However, at field BW SO$_4$-concentration was generally higher as compared to field GW. But with 179.6 mg l^{-1} in 85 cm depth and 168.8 mg l^{-1} in backwater, the concentrations were comparable.

Furthermore, registered DOC of 4.3 mg l^{-1} in groundwater and 4.4 mg l^{-1} in backwater were relatively high, but typically for agricultural use and the application of organic fertilizers in the investigated area (Ackermann, 2016).

Regarding the mean value of NO_2-N and NH_4-N, except in soil solution in 35 cm depth, concentrations were higher at field BW as compared to field GW. Not only the limit values (0.5 mg l^{-1}) were complied but the detection limit lies at 0.05 mg l^{-1}. The most significant differences were determined for NO_3-N. At field BW, the NO_3-N-concentrations (c_{NO3-N}) were comparable. At field GW, c_{NO3-N} was even higher in soil solution as compared to field BW, whereas c_{NO3-N} in drained water was, with 6.6 mg l^{-1} only one third as compared to registered concentration in drained water at field BW (20.5 mg l^{-1}). In groundwater, a mean concentration of only 1.1 mg l^{-1} was determined whereby in the backwater of field BW, 23.2 mg l^{-1} were registered.

Another significant aspect was an iron clogging at field GW, but not at field BW. Iron concentration was not measured, but during water sampling, iron clogging was observed at the drain outlet of field GW.

3.2.2 Crop yields and nitrogen-uptake

Although crop rotation and soil tillage was adjusted at both sites, plants had developed optimal on field BW as compared to field GW (maize: field GW 17.8 t ha^{-1}; field BW 21.4 t ha^{-1}; winter wheat: field GW 5.4 t ha^{-1}; field BW 6.6 t ha^{-1}). As compared to the fields, mean values of the investigated NWGL revealed a maize yield of 26.0 t ha^{-1} (+/- 3.4 t ha^{-1}) in 2014 and a winter wheat yield of 6.8 t ha^{-1} (+/- 0.4 t ha^{-1}) in 2015, being comparable to field BW. Due to the better crop development at field BW, N-uptake by maize was 297.5 kg N ha^{-1}, being 46 % higher as compared to field GW (202.5 kg N ha^{-1}). For winter wheat N-uptake at field BW (163.7 kg N ha^{-1}) was 26 % higher as compared to field GW (129.8 kg N ha^{-1}).

The investigated lysimeters provided a maize N-uptake of 178.9 kg ha^{-1} (+/-27.4 kg ha^{-1}) in 2014, being underestimated as compared to field BW, and a winter wheat N- uptake of 137.7 kg ha^{-1} (+/- 15.6 kg ha^{-1}) in 2015, lying in the range of the results from both fields.

3.2.3 Nitrogen analysis in the soil of field BW and GW

The analyzed N_{min} contents (NH_4-N and mainly NO_3-N) in the subsurface differed at both fields BW and GW, whereas their temporal course was comparable (Figure 3.8 a, b). During hydrological winter (November 2013 until March 2014) N_{min} content decreased from 61 to 40 kg ha^{-1} at field BW. In this time frame, N_{min} was reduced by 19 kg N ha^{-1}, whereas at field GW, N_{min} was reduced by 23 kg ha^{-1}.
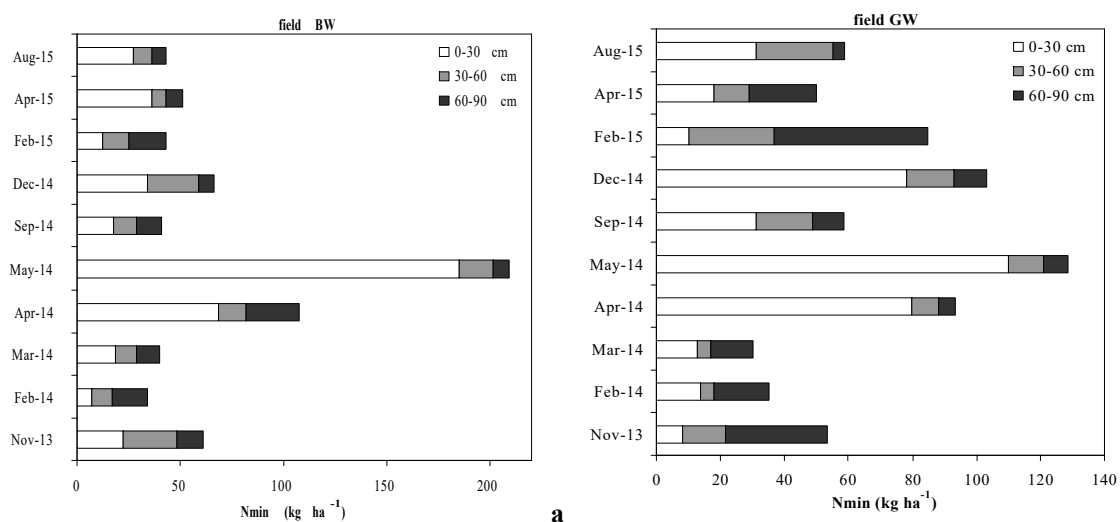
Figure 3.8: Measured mineral nitrogen (N$_{min}$) in 30, 60 and 90 cm depth at a) field BW and b) field GW.

After cattle slurry application (March 2014) and additional mineral N-fertilization (May 2014), at both sites a maximum N$_{min}$ content for the whole observation period was registered in May 2014 (129 kg N ha^{-1} at field GW and 209 kg N ha^{-1} at field BW), whereas the highest values were observed in the top soil (30 cm depth). It was remarkable, that although both fields were managed similarly (soil tillage, fertilization), field BW showed a higher N$_{min}$ content as compared to field GW in May 2014 (surplus of 80 kg N ha^{-1}). During the vegetation period and resulting maize N-uptake, N$_{min}$ at both sites decreased until September 2014. A small increase until December 2014 was measured at field BW, whereas field GW showed an accumulation of N$_{min}$ in the upper soil. N$_{min}$ of 78 kg ha^{-1} from 0 to 30 cm depth was two times higher as compared to registered values at field BW (Figure 3.8 a, b). In addition to that, surveys at field GW in February 2015 showed a very high N$_{min}$ content in 60 and 90 cm depth, presumable caused by N-leaching into deeper soil layers. But this could not be confirmed for field BW.

3.2.4 Soil moisture and NO$_3$-N-concentration in soil solution of field BW and GW

Although soil moisture in the upper 35 cm of both sites was comparable, in 60 and 85 cm depth, field BW showed a smaller water content as compared to field GW (in 85 cm depth saturated) (Figure 3.9 a, b, c, d, e, f). It was obvious that the registered soil moistures of two probes in the same depth were similar at field BW (cf. Figure 3.9 a, b, c) whereas registered moisture data differed between two probes in the same horizon at field GW (cf. Figure 3.9 d, e, f).
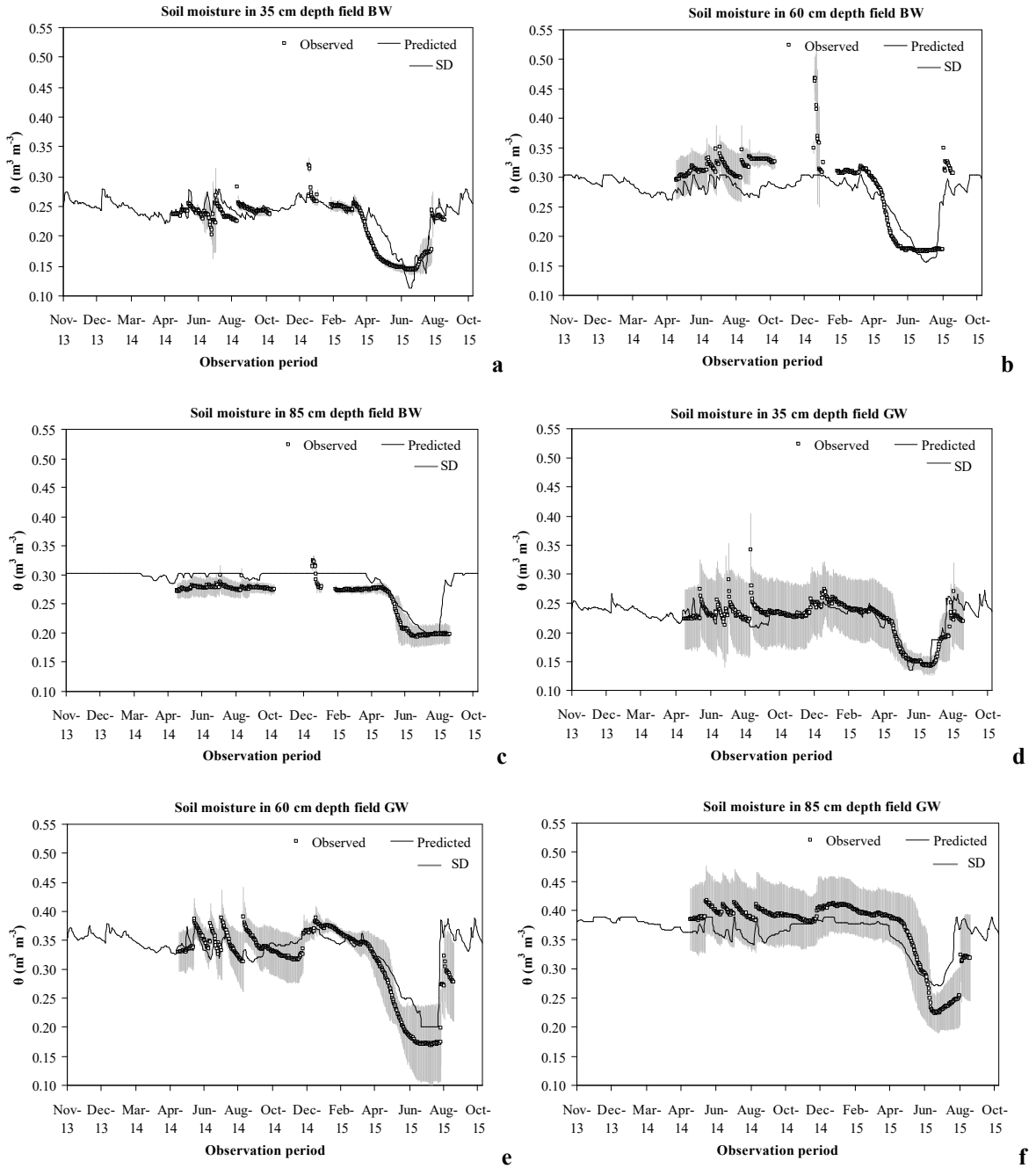
Figure 3.9: Observed (Mean value of two TDR-probes at each horizon & standard deviation SD) and predicted soil moisture in three different depth at field BW (a, b, c) and field GW (d, e, f) observation nodes in the combined model.

During probe-installation it was remarkable, that the subsurface of field BW was very homogenous whereas field GW does not only show a vertical but also a horizontal heterogeneity in soil properties (sandy and very compact loamy materials are lying in an alternating strata). As already stated, next to the TDR probes, in 35, 60 and 85 cm depth suction cups (three in each depth) were installed to get soil solution probes. As illustrated in Figure 3.10

a and b it was remarkable, that the measured NO_3-N-concentration in soil solutions from one depth differed markedly.
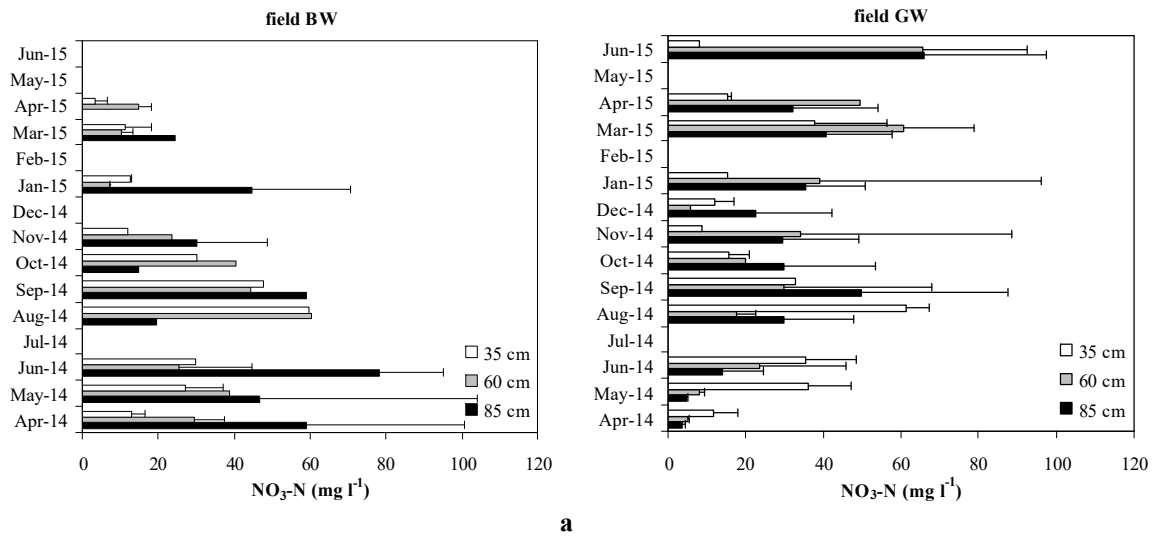
Figure 3.10: Measured nitrate nitrogen (NO_3-N)-concentration in soil solution (mean value of three suction cups at each horizon and standard deviation) of a) field BW, and b) field GW.

In general, in the HY 2014 as compared to field BW, field GW showed smaller concentrations in 60 cm and 85 cm depth, although higher N_{min} contents in deeper soil layers (60-90 cm) were observed. At both sites, in July 2014, c_{NO3-N} increased after rain events and remained on a constantly high level until September 2014. In January 2015, c_{NO3-N} in a depth of 35 cm was three times higher at field GW as compared to field BW. These results were in line with the observed accumulation of N_{min} in December 2014 at this site (cf. Figure 3.8 b). In addition to that, in the vegetation period 2015, field GW showed higher c_{NO3-N} in 85 cm depth compared to field BW, correlating to measured N_{min} contents of the soil. These observations confirmed the suggestion of N leaching into deeper soil layers at field GW. At field BW, unfortunately no soil solution could be sampled due to the low soil water content from May 2015 until October 2015. Thus, there were no evidences for N leaching ascertainable for this site.

3.2.5 Drain flow and NO_3-N-discharge via tile drains

For the whole observation period of two HY, from field GW 17.1 mm and from field BW 150.2 mm were discharged via drains. From the NWGL, in HY 2014 and 2015 124.4 mm were discharged, being comparable to field BW but not to GW. At both sites, BW and GW after rain events, illustrated in Figure 3.11 a), the drain flow rapidly increased. But in contrast to field BW, showing a continuously drain flow throughout the whole study period,

field GW had a very low drain flow, tending to zero for the largest part of the study period (Figure 3.11 b, c).

a

field BW

b

field GW

c
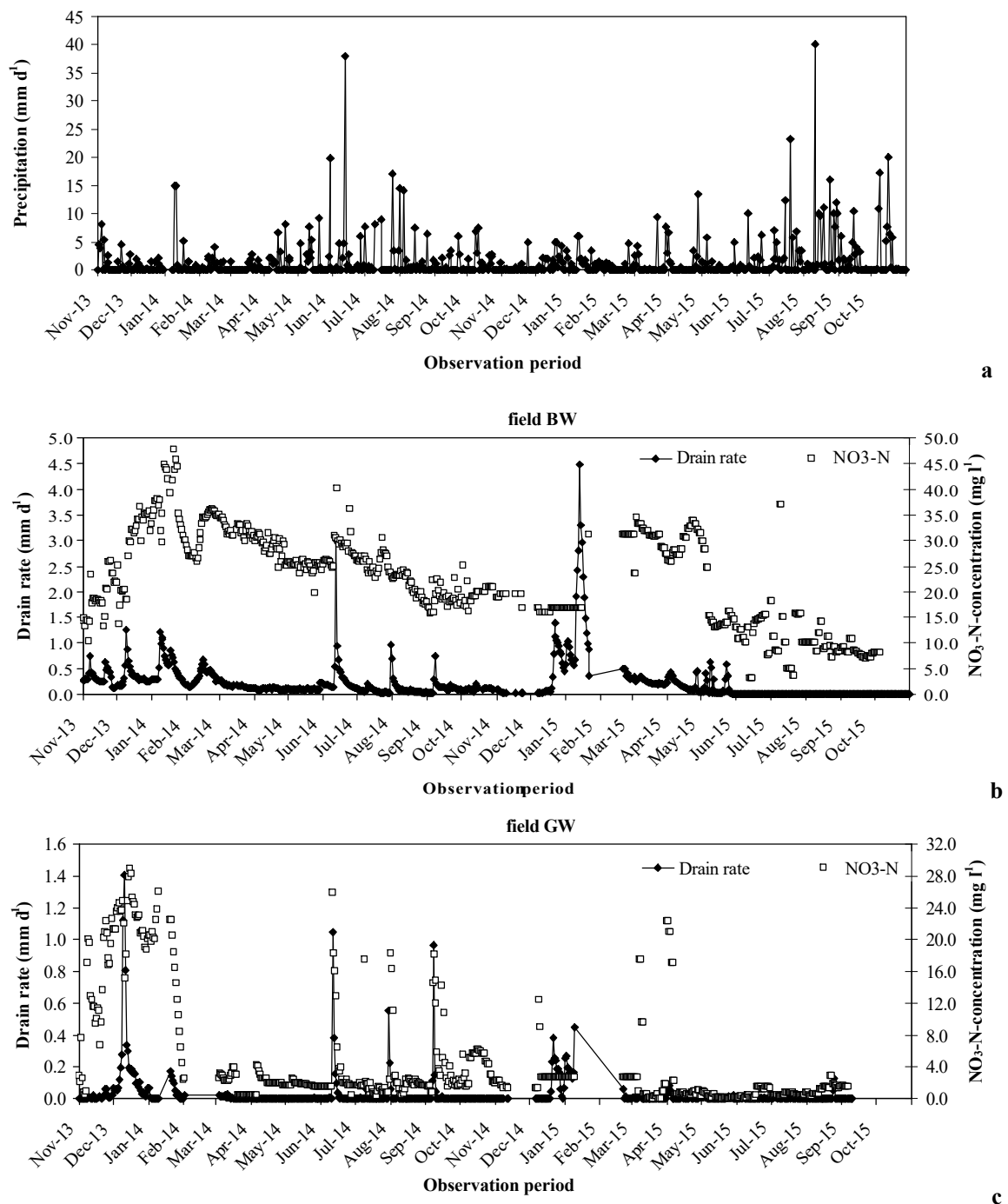
Figure 3.11: a) Temporal course of daily precipitation (P$_{NWGL}$); Daily discharged water and registered nitrate nitrogen (NO$_3$-N)-concentration in drain flow of b) field BW, and c) field GW.

It was assumed, that at field GW precipitated water mainly run off at the surface, being accumulated in present depressions at this field (between borehole 6 and 7, cf. Figure 2.4 b). In addition to that, water percolated slowly into the subsoil of field GW due to smaller

hydraulic conductivities of the field GW soil. Drain flow peaks in general were associated to registered precipitation events for field GW and BW (Figure 3.11 a). Between rain events and drain peak was a time delay of one to four days at both sites. But it was remarkable, that after heavy rain events in summer 2014 no time delay was observed at field GW in contrast to field BW (delay of one day) which was suggested to be caused by a preferential flow at field GW (Figure 3.11 b, c).

At field BW, the NO_3-N-concentration in drained water was generally high, whereas a mean concentration of 20.5 mg l^{-1} was examined for both HY. Field GW showed only a peak-wise increase in concentration, corresponding to high drain flow and rainfall events (Figure 3.11 a). Corresponding to the temporal course of the drain flow peaks, during heavy rain in summer 2014 no time delay between concentration peak and drain flow peak at field GW was determined. In contrast to that, at field BW, a concentration peak was registered one day after the drain flow peak was measured. The mean concentration in drained water from field GW for both HY was only 6.6 mg l^{-1} complying only 30% of the mean concentration in drained water of field BW (20.5 mg l^{-1}). At field GW, concentration-peaks were registered during December 2013, at June/11/2014, August/1/2014, September/8/2014, March/8/2015 and April/1/2015 with maximum concentration in December 2013 (28.8 mg l^{-1}), whereas c_{NO3-N} was below 5 mg l^{-1} at the other sampling dates during the study period (cf. Figure 3.11 b). In contrast field BW showed generally high c_{NO3-N} in drain water for the HY 2014 with maximum concentration of 52.9 mg l^{-1} in January 2014; c_{NO3-N} in drain water decreased slowly during the vegetation period until the end of October 2014 (21 mg l^{-1}). From January 2015 c_{NO3-N} increased associated to increasing drain flow and reaching a constant value of 30 mg l^{-1} until April 2015. Corresponding to an increasing N-uptake of the cultivated winter wheat between May and October 2015, c_{NO3-N} in drain water remains on a low level of 10 mg l^{-1}.

Regarding the monthly amount of discharged NO_3-N via drains (amount of water, multiplied with registered concentration) revealed that a relevant NO_3-N discharge from field GW was registered in December 2013 with 1.5 kg N ha^{-1}, and June 2014 after heavy rain events with 0.4 kg N ha^{-1} (Figure 3.12 a). In contrast to that, maximum NO_3-N-loads at field BW were registered in January 2014 and 2015 with 6.7 kg N ha^{-1} and 8.7 kg N ha^{-1}. But also here, after heavy rain events in June 2014, 3.2 kg N ha^{-1} were measured.

a

b
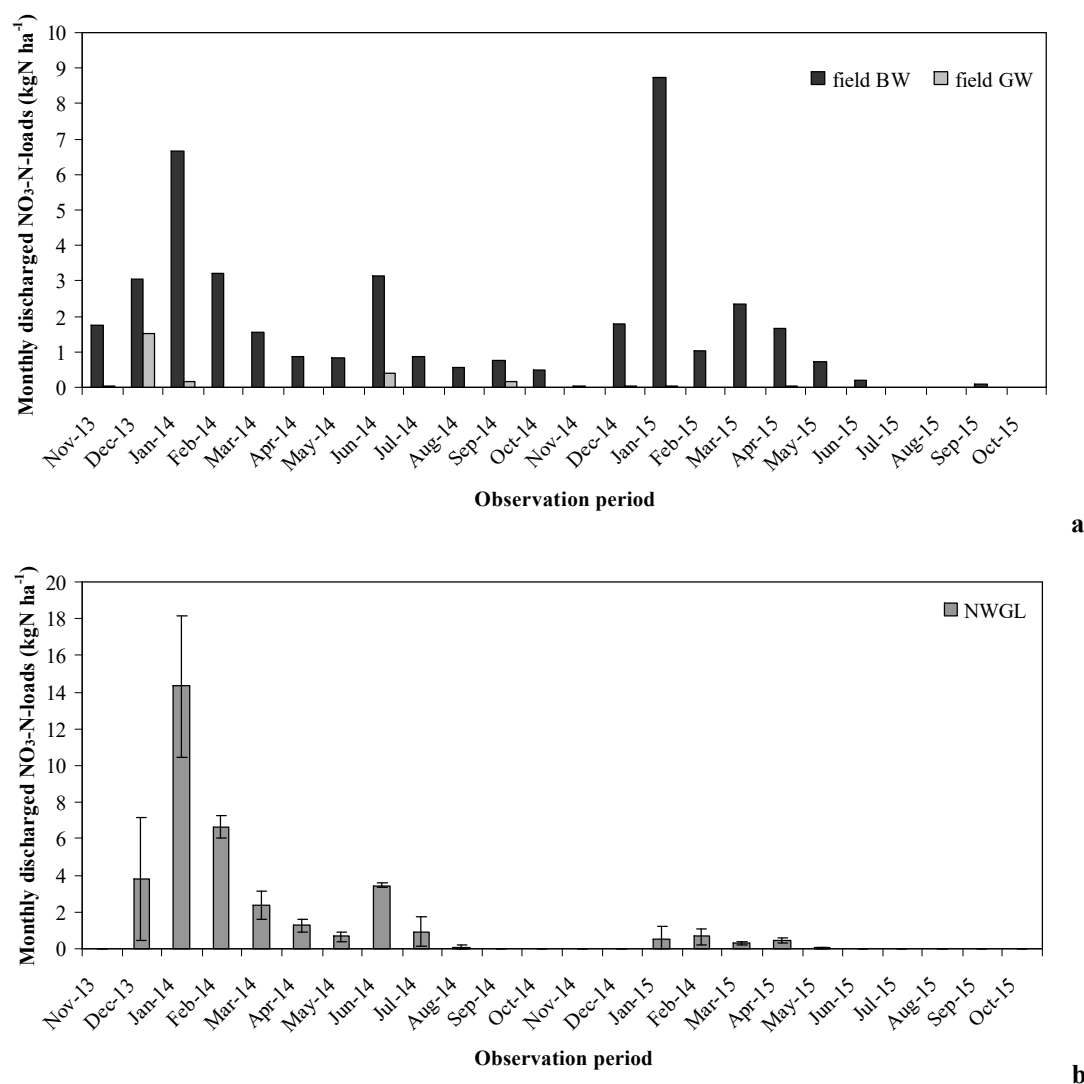
Figure 3.12: Monthly discharged NO$_3$-N-loads from a) field BW and GW; b) the NWGL.

For the whole observation period of two HY, from field GW 17.1 mm water and 2.5 kg N ha^{-1} were discharged via drains. In contrast to that total drain flow was 150.2 mm at field BW, whereas 40.4 kg N ha^{-1} were discharged. Relating these results showed, that drain flow of field GW compared to field BW was 14.6 % and discharged NO$_3$-N loads 9.5 % for HY 2014 (field GW/ field BW: 11.9 mm; 2.3 kg N ha^{-1}/ 81.4 mm; 23.8 kg N ha^{-1}), and 7.5 % regarding drain flow and 1 % regarding NO$_3$-N-loads in HY 2015 (field GW/field BW: 5.2 mm; 0.17 kg ha^{-1}/ 68.8 mm; 16.6 kg ha^{-1}). In this context it should be noted, that the temporal course of discharged NO$_3$-N-loads from the NWGL in HY 2014 corresponded very well to field BW, with maximum discharge in January 2014 (Figure 3.12 b). But with 33.5 kg N ha^{-1} discharged from the NWGL, the determined N-losses were higher as compared to field BW (23.8 kg N ha^{-1}). Because of smaller discharge rates in the HY 2015

(Figure 3.1 a), with 2.0 kg N ha^{-1}, discharged NO$_3$-N-loads from the NWGL were significantly smaller as compared to 16.6 kgN ha^{-1} from field BW.

3.2.6 NO$_3$-N-concentration in back-/ groundwater of field BW and GW

Measured concentration in groundwater at field GW was generally low (mean for both years 1.1 mg l^{-1}) with maximum concentration in April 2015 with 8.7 mg l^{-1}. In contrast to that, registered NO$_3$-N-concentration in backwater of field BW was constantly high, obtaining a mean value of 23.2 mg l^{-1} (Figure 3.13).
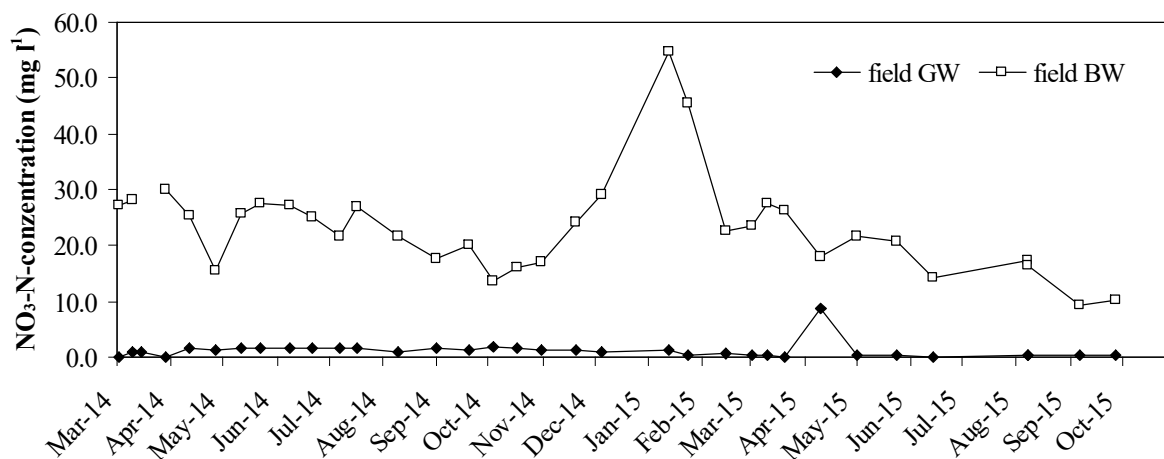
Figure 3.13: Measured nitrate nitrogen (NO$_3$-N)-concentration in groundwater (field GW) and backwater (field BW).

This corresponds very well to the mean concentration in drain flow of field BW with 20.5 mg l^{-1} (cf. Table 3.2). Maximum c$_{NO3-N}$ in backwater was registered in January 2015 (54.6 mg l^{-1}), correlating to maximum drain flow, maximum measured concentrations in discharged water and missing vegetation and root water uptake/ root solute uptake.

3.3 Using lysimeters to simulate the impact of soil heterogeneity

3.3.1 Simulated water balance of both fields based on the NWGL-measurements

As already discussed all input parameters to describe the atmospheric flux at the upper model boundary were determined at the NWGL and directly transferred to the field BW-model, described in Chapter 3.1. In Chapter 3.2 the impact of soil heterogeneity on water flow and N-transport was reproducible. Additionally, the NWGL data should be used to simulate the water balance of both, field BW and GW, combined within one model (Figure 2.5). The initial and the inversely calculated unsaturated soil hydraulic properties for the combined field BW-GW-model are summarized in Table 3.3.

Table 3.3: Initial and calibrated van Genuchten parameters.

	θr_{in}	θr_{cal}	θs_{in}	θs_{cal}	α_{in}	α_{cal}	n_{in}	n_{cal}	Ks_{in}	Ks_{cal}	l_{in}	l_{cal}
	(m^3 m^{-3})		(m^3 m^{-3})		(1 m^{-1})		(-)		(m d^{-1})		(-)	
L1	0.02	0.02	0.35	0.35	1.37	1.60	1.40	1.40	0.36	0.52	0.5	0.5
L2	0.02	0.09	0.35	0.43	2.05	1.00	1.37	1.23	0.37	0.01	0.5	0.5
L3	0.03	0.03	0.32	0.28	1.79	1.79	1.34	1.34	0.16	0.14	0.5	0.5
L4	0.04	0.06	0.32	0.39	2.21	3.89	1.25	1.25	0.04	0.04	0.5	0.5
L5	0.02	0.02	0.33	0.35	0.95	0.95	1.45	1.45	0.21	0.22	0.5	0.5
L6	0.08	0.05	0.33	0.30	4.95	3.00	1.27	1.23	0.05	0.07	0.5	0.5

L-layer; in- initial values; cal-calibrated values; θr-residual water content; θs-saturated water content; a-parameter in the soil water retention function; n-Parameter the soil water retention function; Ks-saturated hydraulic conductivity; l-tortuosity parameter in the conductivity function.

The highest deviations between initial and calibrated unsaturated soil hydraulic properties were determined for layer 2 at field GW (10-30 cm depth, cf. Table 2.2). Whereas the analyzed laboratory data as well as the initial van Genuchten parameters in Table 3.3 revealed that this layer is permeable, during model calibration it was assumed that the conductivity of this layer is very small. Thus, surface runoff and ponding could be simulated. Due to a sealed surface layer, smaller water flow velocities in the upper soil at field GW in contrast to field BW were reproduced. Comparing measured and modelled soil moisture, the model was successfully calibrated, whereby modelled soil moisture was lying in the range of the registered values and the specific standard deviations (Figure 3.9 a-f).

Regarding model validation, as already stated, for the upper boundary condition again the NWGL measurements were used. Furthermore, for field BW, the measured groundwater head was used as a lower boundary (Figure 3.14).
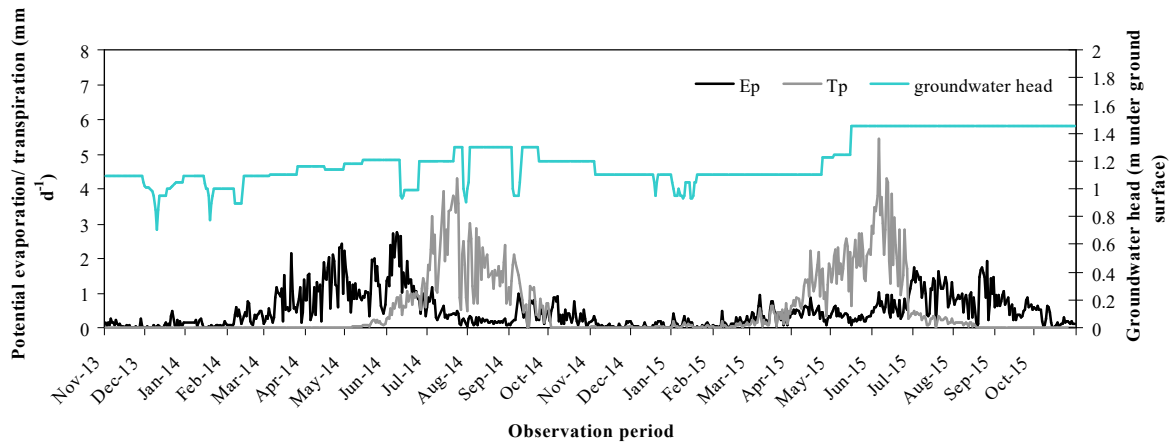
Figure 3.14: Calculated daily potential evaporation and transpiration rate as well as implemented groundwater head.

The combined field BW-GW-model revealed a total outflow of 170.0 mm for both HY. This corresponds to the sum of both fields with 167.3 mm (field GW: 17.1 mm; field BW 150.2 mm) for the whole observation period. Correlation analyses between monthly observed and predicted outflow rates revealed an R of 0.93 and NSE of 0.86, validating the model performance (Figure 3.15 b).
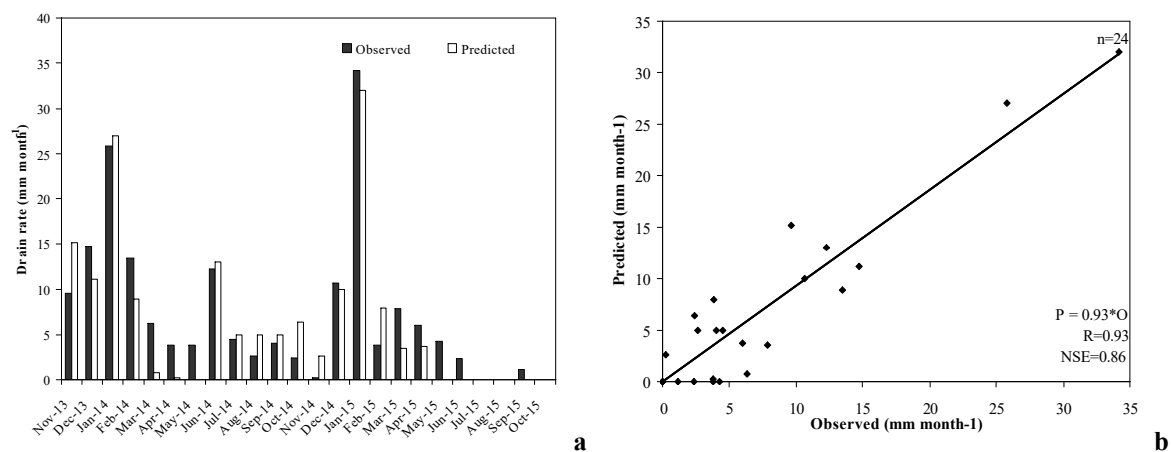
Figure 3.15: a) Observed and predicted monthly drain rate and b) regression analysis between both data sets.

3.3.2 Simplified solute transport model

Based on equations 12 to 16, k_{min} and k_{den} were calculated from registered soil moisture/ temperature at field BW and GW. Although their different pedo-hydrological properties, mineralization and denitrification rates of field BW and GW were comparable (Figure 3.16).
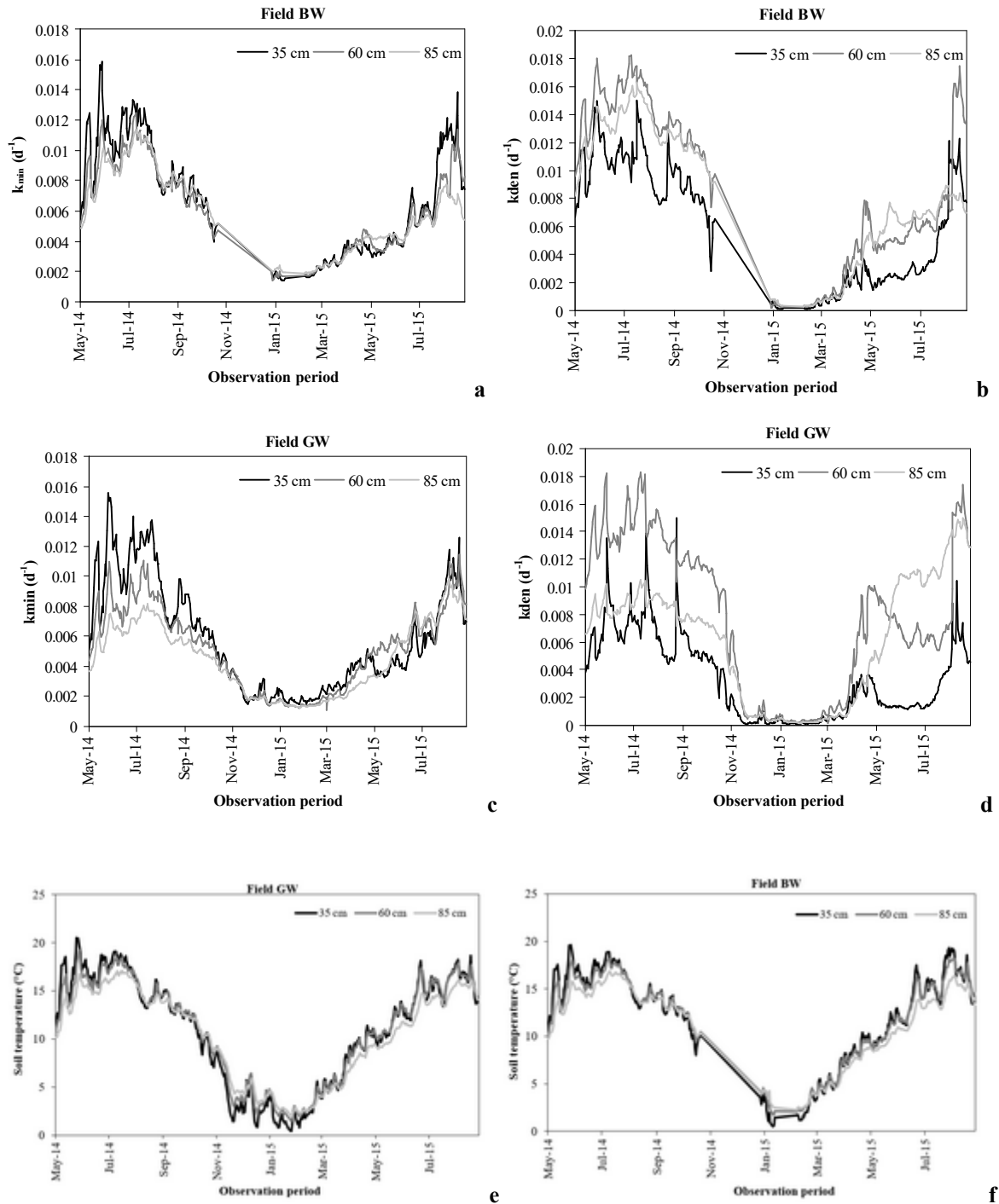
Figure 3.16: Calculated first order rates regarding mineralization k$_{min}$ and denitrification k$_{den}$ for a) and b) field BW; c) and d) field GW in dependence of the soil physical properties; e) soil temperature of field BW; f) soil temperature of field GW.

Maximum mineralization corresponded to generally higher soil temperature, illustrated in Figures 3.16 e and f, in summer 2014, with maximum rates in 35 cm depth (0.016 d^{-1} at field BW and GW).

Maximum denitrification was associated with saturated conditions and thus higher soil moisture. Maximum rates were determined for 60 and 85 cm depth, being 0.018 d^{-1} at both

fields. Because the first order rates were comparable, the amount of mineralized or denitrified N mainly depends on the water residence times and thus on the pedo-hydrological properties.

Based on the validated hydrological model, the simplified transport-model was implemented. Figure 3.17 shows the temporal course of the non-reactive component at the three observation points at field BW and GW, as well as in 100 cm depth.
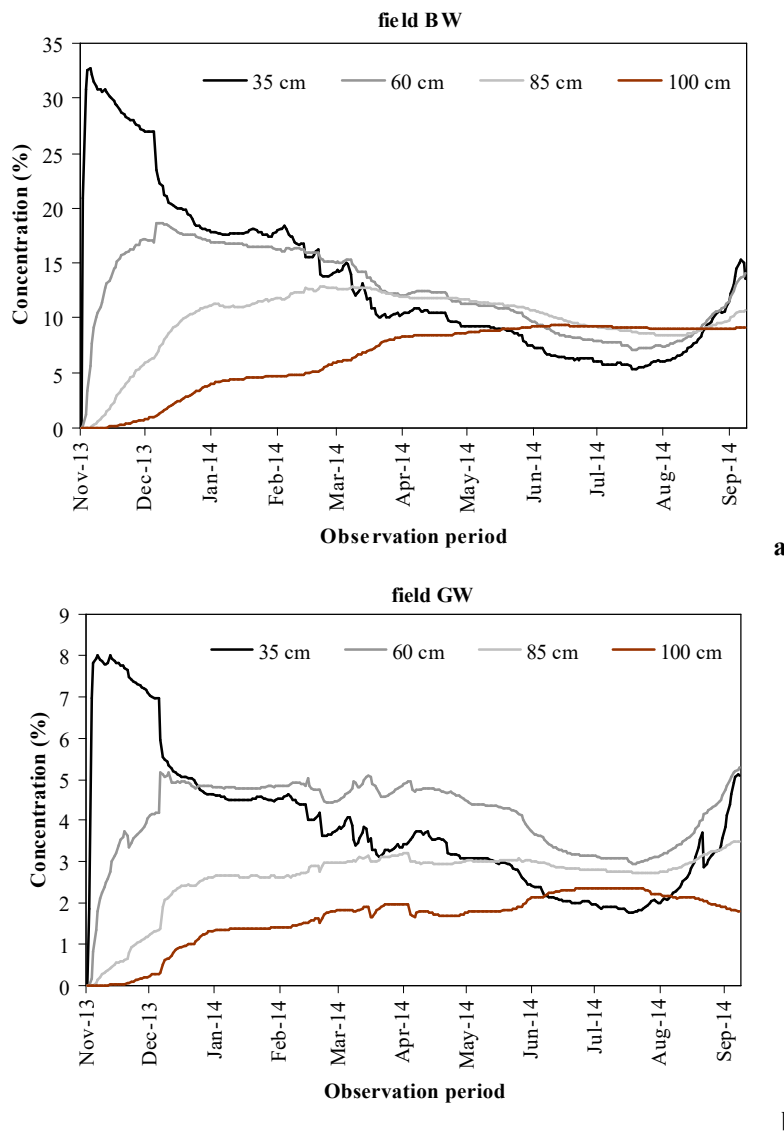
Figure 3.17: Depth depending temporal course of the non-reactive component at a) field BW and b) field GW.

It was significant, that the solute concentration in each depth was higher at field BW as compared to field GW. Thus, constantly for each depth a surplus of 50 % was calculated. But the rapid change from high concentration in soil solution to very small concentration in groundwater could not be reproduced in the model describing field GW part. This could be explained because no denitrification was assumed within the numerical simulations.

3.4 The impact of the lower boundary on the flow regime of lysimeters

3.4.1 Measured water balances at the TL and the GL

To determine the impact of the lower boundary condition within the second lysimeter study, the water balance of the tension-controlled (TL) and the gravitation lysimeter (GL) was compared. As a first step, the monthly climatically water balance (CWB) and resulting from this, the difference of registered monthly precipitation and monthly calculated potential evapotranspiration (ETp) was compared to the water balance of the lysimeters (Table 3.4).

Table 3.4: Monthly registered precipitation (P) and calculated evapotranspiration (ETp) for determining the climatic water balance (CWB) compared to the monthly outflow rate and water balance of the TL and the GL.

Datum	P	Etp	CWB	Outflow TL	Outflow GL	WB_{TL}	WB_{GL}
				mm month^{-1}			
Jun-14	22.8	22.2	0.6	10.8	8.8	3.2	12.9
Jul-14	79.7	57.3	22.4	26.2	28.8	38.4	50.0
Aug-14	62.0	37.4	24.7	101.9	106.3	38.1	51.1
Sep-14	19.6	18.5	1.1	11.9	4.7	-23.8	-17.3
Oct-14	37.5	8.1	29.4	6.7	0.9	16.0	6.4
Nov-14	6.8	3.1	3.7	2.6	0.0	-6.5	-3.1
Dec-14	38.2	3.6	34.6	0.1	0.0	42.2	40.6
Jan-15	67.0	4.3	62.7	12.1	52.0	66.8	73.5
Feb-15	6.2	4.5	1.7	17.8	23.4	-10.6	-2.7
Mar-15	30.6	12.3	18.3	6.6	8.3	7.0	10.5
Apr-15	13.4	13.4	0.0	0.0	1.2	-62.3	-56.2
May-15	16.1	41.7	-25.6	0.3	0.0	-84.7	-89.9
Jun-15	35.4	56.0	-20.6	0.0	0.0	-31.9	-36.0
Jul-15	38.7	52.8	-14.1	0.2	0.0	-23.5	-35.1
Aug-15	26.2	71.2	-45.0	0.0	0.0	-35.5	-31.2
Sep-15	31.7	39.2	-7.5	0.0	0.0	27.2	25.3
Oct-15	60.2	18.2	42.0	0.0	0.0	36.5	37.6
				mm			
Sum	592.2	464.0	128.3	197.2	234.4	-3.5	36.4

P- Precipitation; ETp- potential evapotranspiration; CWB: Climatic water balance (P-Etp); TL-tension controlled lysimeter; GL-Gravitation lysimeter; WB_{TL} (monthly mass change of TL - Outflow of TL); WB_{GL} (monthly weight change of GL-Outflow of GL).

The water balance of the TL (WB_{TL}) and the GL (WB_{GL}) was calculated from the registered outflow and mass changes, representing the difference of precipitation and actual evapotranspiration (Eta). Regarding the whole observation period, CWB was 128.3 mm, whereas WB_{GL} was only 36.4 mm and WB_{TL} -3.5 mm. In the hydrological summer 2014 (June until October) and the following hydrological winter (November 2014 until April 2015) positive water balances were calculated (summer: CWB/ WB_{TL}/ WB_{GL}: 78.0/ 72.0/

103.2 mm; winter: CWB/ WB$_{TL}$/ WB$_{GL}$: 121.0.0/ 36.6.0/ 62.7 mm). In the hydrological summer 2015, due to general small precipitation (Table 3.4), water balances were negative (CWB/ WB$_{TL}$/ WB$_{GL}$: -70.8/ -112.1/ -129.3 mm). Deviating water balances between both lysimeters resulted partly because of deviating registered mass changes. Because of tension regulation at the TL water was pumped into or out of the TL, influencing of course its mass. Additionally, the monthly outflow rates were also different between the TL and the GL, also influencing the mass changes (cf. Table 3.4). Regarding the total outflow, from the TL 197.2 mm, and from the GL 234.4 mm were discharged. The resulting difference of 37.2 mm could be explained with a reduced outflow from the TL in January 2015 as compared to the GL. For the whole observation period, two discharge periods were reproducible - the first one from June until September 2014, and the second one from January until March 2015. For the remaining part of the observation period the daily discharge rate was generally below 2.0 mm d^{-1} (Figure 3.18 a).
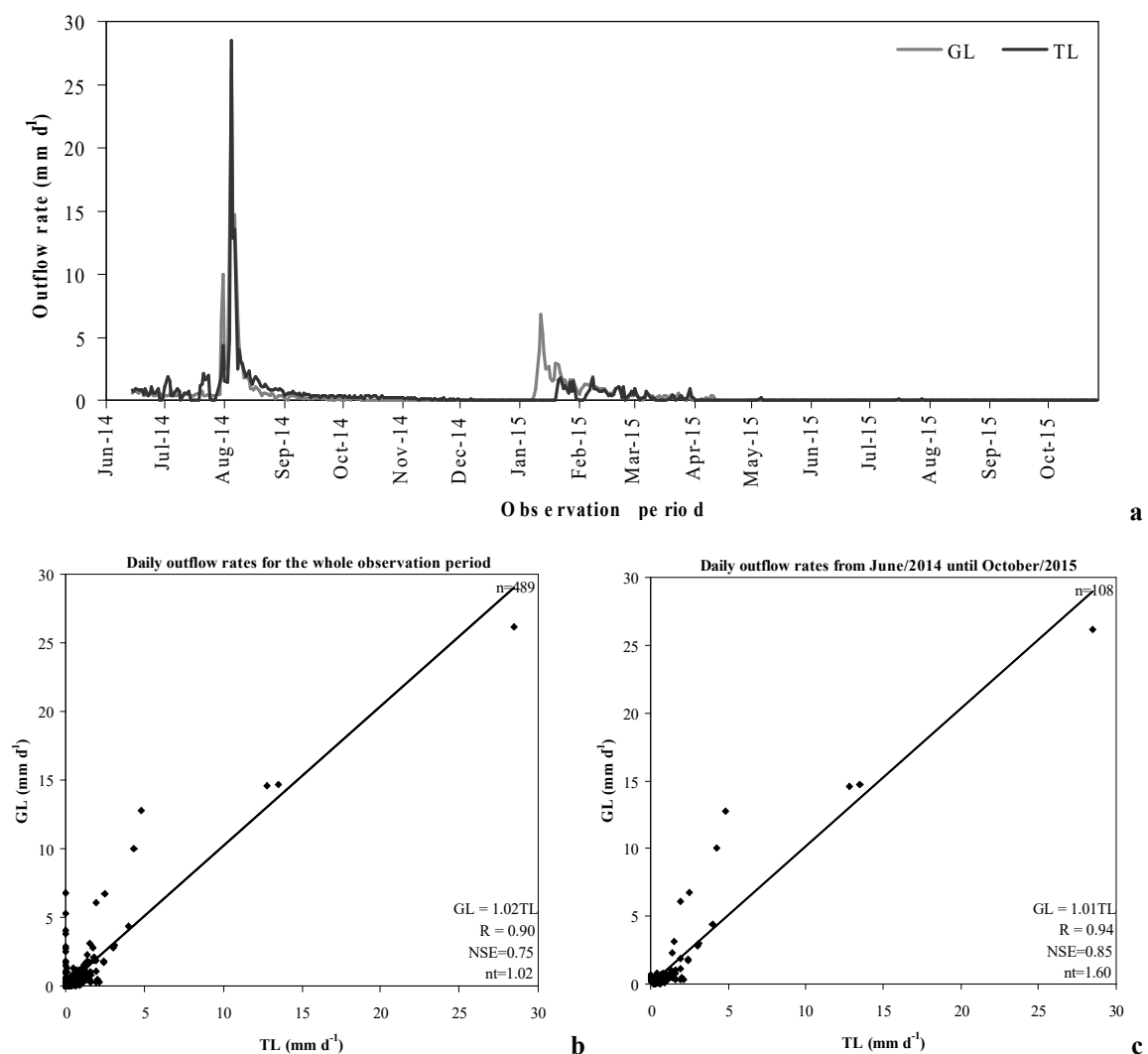
Figure 3.18: a) Daily outflow rates from the TL and the GL; Regression analyses between daily TL-/ GL outflow rates for b) the whole observation period; c) for a discharge event in 2014.

Regarding the whole observation period, correlation analyses between daily outflow rates from the TL and the GL revealed NSE of 0.75, n_t of 1.02, R of 0.90 and a gradient of the regression line of 1.02 (Figure 3.18 b). Correlation analysis between monthly outflow rates, listed in Table 3.4 revealed R of 0.93, a gradient of 1.01, NSE of 0.83 and n_t of 1.41. According to the quality criteria discussed in chapter 2.3.4, both data series correlate with each other. With regard to the two discharge periods it was remarkable, that daily outflow rates of both lysimeters were only comparable for the first period from June until September 2014 (gradient of the regression line=1.01; R=0.94; NSE=0.85; n_t=1.60), whereas no correlation could be determined for the second discharge period (January to March 2015). After drying up, from the GL water began to discharge from January/7/2015, whereas from the TL outflow was registered from January/19/2015. Thus, there was a time delay of twelve days. Additionally, the daily discharge rate in January 2015 was higher from the GL with a maximum flow rate of 7 mm d^{-1} as compared to 1.9 mm d^{-1} from the TL (Figure 3.18 a).

3.4.2 Measured depth depending soil moisture of the TL, GL and the undisturbed soil

The temporal course of the depth depending soil moisture of the TL, the GL and the undisturbed, natural soil is illustrated in Figure 3.19 a to d.
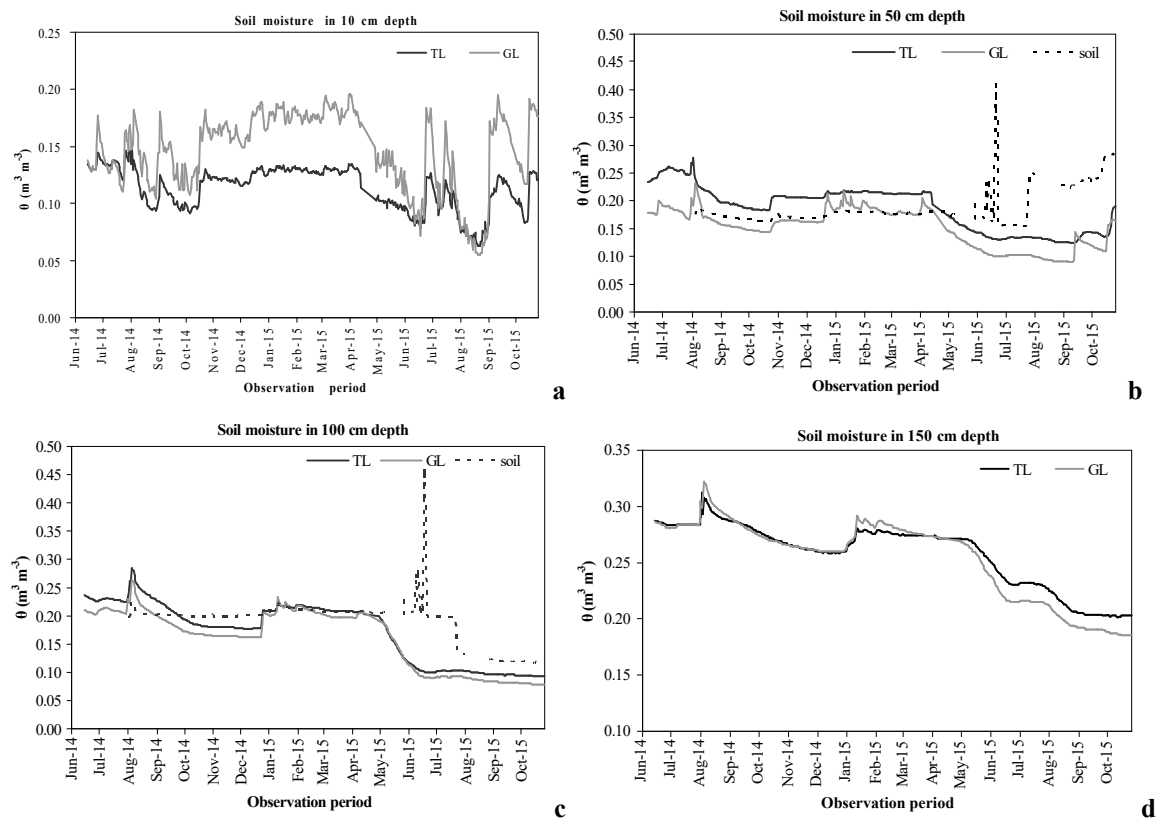
Figure 3.19: Temporal course of registered soil moisture of the TL and the GL in a) 10 cm; b) 50 cm; c) 100 cm and d) 150 cm depth.

In each depth, soil moisture showed a peak-shaped increase in August 2014, decreasing after that, being on a constantly low level until the end of December 2014. In January 2015, soil moisture increased, being constantly high during April 2015. From the end of April 2015, the water content from 50 cm to 150 cm rapidly decreased, whereas in 10 cm the water content showed peak wise arises after rain events. In 10 cm depth, registered soil moisture of the TL was 5 Vol. % lower as compared to the GL for the main part of the observation period (Figure 3.19 a). But correlation analyses revealed R of 0.86 between both data series, implying that their temporal course was comparable. In contrast to that in 50 cm depth, registered soil moisture of the TL was about 4 Vol.% higher as compared to the GL, corresponding to a higher porosity of this soil layer at the TL (cf. Table 2.5, Figure 3.19 b). But also here, the temporal course between both data series was comparable, described by R of 0.93. Although their different lower boundary conditions, no significant deviations regarding their water content in 100 and 150 cm depth could be determined (lying in the range of the measurement accuracy of +/- 2 Vol.%) expressed with R of 0.97 for each depth (Figure 3.19 c, d). From June 2014 until May 2015, in 50 and 100 cm depth, registered water content of the surrounding soil corresponded to registered soil moisture of the TL and the GL. But whereas water content at both lysimeters decreased from April 2015, at the surrounding soil peak wise increases in June 2015 were registered, corresponding to increasing water content in 10 cm depth of the TL and the GL in this time frame (Figure 3.19 a, b & c). As already noted, this peak was not registered in the other depths at both lysimeters.

3.4.3 Measured tension at the lower boundary of the TL, GL and the undisturbed soil

The temporal courses of the registered and the controlled tensions in 175 cm depth of the TL, the GL and the natural field soil are illustrated in Figure 3.20 a and b.
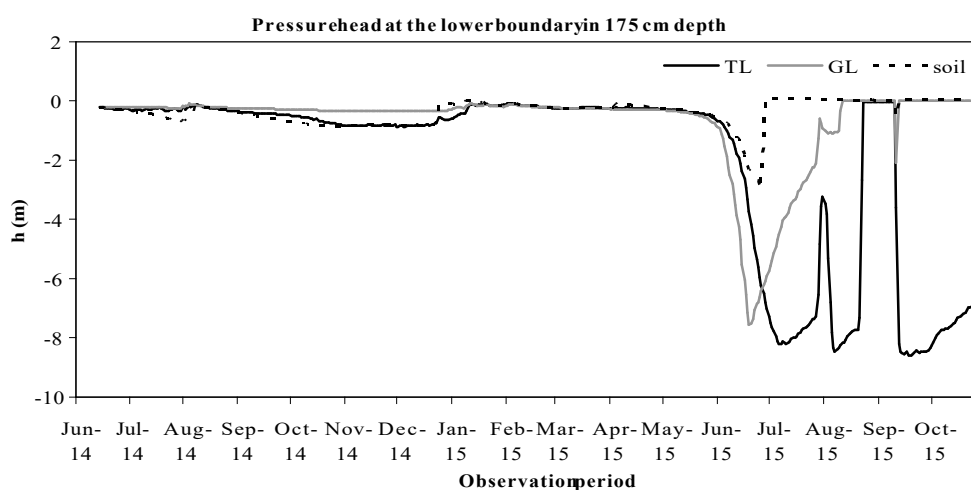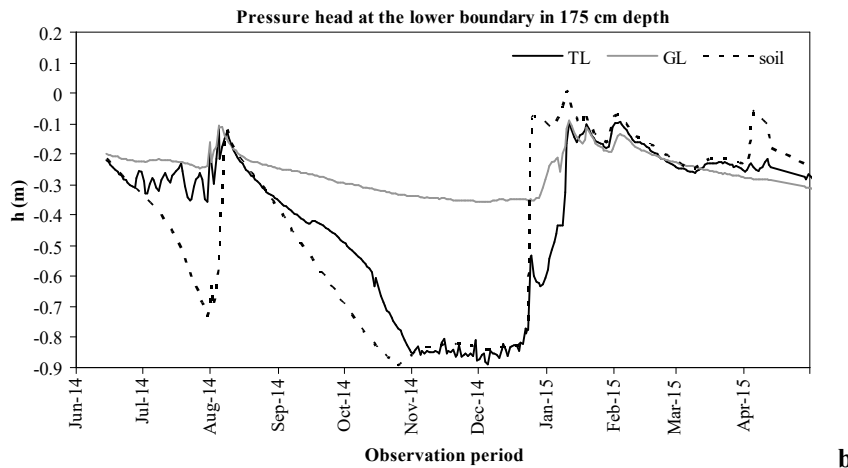
Figure 3.20: Temporal course of the pressure head (h) in transition of filling material to filter layer of the TL, the GL and the field soil for a) the whole observation period; b) June 2014 until April 2015.

From June 2014 until the end of April 2015 the TL, the GL and the field soil revealed a comparable temporal course of registered pressure head in 175 cm depth, whereas from May 2015, unreasonable values were registered by the tensiometer inside the TL (Figure 3.20 a, b). Corresponding to the discharge event at the end of July/ August 2014 and increasing soil moisture during this time frame, pressure head h was only -0.1 m, revealing near saturation conditions. From August 2014, corresponding to low water content, pressure head rapidly decreased, being constantly low until December 2014. In this timeframe, the regulated, registered pressure head of the TL corresponded very well with the tension measured in the surrounding soil. Furthermore, a pressure head of -0.3 m inside the GL as compared to -0.85 m in the TL and the undisturbed field soil revealed wetter conditions in the GL. But it was remarkable, that after this dry period, from December 2014 registered pressure head of the surrounding soil rapidly increased, revealing near saturation conditions from December/27/2014, whereas the regulated tension in the TL obtained this peak with a time delay of 16 days. Furthermore, resulting in the near saturation conditions of the GL in 175 cm depth, pressure head and thus water content was higher as compared to the TL. This corresponded to the beginning of discharging water from the GL at January/7/2015. Thus, pressure head of the TL does not correspond neither to the field soil nor to GL and water discharge began later and underestimated as compared to the GL (cf. Figure 3.18). Another important aspect was that from May 2015 (very dry period), the registered tension of the TL could not be regulated via the pumping system, whereby the tensiometer inside the TL registered unreasonable data. Registered pressure head at the GL revealed -7.6 m at June/20/2015, implying dryer conditions as compared to the undisturbed soil (-2.98 m). Moreover, in the field soil pressure head raised, revealing saturated condi-

3. Results

tions after June/20/2015, whereas registered pressure head of the GL approached zero with a time delay (August/12/2015). In this context it should be noted, that from June 2014 until the end of April 2015 discharge events corresponded to rain events, whereas no correlation to precipitation from May 2015 until October 2015 was determined.

3.4.4 Simulated water balances of the TL and the GL

3.4.4.1 Model calibration

The unsaturated soil hydraulic properties were inversely calculated within HYDRUS, based on the initial van Genuchten parameters, listed in Table 3.5. For calibrating the GL-model, a seepage face was used, for the TL- model the tension controlled lower boundary ("tension TL") was implemented. The best fit between measured and modelled soil moisture and pressure head (R of 0.99 TL; R of 0.99 GL) was determined with the parameters, summarized in Table 3.5.

Table 3.5: Calibrated van Genuchten parameters of the TL- and the GL- models.

z in m	θr $(m^3 m^{-3})$	θs $(m^3 m^{-3})$	a $(1\ m^{-1})$	n $(-)$	Ks $(m\ d^{-1})$	l $(-)$
TL						
0.00-0.20 m (L1)	0.07	0.22	2.00	1.83	3.0	0.50
0.20-1.85m (L2)	0.05	0.38	3.00	1.41	1.6	0.50
1.85-1.95 m (F1)	0.04	0.43	17.00	5.12	8.10	0.50
1.95-2.00 m (F2)	0.03	0.45	17.40	10.00	15.0	0.50
GL						
0.00-0.35 m (L1)	0.07	0.30	1.81	1.92	2.1	0.50
0.35-0.90 m(L2)	0.10	0.38	2.97	1.90	1.6	0.50
0.90-1.50 m (L3)	0.10	0.38	2.97	1.90	1.9	0.50
1.50-1.85 m(L2)	0.10	0.38	2.97	1.90	1.6	0.50
1.85-1.95 m (F1)	0.04	0.43	17.00	5.12	8.10	0.50
1.95-2.00 m (F2)	0.03	0.45	17.40	10.00	15.0	0.50

L-layer; F-filter layer; θr-residual water content; θs-saturated water content; a & n-parameters of the soil water retention function; Ks-saturated hydraulic conductivity; l-tortuosity parameter in the conductivity function.

The most significant differences between both, TL and GL, were calculated for the surface layer 1, whereas the saturated water content of this layer at the TL is significant lower. Except n, the remaining part of the soil layer of both lysimeters is comparable. Due to the inhomogeneous compaction of the GL, in 100 cm depth bulk density was smaller as compared to 50 and 150 cm depth (cf. Table 2.5). As a result, the van Genuchten parameters in

- 65 -

this layer 3 are the same as compared to layer 2, but hydraulic conductivity was slightly higher with 1.9 m d^{-1} compared to 1.6 m d^{-1} (Table 3.5). The observed and, based on the parameters in Table 3.5, calculated soil moisture and the pressure head in 175 cm depth for the calibration period from June/15/2014 until September/30/2014 are illustrated in Figure 3.21 a, b, c, d.
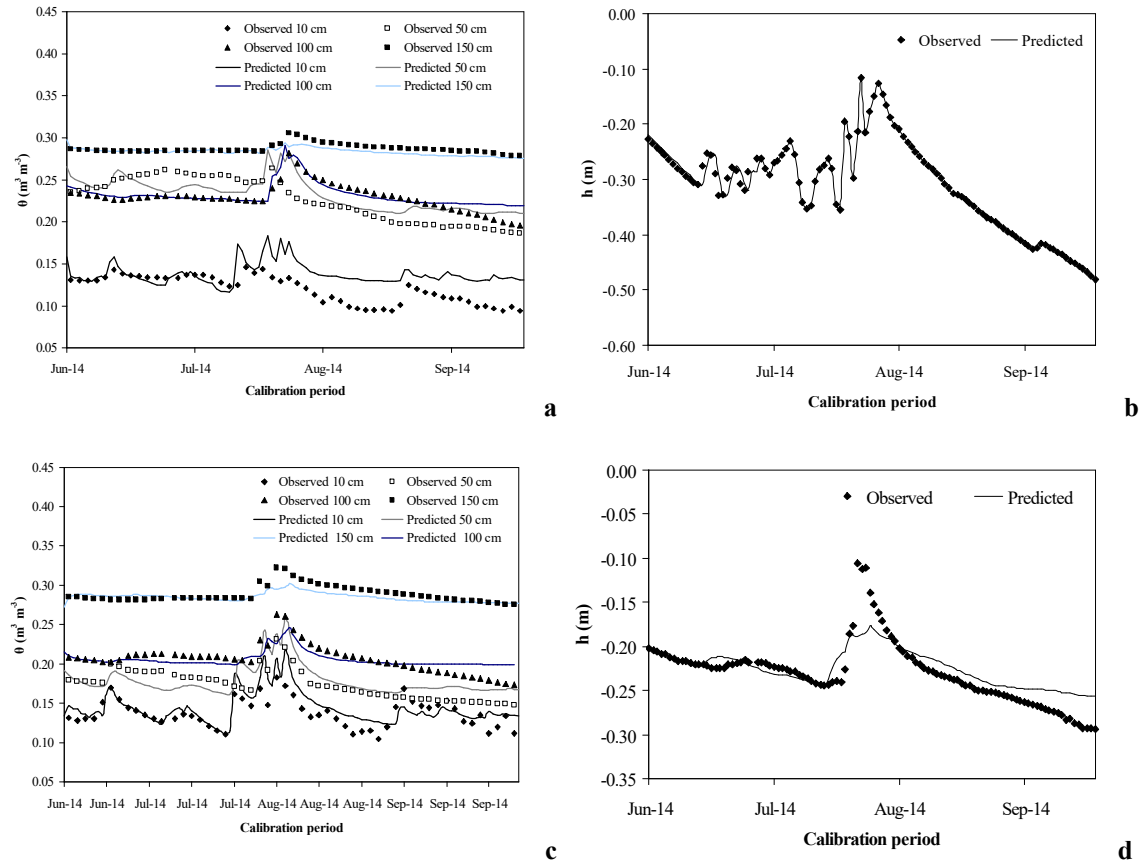
Figure 3.21: Calibration results – Comparison of observed and predicted a) soil moisture TL; b) pressure head TL; c) soil moisture GL; d) pressure head GL.

3.4.4.2 Model validation

GL, as well as the seepage face treated TL-model were validated from June 2014 until October 2015. TL and GL were described with a seepage face and a tension controlled ("tension TL" and "tension soil") boundary. Because from May 2015 registration of soil moisture as well as registration of the tension in TL was erroneous, for model validation the observation period was splitted into two sub periods. The first one (sub period I) from June 2014 until April 2015 and the second one (sub period II) from May until October 2015. For the whole modeling period, the actual atmospheric flux was 359.65 mm, whereas actual root water uptake amounted 212.4 mm. A difference of 147.25 mm was determined. Because 197.2 mm from TL and 234.4 mm from GL were discharged, the water balance of both lysimeters was negative regarding the whole observation period (Figure 3.22).
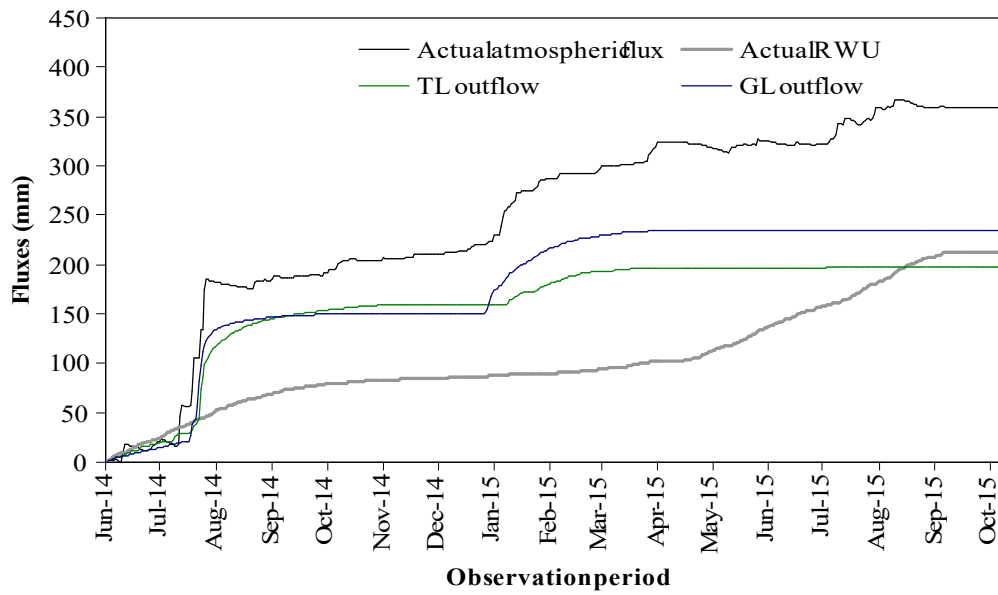
Figure 3.22: Actual atmospheric flux and root water uptake (RWU) as compared to cumulated daily outflow rates of the TL and the GL.

TL-model

The depth depending course of the soil moisture was reflected by the TL-models, treated with the tension-controlled lower boundaries "tension in TL" and "tension in soil" for the first sub period. But in sub period II, both tension controlled models over predicted water content in 50 cm and 100 cm depth. In this time frame, in 150 cm the simulations revealed unrealistic soil moisture data due to the erroneous tensiometer measurements inside the TL (Figure 3.23 a, b, c, d).

Soil moisture in 50 cm depth

b

Soil moisture in 100 cm depth

c

Soil moisture in 150 cm depth

d
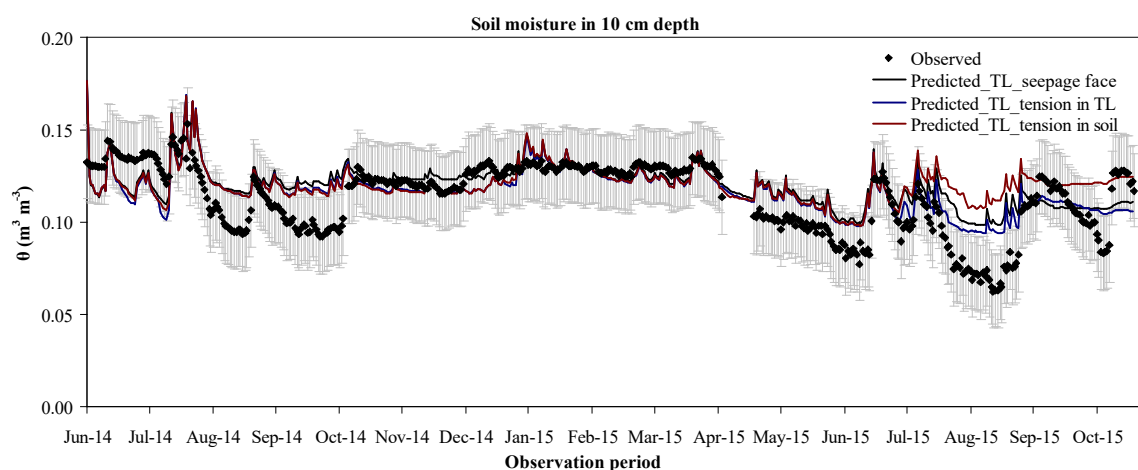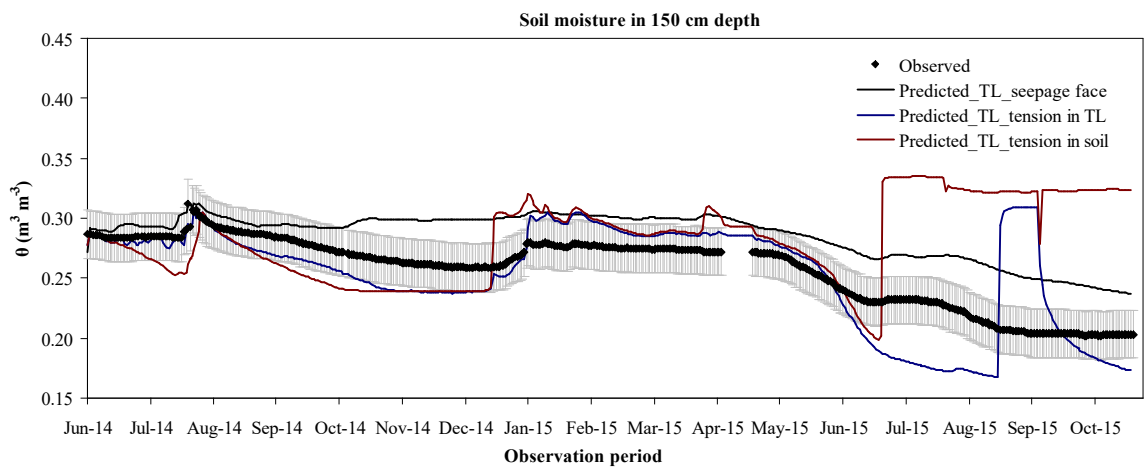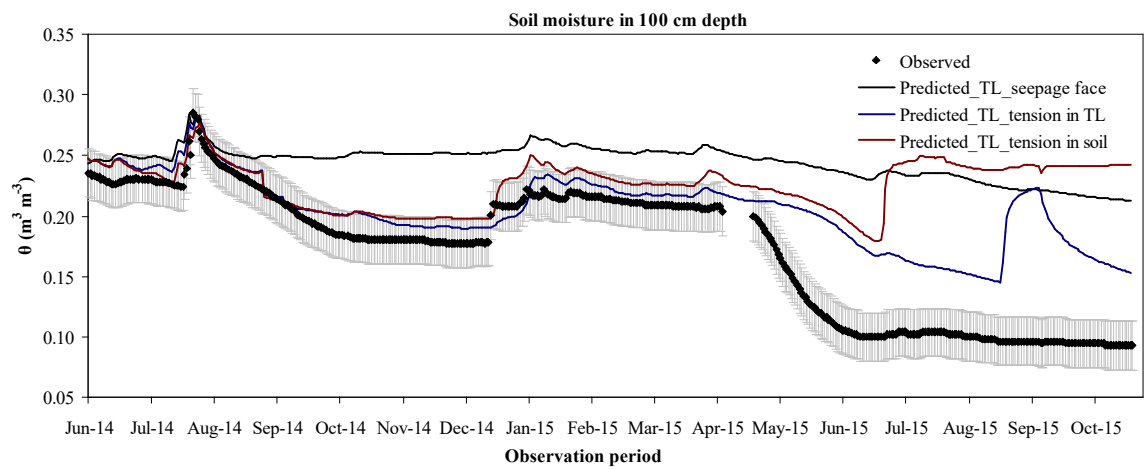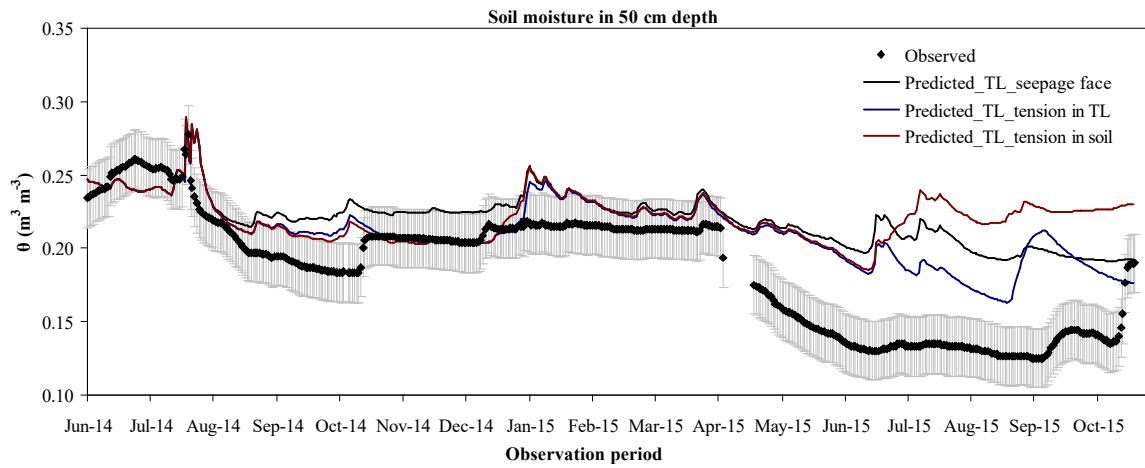
Figure 3.23: Observed and predicted soil moisture in 10 cm, 50 cm, 100 cm, 150 cm, and 175 cm depth of the TL-models with the lower boundaries seepage face, tension in TL, and tension in the surrounding soil (a-e).

Comparing the depth depending course of soil moisture between the seepage face and the tension controlled TL-models led to the conclusion that the type of lower boundary conditions had only a slightly impact on the water content in 10 cm and 50 cm depth. The impact of the lower boundary type could be reproduced for soil moisture in 100 and 150 cm depth. In these depths, the seepage face treated TL-model over predicted measured values, whereby in addition to that, at the lower boundary near saturation conditions were simulated (Figure 3.23 e). Corresponding to a delayed tension control in the TL as compared to registered tension in the surrounding soil, at the end of December 2014, the model with the implemented "tension in soil" reached near saturation conditions at December/27/2014 whereby the model with the registered "tension in TL" simulated these conditions16 days later (Figure 3.23 e).

Regarding the discharge behavior of the TL-models, the best fit between observed and predicted daily outflow rates could be examined with the lower boundary seepage face and "tension in soil" (Figure 3.24).
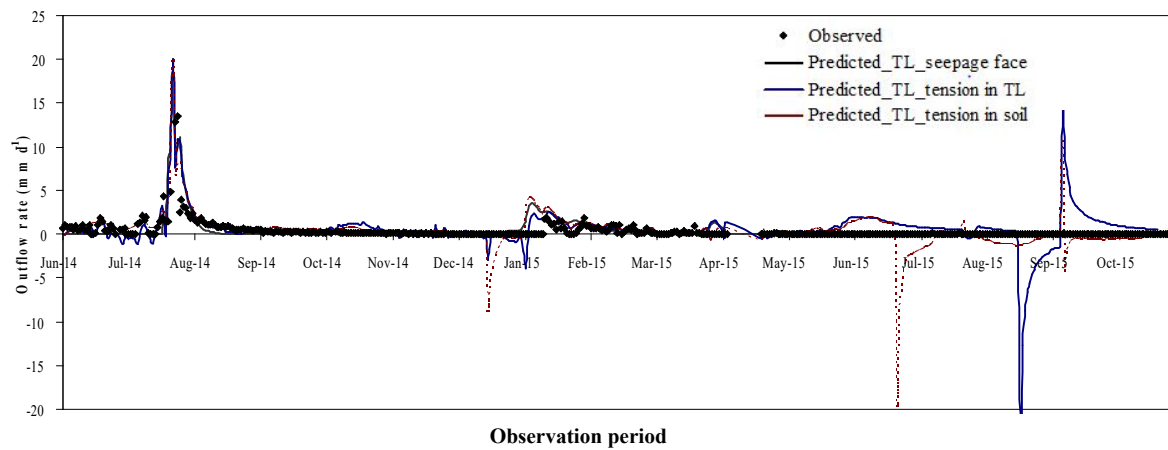
Figure 3.24: Observed and predicted daily outflow rates of the TL-models with the lower boundaries seepage face, tension in TL, and tension in the surrounding soil.

But it should be noted, that mainly the first discharge event from June until September 2014 was reproduced in contrast to the second one from January 2015 (Figure 3.24). Negative flow in Figure 3.24 characterizes the amount of water that should have been pumped back to the TL during tension regulation, whereas this was not reproduced by the registered mass of the TL.

As a result, water was not pumped back into the system adequately. Observed predicted analyses of daily outflow rates from the TL-models "seepage face" (NSE of 0.65 and n_t of 0.67), "tension in TL" (NSE of 0.25 and nt of 0.15) and "tension in soil" (NSE of 0.69, n_t of 0.80) revealed no correlation between measured and the respective modelled outflow rates. This could be explained on the one hand by the fact that the pumping system did not work in sub period I leading to a time delayed adjustment of the tension inside TL in December 2014, and on the other hand that the measured tension in sub period II was erroneous. As already stated in sub period I in January 2015, with 12.1 mm measured outflow from TL was drastically reduced as compared to measured 52.0 mm from the GL (Table 3.6).

Table 3.6: Observed and predicted outflow rates for the TL and the GL.

	Tension-controlled lysimeter TL				Gravitation lysimeter GL			
	Observed	Predicted seepage face	Predicted tension TL	Predicted tension soil	Observed	Predicted seepage face	Predicted tension TL	Predicted tension soil
	mm month-1							
Jun-14	10.8	0.0	5.9	7.2	8.8	8.6	8.6	8.5
Jul-14	26.2	1.7	18.6	27.2	28.8	20.9	26.4	33.9
Aug-14	101.9	108.9	113.4	105.8	106.3	110.0	124.9	120.4
Sep-14	11.9	0.0	6.5	16.0	4.7	0.1	8.2	17.4
Oct-14	6.7	0.0	21.0	15.3	0.9	0.4	18.9	10.9
Nov-14	2.6	2.2	10.8	5.0	0.0	0.2	9.8	5.2
Dec-14	0.1	3.8	4.6	3.2	0.0	3.7	3.2	2.6
Jan-15	12.1	50.6	33.7	49.6	52.0	52.9	36.8	50.4
Feb-15	17.8	21.2	23.7	23.8	23.4	22.8	27.2	27.3
Mar-15	6.6	6.3	7.0	7.0	8.3	7.9	7.6	7.8
Apr-15	0.0	8.3	10.7	6.3	1.2	5.3	10.0	7.3
May-15	0.3	0.0	7.2	7.6	0.0	1.2	15.1	14.2
Jun-15	0.0	0.0	47.3	36.7	0.0	0.0	34.0	32.0
Jul-15	0.2	0.0	21.0	2.6	0.0	0.0	9.0	1.8
Aug-15	0.0	0.0	11.1	0.0	0.0	0.0	4.2	0.0
Sep-15	0.0	0.0	72.7	10.7	0.0	0.0	62.5	12.9
Oct-15	0.0	0.0	19.8	0.0	0.0	0.0	19.5	0.0
	mm							
OP	197.2	203.0	435.0	323.9	234.4	233.9	425.9	352.4
SP I	196.7	203.0	255.9	266.3	234.4	232.7	281.6	291.6
SP II	0.5	0.0	179.1	57.6	0.0	1.2	144.3	60.8

OP – Observation period; SP I – Subperiod I; SP II – Subperiod II.

In January 2015, the TL-model with registered "tension in TL" revealed an outflow of 33.7 mm, the model with the tension of the surrounding soil simulated 49.6 mm. This corresponded very well to 50.7 mm, calculated within the TL-model "seepage face" and the measured 52 mm from the GL (Table 3.6).

Treating the TL-model with a seepage face revealed a total outflow of 203.0 mm, being slightly higher than the measured outflow from the TL (197.2 mm), whereas with "tension in TL" 434.9 mm and with "tension in soil" 323.9 mm were calculated (Table 3.6).

The unrealistic total outflow of the "tension-controlled" models could be explained with the erroneous TL-measurements in sub period II. Whereas in this time frame, the seepage face treated model simulated no outflow, TL with "tension in soil" calculated 57.6 mm, whereby due to the unreasonable tensiometer measurements inside TL 179.1 mm were calculated. But neither at the TL nor at the GL was any outflow registered for this time frame. In sub period I the model "tension TL" simulated 255.9 mm, and "tension soil" calculated 266.3 mm that should have been discharged. This corresponded to measured 234.4 mm from GL, being slightly higher due to the controlled lower boundary.

GL-model

The GL-model with a seepage face lower boundary reproduced measured soil moisture in each depth for the first sub period I (Figure 3.25 a, b, c, d).
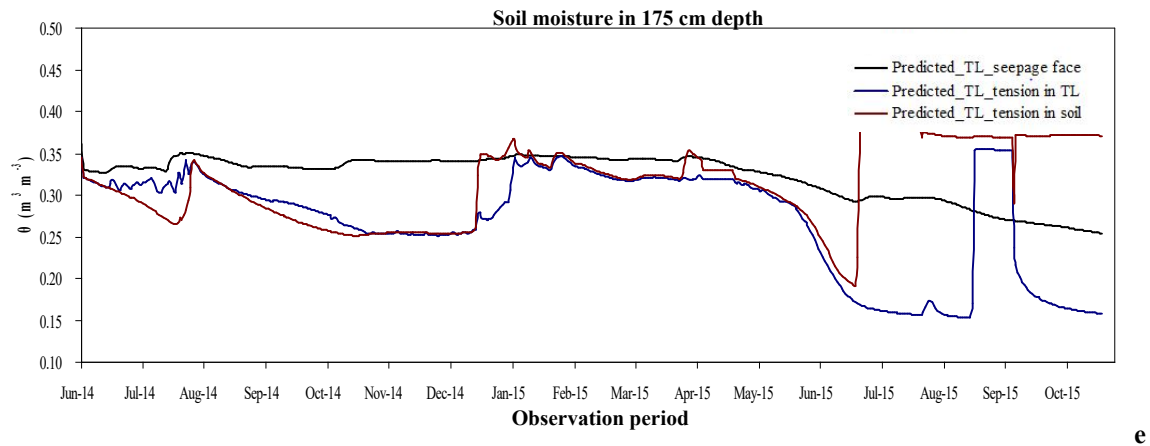

a

b

c

d

e
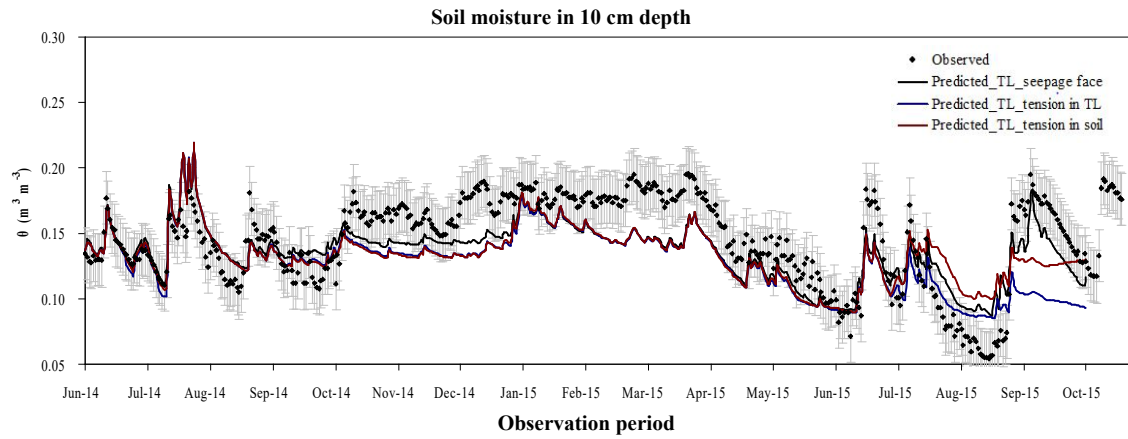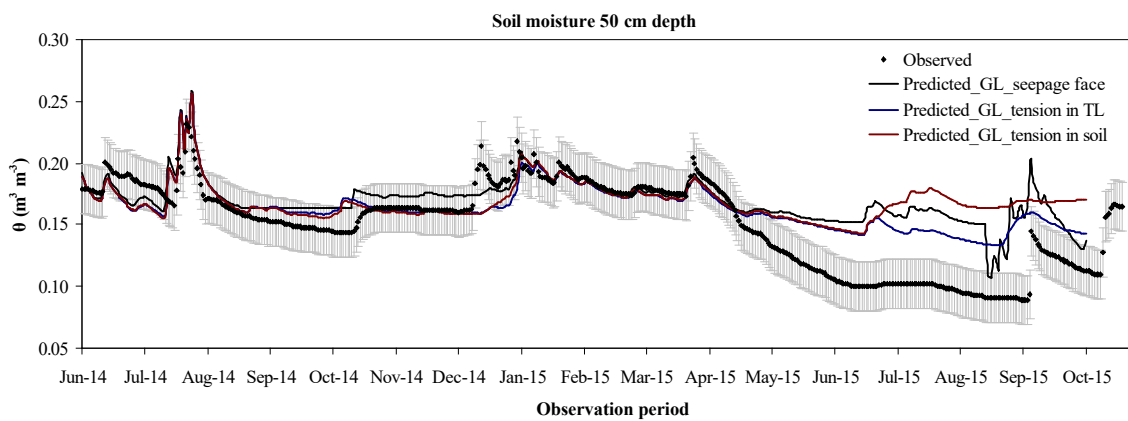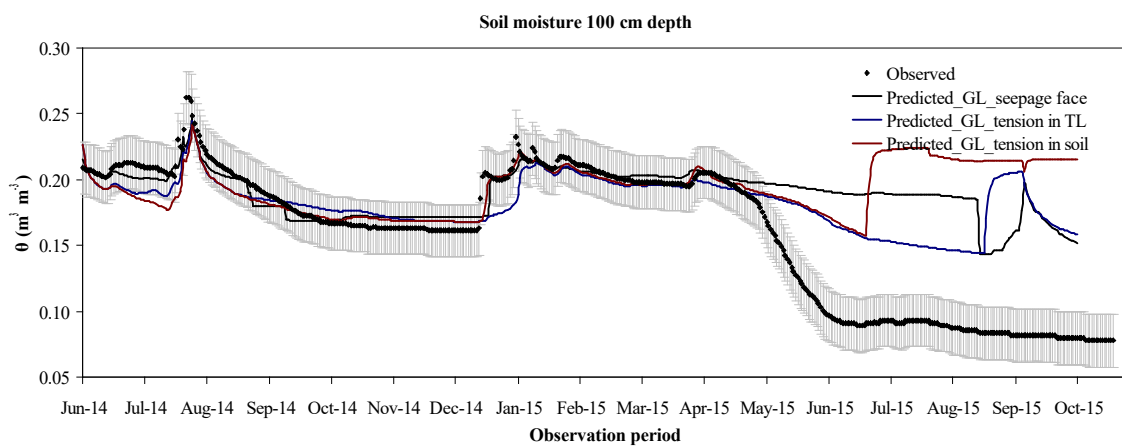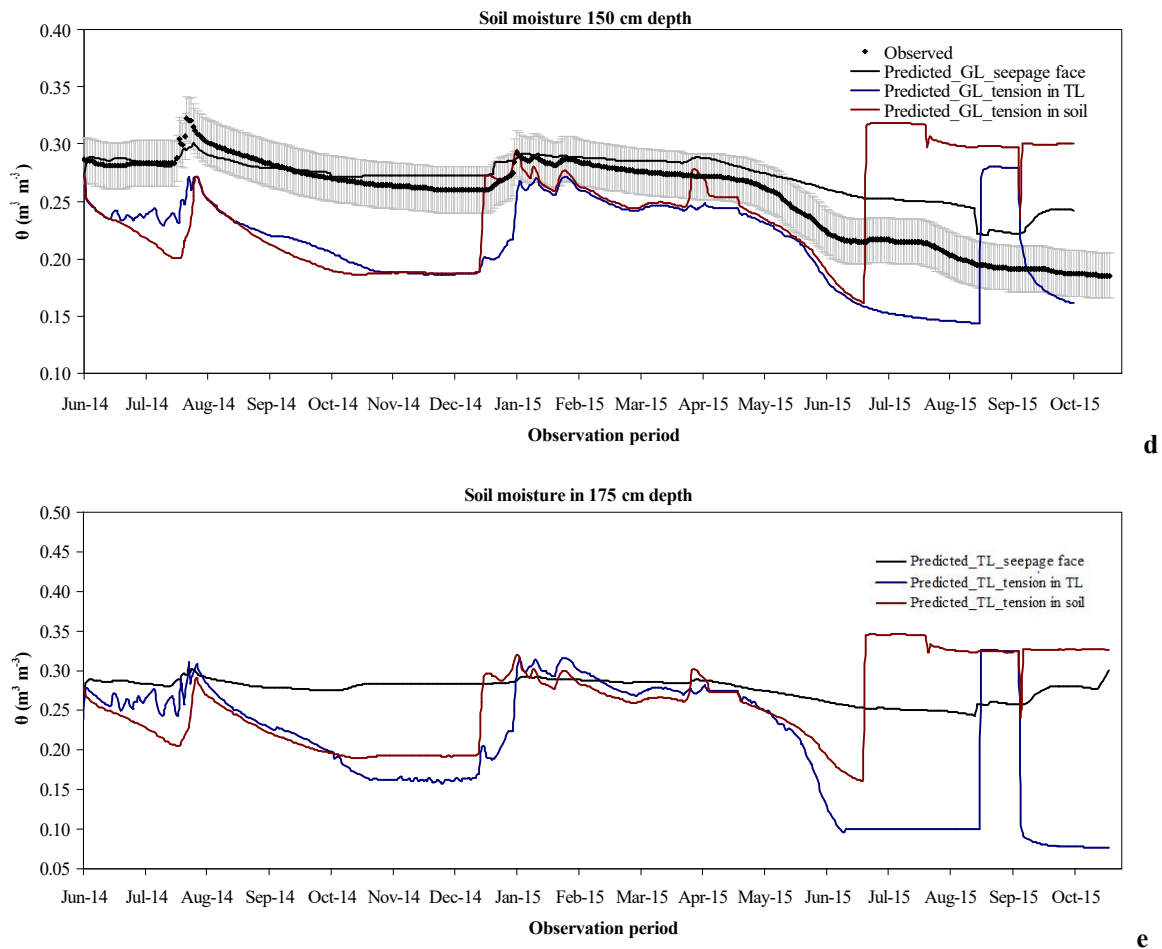
Figure 3.25: Observed and predicted soil moisture in 10 cm, 50 cm, 100 cm, 150 cm, and 175 cm depth of the GL-models with the lower boundaries seepage face, tension in TL, and tension in the surrounding soil (a-e).

The highest deviations between observed and predicted values were determined for soil moisture in 100 cm depth in sub period II. Both tension controlled GL-models lead to the conclusion that there is only a slightly impact of the type of lower boundary condition on the temporal course of soil moisture in 50 and 100 cm depth, whereas there is a significant impact on the water content in 150 cm depth (Figure 3.25). Thus, the tension-controlled models simulated a smaller water content in transition to the filter layer as compared to the seepage face model (Figure 3.25 e). Treating GL with a seepage face, implying natural gravitational flow, simulated a total outflow of 233.9 mm, corresponding very well to registered outflow (Figure 3.26, cf. Table 3.6).
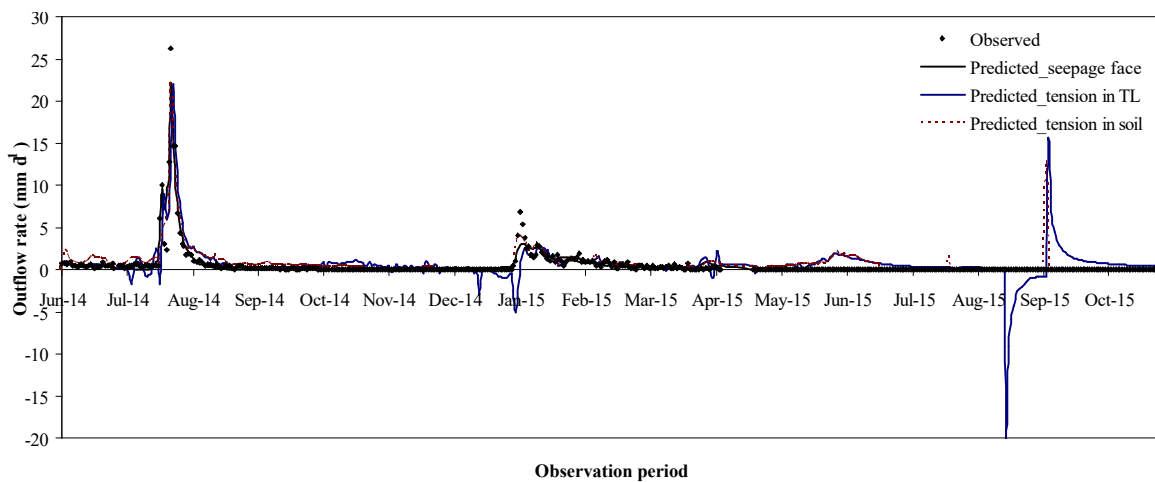
Figure 3.26: Observed and predicted daily outflow rates of the GL-models with the lower boundaries seepage face, tension in TL, and tension in the surrounding soil.

Correlation analysis between observed and predicted (seepage face) daily outflow rates revealed an R of 0.95, a gradient of the regression line of 0.95, NSE of 0.91 and n_t of 2.3, verifying the high model quality. Comparing monthly measured and simulated (seepage face) outflow rates, with NSE of 0.99, n_t of 11.38, a gradient of 1.00 and R of 1.00 a perfect fit could be determined. The GL-models with controlled lower boundaries simulated for "tension TL" 425.9 mm and for "tension soil" 352.4 mm. These results are not realistic and they are caused by wrong tension measurements in sub period II. For sub period I, both tension controlled models simulated a surplus of approximately 50 mm as compared to registered 234.4 mm. This was verifiable because the GL is free draining and thus, the tension controlled GL-models should of course calculate higher outflow rates.

4. <u>Discussion</u>

4.1 The transferability of lysimeter data to describe water flow on field scale

Comparing measured and modelled outflow rates of the NWGL and field BW reveals that the monthly discharge behavior on field scale could be described by the monthly discharge rates of simple constructed lysimeters with the preconditions, that not only meteorological data and agricultural management, but also pedo-hydrological conditions are comparable. Furthermore, not only measured rates, but also the HYDRUS model input parameters like stand precipitation, potential evaporation/ transpiration and resulting from this root water uptake, derived from NWGL measurements can be used to simulate the water flow of the investigated field BW for the whole observation period (cf. Figures 3.1, 3.5, 3.6). But as compared to HY 2013 and 2014, in HY 2015 neither measured outflow of the NWGL (49.2 mm) and the field (68.7 mm) corresponded with each other, nor the NWGL-model (89.0 mm) reproduced the measured discharge of the lysimeters (49.2 mm) in this time frame, although the model input parameters were determined at the NWGL (cf. Figure 3.4 a). Within this thesis, based on measurements and simulations various influencing parameters, which could lead to these deviations between both scales, were examined. Deviating outflow rates can be explained by the measured temporal course of discharging water. The NWGL generally fell dry during and after vegetation periods, whereas water still discharged from field BW (cf. Figure 3.1 a). This can be explained by two different aspects. On the one hand, capillary rise of water during vegetation periods is hindered because lysimeters are isolated blocks, and on the other hand, a water logged zone has to form at the bottom of the NWGL before water can discharge (Flury et al., 1999; Shirmohammadi et al., 2005; Gee et al., 2009; Wegehenkel and Gerke, 2015). But correlation analysis between monthly discharge rates from the NWGL and field BW for the first two HY revealed their comparability, yielding that these effects are not significant in HY 2013 and 2014 (cf. Figure 3.1 b, c). As already stated, although the unsaturated soil hydraulic properties of the NWGL filling material and the field BW soil are comparable, they are not the same, being a possible source for deviating outflow rates between both scales. Within the numerical simulations, the influence of different soil properties was taken into account via transferring the calibrated NWGL van Genuchten data, listed in Table 3.1, to the field model. Additionally, differences in precipitation registered at both testing sites were also examined because deviating P_{NWGL} and P_{field} would be the most evident reason for different discharge rates at both scales. The simulated results regarding the transferability of the unsaturated soil hydraulic properties as well as the comparison of precipitation revealed that these facts

do not explain smaller monthly outflow rates of the NWGL as compared to field BW in HY 2015. But the models were helpful to find the most appropriate reason therefore, which is in this case study a combination of heavy rain, wind and the ratio of surface cover fraction, height and relatively small surface of the investigated NWGL (cf. Figure 3.7). Thus, the main part of precipitation did not match the NWGL surface because the leaves of the cultivated maize protruded beyond the NWGL edge. Implementing this modified precipitation ($P_{modified}$) in the NWGL-model, excluding heavy rain in July and August 2014, the calculated discharge in HY 2015 (47.7 mm) fits to the measured outflow of 49.2 mm. Regardless of the in literature highlighted impact of the lower boundary condition, either tension-controlled or gravitation lysimeters would show the same error, which depends mainly on the type of the cultivated crop. A disadvantage of lysimeter measurements is their size in combination with the height and planophile behavior of the grown crop (Bavel et al., 1963; Allen et al., 1991; Allen et al., 2011). But surrounding the NWGL with the same vegetation that is cultivated on it, highlighted by Bavel et al. (1963), would not minimize this error. It is out of question, that weighable lysimeters are better suitable to record precipitation matching the surface of the lysimeter compared to the real amount of precipitation. But as stated by Meissner et al. (2007) weighable lysimeters, obtaining a large surface area, which would at least minimize the canopy effect, are expensive, increasing the maintenance requirements. Additionally, other factors like wind and evaporation losses would also lead to systematic errors in precipitation registration at weighable lysimeters. Thus, also here an appropriate data filtering is needed (Hoffmann et al., 2016). If simple constructed NWGL are present, measurement results can be used to characterize water flow on field scale when critically observing the development of the cultivated crop to describe deviating outflow rates at both scales. Surface cover fraction of the NWGL should be determined at least with a biweekly rhythm to ensure that protruding leaves would be taken into account in the case of rain events. Especially in the main vegetation period, around the edge of the NWGL surface precipitation collectors should be installed to record the amount of precipitation which did not match the surface due to dropping off from leaves. Furthermore, to exactly determine the amount of precipitation that matches the NWGL, a rain gauge directly on their surface should be installed. Additionally, due to the simple construction of NWGL (at least delivering outflow data but not registering mass changes which described not only outflow but also inflow) it is more liekly not to cultivate planophile plants, whereas the maximum height of the crop should not exceed the diameter of the NWGL surface. When using NWGL, it should be considered that they work like a

black box, only delivering in- and output data describing the water balance. Field meausrements are absolutely requiered to determine NO_3-N-losses from drained arable fields. But when critically observing all influencing parameters, being aware of possible errors, NWGL meausrements could be additionally used for hydrological studies and to determine water balance parameters.

4.2 The impact of soil heterogeneity on water flow and nitrogen-dynamic at field scale

The measured and modelled results clearly indicated that the pedo-hydrological properties of both fields differed. These properties mainly determine the flow regime and hydraulic residence times, influencing in this context NO_3-N-leaching.

Flow regime

The calibrated unsaturated soil hydraulic properties revealed a nearly impermeable layer from 10 to 30 cm depth in the top soil of field GW (cf. Figure 2.5 and Table 3.3, Layer 2). Thus, in contrast to field BW, ponding, surface runoff and a hindered percolation is of major concern. The soil of field BW shows constantly increasing clay content with increasing depth, being nearly impermeable in 1.25 m. But water percolates freely into the top soil. As a result, the discharge behavior between both fields has to be distinguished.

When evaluating the impact of agriculture on NO_3-N leaching via tile drains, according to Gooday et al. (2008), characterizing the flow regime and quantifying the amount of drained water is a precondition, because higher discharge rates correlate to higher discharged NO_3-N loads in general. Total drain flow from field GW (17.1 mm) was only 10 % as compared to field BW (150.2 mm) within the observation period of two HY. Because field BW is permeable at its surface but impermeable in 1.25 m depth, the whole amount of backwater, resulting from percolating seepage water, is discharged via drains. In contrast to that, at field GW, groundwater is the main component of the discharged drain water, whereas drain water is only affected by seepage water after heavy rain events. This was described within the numerical simulations by the implementation of a nearly impermeable layer 2 (cf. Tables 2.2, 3.3). The theory of a low permeable surface at this site was substantiated by the measured mean c_{NO3-N} in each compartment of both fields (see Table 3.2). Resulting from low hydraulic conductivities at field GW the flow velocities in the top soil are generally smaller as compared to field BW, influencing the N transformation.

Correlating discharge and rain events reveals a time delay of one to four days (depending on the intensity of precipitation) between precipitation and drain rate peak at both sites,

whereas higher drain peaks were measured at field BW as compared to field GW (cf. Fig. 3.11 a, b, c). But after a heavy rain event in June 2014, in contrast to field BW, at field GW no time delay between drain peak and rain event was registered, being a hint for a preferential flow here.

NO₃-N-transport

Because in HY 2014 and 2015 total drain flow at field GW was 10 % as compared to field BW, also the amount of discharged NO_3-N was only 10 % at this site as compared to field BW. These observations are in line with other studies of Warsta et al. (2013), reporting that the quantification of nutrient transport directly depends on the quantification of the water movement, whereas NO_3-N-leaching increases with an increasing drainage flow. But as illustrated in Figure 3.12, the NWGL measurements suggest that the general discharge behavior of field BW fits to this region with regard to the applied agricultural management, whereas there seems to be an impact at field GW.

But not only the amount of discharged NO_3-N and thus ecological interrelations, but also nutrient availability for plants and resulting from this yield development as an economical objective for agriculturalists is influenced by soil texture or soil moisture (Adamchuk et al., 2004). In this context, N uptake by plants is optimized at field BW as compared to field GW. This can be explained by the fact that the subsurface of field BW is homogenous, whereas the topsoil shows a relatively high hydraulic conductivity (0.5 to 0.14 m d^{-1} from 0 to 50 cm depth). At field GW, a low conductivity of 0.01 m d^{-1} in the top soil is assumed whereas in addition to that the vertical and horizontal heterogeneous soil structure from sandy to compact and clayey yields in a hindered crop development. Although the soil at field GW shows higher soil moisture in general, dryer periods are compensated better at field BW due to a constantly increasing and higher clay content, whereas the water holding capacity, expressed by a and n, is optimized at field BW (see Table 2.2). Resulting from this, at field GW maize in 2014 showed a deficit of 95 kg N ha^{-1} and winter wheat in 2015 a deficit of 34 kg N ha^{-1} as compared to field BW, correlating to lower yields in 2014/2015 at field GW. Mean values of the investigated NWGL revealed a maize yield of 26.0 t ha^{-1} (+/- 3.4 t ha^{-1}) in 2014 and a winter wheat yield of 6.8 t ha^{-1} (+/- 0.4 t ha^{-1}) in 2015, being comparable to field BW. Whereby maize N-uptake in 2014 was underestimated as compared to field BW with 178.9 kg ha^{-1} (+/-27.4 kg ha^{-1}), winter wheat N-uptake (137.7 kg ha^{-1} (+/- 15.6 kg ha^{-1})) was lying in the range of both fields.

For the numerical simulations, atmospheric flux at the upper boundary and thus not only precipitation but also potential evaporation, transpiration and root water uptake was equal for field BW and GW. Because the model was calibrated and validated successfully with the assumption of an equal plant development although the yields are different, it can be assumed that the crop development is very heterogeneous at field GW in contrast to field BW.

Partially, crops develop as optimal as at field BW, whereas in certain areas at field GW development is hindered due to surface runoff and ponding. This was also reproducible on a purely visible level during field campaigns. Due to a smaller N-uptake by plants at field GW, deviations in N_{min} content in soil between both fields after harvest in December 2014 and August 2015 are reproducible (cf. Figure 3.8 a, b). As already stated, N_{min} was accumulated in the upper 30 cm of the soil at field GW, being with 78 kg ha^{-1} two times higher as compared to measured values of field BW. These results correspond very well to registered c_{NO3-N} in soil solution in 35 cm depth in January 2015 with 46.3 mg l^{-1} at field GW and 12.6 mg l^{-1} at field BW (cf. Figure 3.10 a, b).

As stated by Abdirashid et al. (2004), the different potentials of accumulating NO_3-N in the soil should be taken into account due to the fact that NO_3-N leaching is influenced by this. The higher c_{NO3-N} in 85 cm depth at field GW as compared to field BW for the vegetation period 2015 correlating to N_{min} measurements are enforcing the assumptions of a higher N-leaching potential at field GW, corresponding to studies of El-Sadek et al. (2002). But beside the flow regime also N-transformation processes might affect NO_3-N leaching in a relevant way. NO_3-N-leaching via drains is negatively correlated to N_{min} contents of the soil at field BW whereas no correlation between both is found at field GW suggesting different N transformation rates at both fields. During November 2013 until March 2014 a high amount of NO_3-N (18 kg N ha^{-1}) was discharged via drains at field BW which was associated with the observed decrease of N_{min} (19 kg N ha^{-1}) in soil in the same time (cf. Figure 3.8 a). At field GW, N_{min} content of the soil also decreased by 23 kg N ha^{-1} during hydrological winter. But in contrast to field BW only 1.8 kg N ha^{-1} were discharged via drains due to smaller drained water amounts and lower NO_3-concentrations. This is a clear indication for a possible denitrification at field GW. Additionally, SO_4-concentration in soil solution (85 cm depth) and groundwater (1 m depth) differed markedly at field GW with an increase of mean concentrations from 25.4 mg l^{-1} to 69.8 mg l^{-1} respectively. In contrast no differences between SO_4-concentrations in soil solution (85 cm depth) and backwater were observed at field BW (cf. Table 3.2). According to DVWK (1994) occur-

ring SO_4 concentrations of naturally groundwater are in the range of 20 to 50 mg L^{-1}. Kunkel et al. (2002) stated that higher values could result on the one hand due to agricultural use and on the other hand due to an iron-sulfide oxidation in reductive aquifers. Increasing SO_4-concentrations in groundwater could be an indication for reductive conditions and a pyrite oxidation, which is coupled to NO_3-N-reduction in natural water (Kölle et al., 1983; Ashok and Hait, 2015). This is confirmed by higher NO_3-N concentrations at field BW which were similarly high for soil solution, drained water and backwater (Table 3.2). In contrast at field GW, discharged water and groundwater showed very small concentrations (mean of 6.6 mg l^{-1} in drained water and 1.1 mg l^{-1} in groundwater) whereas in soil solution of 35, 60 and 85 cm depth markedly higher concentrations of 31.3, 34.3 and 36.5 mg l^{-1} were detected. It should be stated, that calculated denitrification k_{den} was comparable at both fields, illustrated in Figure 3.16. This can be explained by the fact, that the respective equations mainly use soil moisture and temperature as influencing parameters.

It should be concluded that restrictions with regard to water protection have to be adapted to site specific conditions (Refsgaard et al., 2014). This implies the site specific improvement of soil tillage and fertilization application with regard to spatial and temporal variations on field scale (Robert, 2002). Whereas NO_3-N-discharge is higher at field BW due to a higher drain rate, there is a potential risk at field GW. The by Abdirashid et al. (2004) highlighted effect, that the accumulation potential for NO_3-N in the soil, which is higher at field GW due to the nearly impermeable layer 2, also plays a major concern is reproduced in the presented case study. At this site, the potential for N-accumulation and a potential NO_3-N breakthrough during fall and winter is higher as compared to field BW. But the benefits at this site are that (i) the amount of discharged water is very small, (ii) groundwater is protected due to a nearly impermeable clay material and (iii) the soil shows a higher denitrification potential as compared to field BW due to a pyrite oxidation. Thus, at field GW NO_3-N is reduced naturally in contrast to field BW.

Mainly in quaternary shaped landscapes, which also characterize the subsurface of the fields in the presented study, soil heterogeneity is of major concern. As highlighted by Refsgaard et al. (2014), water flow and solute transport at catchment scale models should obtain the predictive capability on small spatial scales in order to provide support for agricultural management decisions. Furthermore, according to Refsgaard et al. (2014), characterizing robust (higher denitrification potential) and vulnerable sites with regard to NO_3-N-leaching is of great importance because it would be more expedient and cost effective to adopt restrictions at areas, where no subsurface nitrate degradation takes place naturally.

As stated by Warsta et al. (2013), the local scale and especially local tile-drain network has a key impact on groundwater and surface water flow. As a result, each case is unique.

It is out of question that describing NO_3-N-transformation and transport is a multidisciplinary problem. In this context, several scientific fields like hydrology, hydrological engineering, physical chemistry or microbiology should be combined to examine the different processes and to develop scientifically based predictive models that can be used for a general application at different pedological, hydrological, climatically or management conditions. Within this study, it is focused mainly on the pedo-hydrological and the agronomic aspect. Based on the results it can be stated that different pedo-hydrological properties lead to a deviating flow regime, and deviating flow velocities, which have a significant impact on the NO_3-N-transport and N-transformation (Jury and Nielson, 1989; Pärn et al., 2012; Filipovic et al., 2014). Constantly high c_{NO3-N} in soil solution, drained water, and backwater of field BW suggest low residence times for water and resulting from this, missing denitrification. Thus, the main part of NO_3-N passing the root zone is intercepted by the drains, being discharged to surface waters (David et al., 1997; Hatfield et al., 1999; Blann et al., 2009; Warsta et al., 2013). In contrast to that, at field GW percolation is hindered. Furthermore high SO_4 concentrations in combination with low c_{NO3-N} and a visible iron clogging at the drain outlet are a clear indication for reductive conditions and pyrite oxidation with a coupled NO_3-N-reduction (Kölle et al., 1983; Ashok and Hait, 2015). Only based on the simplified water flow model, the key differences between both sites could be determined.

4.3 Combined lysimeter measurements and simplified simulations to predict water flow and nitrogen-transport at field scale with spatial soil heterogeneity

The possibility of directly upscaling measurement results from NWGL to describe the water balance of field BW was already discussed in chapter 4.1. This transferability is ensured because of the comparability of their pedo-hydrological conditions.

Additionally, based on the NWGL measurements and the resulting calculated atmospheric flux and root water uptake, numerical simulations, combining both fields BW and GW, were performed. The upper boundary suggests a homogeneous development of the plants at both sites, whereby it was reproducible during field campaigns, that field GW showed a very heterogeneous plant development. Furthermore, as described in chapter 4.2, not only yield but also N-uptake by plants was optimized at field BW as compared to GW. But the field BW-GW-model was successfully calibrated and validated with the assumed atmos-

pheric flux and "homogeneous" root water uptake, determined at the NWGL. Thus, only via implementing the specific soil physical properties (Table 2.2) and calibrated van Genuchten parameters (Table 3.3), depth depending soil moisture at each field as well as monthly outflow rates were simulated adequately (cf. Figures 3.9, 3.15).

The water flow and the simplified transport model showed, that deviations in the depth depending concentration and N-leaching result because of different soil properties in general, whereas c_{NO3-N} was higher at field BW as compared to field GW. But rapid changes in c_{NO3-N} between soil solution and groundwater at field GW could not be reproduced with the model (cf. Figure 3.17 a, b). Because a conservative component was assumed, no denitrification was implemented in the numerical simulations. This leads to deviations for the measured and the modelled relationship between c_{NO3-N} in soil solution, drained water and groundwater, being a hint for deviating transformation rates. These deviations were already explained by a pyrite oxidation at field GW.

When focusing on a site-specific N-management as a requirement to fulfill the objectives of the water protection policy, it is not possible to carry out separate case studies and further numerical simulations for every site-specific problem, because it is time and cost consuming. Schepper et al. (2015) summarize simplifications in numerical simulations with regard to the impact of small scale soil-heterogeneity on tile-drains. In this context for more robust areas, simplified local scale models should be used with a smaller temporal resolution of influencing parameters, a coarser mesh and simplified numerical implementation of drain layers. In contrast to that, at vulnerable areas, detailed meshes or dual porosity concepts are recommended for more detailed studies on solute transport.

These approaches could be combined with each other, and NWGL-measurements could be used as point information for larger hydrological scales like catchment scale models.

To make generalizations and to draw conclusions, a multidisciplinary approach for considering the specific impact of influencing parameters on NO_3-N-transformation and leaching is absolutely required. Measurements at different scales from laboratory via lysimeter and field to catchment scale, and further numerical simulations from detailed to simplified would be helpful to determine key processes and make generalizations in order to predict the influence of soil heterogeneity on NO_3-N-losses from subsurface tile drainage.

4.4 Advantages and drawbacks of recent lysimeter technologies

The most controversially discussed aspect in literature when examining the reliability of lysimeter measurements to predict the flow regime of larger scales is their lower boundary condition, which could be tension-controlled or gravitational. In this context, the reliable reproducibility of data, gathered from gravitation lysimeters is questioned in general. But within the second lysimeter study in Müncheberg (Brandenburg), the measurements and the numerical simulations reveal that the advantages of a tension controlled lower boundary, which could be reproduced within the presented study, were nogated by the technical problems in tension regulation. As compared to gravitational devices, the main advantage of tension controlled lysimeters is their more natural hydraulic gradient because the pressure head at their lower boundary is adjusted to measured tension at the same depth in the surrounding field soil (Groh et al., 2016). Based on measurements and simulations it was proven, to which extend the type of the lower boundary condition influences the water balance of the respective lysimeter devices, and if a dynamic tension control involves an increasing reliability of lysimeter measuring results.

Measured pressure head (cf. Figure 3.20 a, b) indicated wetter conditions at the lower boundary of the GL, which could be examined by the modelled soil moisture in transition to the filter layer (Figure 3.23 e, 3.25 e). Thus, the seepage face treated TL- and GL-models simulated a higher water content in this depth as compared to the tension controlled TL- and GL-models (Figure 3.23 e; Figure 3.25 e). These results correspond to studies of Abdou and Flury (2004), providing that tension controlled lysimeters with fixed or variable tension would prevent wetter zones above the drain face. Another benefit of a tension control, which was also reproducible within the study, is that drain flow is more continuous as compared to gravitation lysimeters. Whereas from October until December 2014 the GL fell totally dry, from the TL water was still discharged in this time frame (cf. Figure 3.18 a, Table 3.6). These results are in line with studies of Vereecken and Dust (1998), Zhu et al. (2002) or Abdou and Flury (2004) and could be reproduced by the measurements and the tension controlled TL- and GL-models (cf. Table 3.6). Furthermore, the lysimeter experiments in the Altmark region also revealed, that the NWGL fell dry during and after vegetation periods, whereas water was continuously discharged from the investigated fields (cf. Figure 3.1 a).

Despite Abdou and Flury (2004), Gee et al. (2009) or Peters and Durner (2009), stating that the leachate flux of gravitation lysimeters is underestimated as compared to tension-controlled devices, a deficit of 37.2 mm was measured from the TL (197.2 mm) as com-

pared to the GL (234.4 mm) for the whole observation period. This deficit resulted mainly from deviating outflow rates in January 2015, whereas from the TL 12.1 mm and from the GL 52.0 mm water was discharged (cf. Table 3.4). Barkle et al. (2014) stated that after rain fall the volume of drained water would be larger if near-saturation conditions exist in contrast to the undisturbed soil profile. These near saturation conditions were measured for the GL and simulated in both seepage face treated models (Figure 3.23 e, 3.25 e). But another important aspect in this context is that pressure head in the TL approached tension of the surrounding soil with a time delay (cf. Figure 3.20 a, b). Thus, from the TL water was discharged from January/19/2015 whereas the GL started discharging water from January/7/2015. Furthermore, the TL-model with "tension in TL" simulated an outflow of only 33.7 mm in January 2015, whereas the model "tension in soil" simulated 49.6 mm and the seepage face treated one 50.6 mm, fitting very well to measured outflow of the GL (52 mm) (Table 3.4). As a result, a higher outflow at the GL was not primary caused due to near saturation conditions. It was more likely that the TL outflow was reduced due to an inadequate and erroneous pumping system and tension control.

Not only measurements but also the numerical simulations show that a wrong tension registration leads to unreliable data. Treating the TL-model with "tension in soil" revealed an outflow of 57.6 mm in sub period II, whereby with "tension TL" 179.1 mm were calculated in this time frame, being unrealistic. In contrast to that, for the first sub period, 255.9 mm ("tension TL") and 266.3 mm ("tension soil") were calculated, being verifiable. At the GL-model treated with a tension control, for the first sub period 281.6 mm ("tension TL") and 291.5 mm ("tension soil") were calculated, whereas here also in the second sub period 144.3 mm and 60.8 mm water should have been discharged, being again not realistic. The GL-model with a seepage face reproduced measured outflow with 233.9 mm (cf. Table 3.6).

A disadvantage of lysimeter devices with variable tension is not only the fact that they are expensive and difficult to install, but also an increase in maintenance requirements, stated by Weihermüller et al. (2007). The correct control of the lower lysimeter boundary directly depends on the correct registration of the pressure head. Tension measured in the TL was wrong from May 2015 because the minimum pressure range (-85 kPa = -8.5 m) was exceeded due to dryness. After that unreasonable values were measured.

Regarding the whole observation period, the comparison of measured daily and mainly monthly outflow rates of TL and GL provide that the data series correlate with each other (cf. Figure 3.18 a, b), corresponding to studies of Meissner et al. (2010) that there are no

significant differences between both lysimeter types for larger observation periods. Furthermore, by switching the boundary conditions in each model it could be proven, that the temporal course of soil moisture in the upper 50 cm of the devices is not influenced by the type of lower boundary condition whereas a significant impact from 100 cm depth is examined (cf. Figure 3.23 c, d; Figure 3.25 c, d). Treating both, the TL- and the GL-model with a seepage face, regarding their total outflow a difference of 30 mm between the TL (seepage face) and the GL would result although the pedo-hydrological properties were comparable. As already mentioned for the experiments, the lysimeters were filled non-monolithically to exclude natural occurring heterogeneity. But in this context, it should be questioned if the impact of spatial heterogeneity would cover the potential impact of the lower boundary on deviating outflow rates in general.

Both lysimeter types obtain their specific disadvantages, not only for hydrological but also for solute transport questions. Due to the near-saturation conditions at GL anaerobic conditions could occur on the bottom which could influence solute reaction. But in accordance with Weihermüller et al. (2007) also at TL, there is an impact on the solute behavior and reactions due to the material of the investigated suction cups and the influence of the steering procedure to establish the natural equivalent pressure head. The experimental and techniqual setup depends on the specific scientific question. But the technical ambicious tension controlled boundary could only hardly be implemented when lysimeters are installed at regions, were the performance of the registration and controll system is not continously monitored. For long term measurements with a generally small temporal resolution of observed data, gravitation lysimeters would also deliver reliable data and could be used for awnsering practical hydrological questions.

This could also be examined within the experimental studies in the Altmark region. Thus, not only the transferability of meausred data from the NWGL to field BW, but also the application of the NWGL data as point information to numerically describe water flow of field BW and GW was verified.

5. __Conclusions__

Within two separate studies, the transferability and the reliability of data, measured with different lysimeter types, to predict the flow regime of larger scales was evaluated.

The coupled NWGL experiments and field trials in Saxony-Anhalt served to examine the possibility to directly upscale measured and modelled NWGL data to predict the water flow of two neighboring tile-drained arable fields.

Additionally, the impact of heterogeneous pedo-hydrological properties on NO_3-N-leaching via drains was determined because one field is backwater influenced (field BW), corresponding to the flow regime of the NWGL, and the other field shows confined groundwater conditions (field GW). In this context, it was proven if the measured NWGL data can only be used to describe the flow regime of field BW, or if these data can be implemented as point information to numerically describe the water regime of both, field BW and field GW.

The review of actual literature provides that the application of gravitation lysimeters to predict the water regime of larger scales is questioned in general due to their free draining lower boundary. But it should be noted, that the NWGL were mainly constructed to answer practical questions with regard to water protection. Therefore, the evaluation of the monthly discharge behavior is sufficient. The in literature highlighted impact of the lower boundary condition on the discharge behavior of lysimeters is mainly important when evaluating and upscaling registered values with a daily temporal resolution or even higher. In this context, another lysimeter experiment in Brandenburg, comparing the flow regime of a tension-controlled and a gravitation lysimeter was performed, revealing information about the impact of the lower boundary on the depth depending course of soil moisture and the daily discharge behavior. Resulting from both studies and regarding the three main objectives the following conclusions were drawn.

Could measurement data from simple constructed non-weighable gravitation lysimeters (NWGL) be transferred to describe the water flow on field scale?

- Directly describing the monthly water balance on field scale with the measured water balances of the simple constructed lysimeters is possible on the conditions, that not only meteorological parameters and agricultural management but also pedo-hydrological conditions between NWGL and field site are comparable. This is achieved by the comparability of monthly discharge rates of the NWGL and field BW in HY 2013 and 2014.

- A disadvantage of the simple design of the investigated NWGL is clarified with the measured deficit in the water balance of the NWGL as compared to the field BW in the third HY 2015. This deficit was induced by a canopy effect, caused by the plano-phile grown maize and heavy rain events in the main vegetation period, whereas precipitation did not match the NWGL surface.

- The development stages of the cultivated crop have to be observed regularly and critically when determining the real stand precipitation to interpret measured outflow differences between both scales. Rain gauges on and surrounding the NWGL should be installed due to the missing weighing mechanism because this would optimize the reliable reproducibility of the measurements.

- Further research is necessary to examine the canopy effect to guarantee the integrative interpretation of deviating outflow rates at both scales.

- The impact of the lower boundary condition on the monthly discharge behavior of the lysimeters does not play a concern in this study.

To which extend do different soil properties influence the water balance and the resulting N-dynamic at drained arable fields and could NWGL-measurements be used as point information for further field scale simulations?

In general, experiments and models describing the role of drains on a national level suggest that tile drains are one of the major sources for diffuse N inputs into surface waters. Additionally, the investigations described in this thesis showed that

- Different soil properties on field scale mainly affect the water flow regime and resulting NO_3-N-leaching, whereas agricultural management is of minor importance for the observed differences at both considered fields BW and GW.

- The compliance with authorized threshold values for nitrate in groundwater ($NO_3^- = 50$ mg l^{-1} →NO_3-N=11.3 mg l^{-1}) in agricultural practice is very difficult because restrictions for agricultural management are not enough site specific. A spatial adaption of management strategies is absolutely required to fulfill the objectives of the EU Water Framework Directive. At field GW, a fertilization that conform the regulations of best management practice would be sufficient due to the small amount of discharged NO_3-N, whereas fertilization and agricultural management at field BW should be optimized to reduce N-losses.

- Further investigations regarding N-transformation, mainly pyrite oxidation in combination with NO_3-N-degradation and leaching are mandatory to understand the impact of the site-specific effect at field scale and to transfer it to catchment scale.

- Separate case studies for every site-specific problem are not workable because it would be not only cost but mainly time consuming. Thus, further research is required to draw generalizations on NO_3-N-transport and transformations in dependence of the pedo-hydrological and site-specific conditions.

- Not only field BW, but also the water flow of the combined model field BW-GW was simulated adequately based on the NWGL-measurements. Although the model input parameters suggest homogeneous plant development and root water uptake, which was clearly not the case, the simulations could describe the real flow regime of both sites.

- Based on soil maps, areas can be classified into robust and vulnerable. Only a minimum number of soil samples and analyses, delivering at least the basic soil physical properties of the respective fields are needed to describe the internal structure of a modeling domain. The other input data describing the boundary conditions at the borders can be determined at the NWGL.

- The combination of NWGL data and simplified simulations would be an efficient approach to examine the impact of drains on discharged NO_3-N-loads under heterogeneous soil conditions.

Does the development of technically ambitious lysimeter techniques optimize the reliability of lysimeter data to predict water flow on field scale?

- Within the presented lysimeter study in Müncheberg, the impact of the lower boundary on the water balance could be reproduced.

- Inside the tension controlled lysimeter TL, a depth depending hydraulic gradient was measured that was closer to field conditions as compared to the hydraulic gradient inside the GL, where generally wetter conditions above the drain face were registered.

- Reliable data from tension controlled lysimeter systems can only be guaranteed when these devices are continuously and critically supervised to examine different error sources. Currently, it seems that the available technical solutions for a dynamic tension-controlled bottom boundary are not sufficient and further research is necessary to solve this problem.

- In general, tension-measurements on field scale, being the basis for tension-regulation of a TL, also contain several errors, which are then directly transferred to the con-

trolled lysimeters. Furthermore, the measurements only provide point information. Spatial heterogeneity is not taken into account, whereby only the specific probe installation location at the field is described, not being spatially representing another point.

- The advantages of gravitation lysimeters in general are their simple design in combination with the steadiness they are working and delivering data. For long-term measurements with smaller temporal data resolutions which are often used to answer more practical, hydrological questions, simple constructed GL could be applied.

- If these simple lysimeters are deep enough, overcoming the natural zero flux plane, the impact of the lower boundary type on the water balance inside the upper root zone, where root water uptake and thus evaporation and transpiration occurs, could be minimized

- For scientific issues, often requiring data from relatively short observation periods but with a very high temporal resolution, TL data are absolutely required. But the tension-controlled system should be supervised continuously during measurement campaigns.

6. **References**

91/676/EWG (1991). Richtlinie zum Schutz der Gewässer vor Verunreinigung durch Nitrat aus landwirtschaftlichen Quellen.

2000/60/EG (2000). Richtlinie zur Schaffung eines Ordnungsrahmens für Maßnahmen der Gemeinschaft im Bereich der Wasserpolitik.

2006/118/EG (2006). Richtlinie zum Schutz des Grundwassers vor Verschmutzung und Verschlechterung.

Abdirashid, E., Madramootoo, C., Egeh, M. & Hamel, C. (2004). Water and fertilizer nitrogen management to minimize nitrate pollution from a cropped soil in southwestern Quebec, Canada. *Water, Air and Soil Pol.*, 151, 117-134.

Abdou, H.M. & Flury, M. (2004). Simulation of water flow and solute transport in free-drainage lysimeters and field soils with heterogenous structures. *Eur. J. Soil Sci.*, 55, 229-241.

Ackermann, A. (2016). Simulation des Austrags von gelöstem organischen Kohlenstoff aus landwirtschaftlich genutzten Mineralböden. PhD Thesis, Helmholtz Centre for Environmental Research-UFZ, 144 pp.

Adamchuk, V.I., Hummel, J.W., Morgan, M.T. & Upadhyaya, S.K. (2004). On-the-go soil sensors for precision agriculture. *Computers and Electronics in Agriculture*, 44, 71-91.

Allen, R.G., Pereira, L.S., Howell, T.A. & Jensen, M.E. (2011). Evapotranspiration information reporting: I. Factors governing measurement accuracy. *Agr. Water Manage.*, 98, 899-920.

Allen, R.G., Pereira, L.S., Raes, D. & Smith, M. (1998). Crop evapotranspiration: guidelines for computing crop water requirements. Irrig. Drain. Rome: FAO.

Allen, R.G., Pruitt, W.O., Jensen, M.E. & Burman, R.D. (1991). Environmental requirements of lysimeters. In: Allen, R.G., T.A. Howell, W.O. Pruitt, I.A. Walter, M.E. Jensen (Eds.), Lysimeters for Evapotranspiration and Environmental Measurements, Proc. Int. Symp. Lysimetry. ASCE, New York.

Ashok, V. & Hait, S. (2015). Remediation of nitrate-contaminated water by solid-phase denitrification processes-a review. *Environ. Sci. Pollut. Res.*, 22, 8075-8093.

Barkle, G.F., Wöhling, T. & Stenger, R. (2014). Variability of unsaturated Bromide fluxes as measured through a layered volcanic vadose zone in New Zealand. *Hydrol. Process.*, 28, 6080-6097.

Bavel, C.H.M., Fritschen, L.J. & Reeves, W.E. (1963). Transpiration by sudangrass as an externally controlled process. *Science*, 141, 269-270.

Bednorz, D., Tauchnitz, N., Christen, O., Rupp, H. & Meissner, R. (2016). The impact of soil heterogeneity on nitrate dynamic and losses in tile-drained arable fields. *Water Air Soil Pol.*, 227(295), 1-18.

Bergström, L.F. (1990). Use of lysimeters to estimate leaching of pesticides in agricultural soils. *Environ. Pollut.*, 67, 325-347.

BGR. (2007). Bodenarten der Böden Deutschlands - Bericht über länderübergreifende Auswertungen von Punktinformationen im FISBo BGR.

Blann, K.L., Anderson, J.L., Sands, J.R. & Vondracek, B. (2009). Effects of agricultural drainage on aquatic ecosystems: a review. *Crit. Rev. Environ. Sci. Technol.*, 39, 909-1001.

BMU & BMELV. (2012). Nitratbericht 2012 - Gemeinsamer Bericht der Bundesministerien für Umwelt, Naturschutz und Reaktorsicherheit sowie für Ernährung, Landwirtschaft und Verbraucherschutz.

Burkart, M.R. & Stoner, J.D. (2008). Nitrogen in groundwater associated with agricultural systems. In: Hatfield, N.L., R.F. Follett (Eds.), *Nitrogen in the Environment: Sources, Problems, and Management* (pp. 177-202). Amsterdam, Niederlande: Elsevier.

Carbon, F., Girard, G. & Ledoux, E. (1991). Modelling of the nitrogen cycle in farm land areas. *Fert. Res.*, 27, 161-169.

David, M.B., Gentry, L.E., Kovacic, D.A. & Smith, K.M. (1997). Nitrogen balance in and export from an agricultural watershed. *J. Environ. Qual.*, 26, 1038-1048.

DIN-4049-3 (1994). Hydrology - Part 3: Terms for the quantitative hydrology: Beuth.

DIN-18130-1 (1998). Soil - investigation and testing; Determination of the coefficient of water permeability - Part 1: Laboratory tests. Beuth.

DIN-EN-1484 (1997). Water analysis - Guidelines for the determination of total organic carbon (TOC) and dissolved organic carbon (DOC). Beuth.

DIN-EN-ISO-10304-1 (2009). Water quality - Determination of dissolved anions by liquid chromatography of ions - Part 1: Determination of bromide, chloride, fluoride, nitrate, nitrite, phosphate and sulfate. Beuth.

DIN-EN-ISO-10523 (2012). Water quality - Determination of pH. Beuth.

DIN-EN-ISO-16634-1 (2008). Food products - Determination of the total nitrogen content by combustion according to the Dumas principle and calculation of the crude protein content - Part 1: Oilseeds and animal feeding stuffs. Beuth.

DIN-ISO-11274. (2009). Soil quality - Determination of the water retention characteristics - Laboratory methods Beuth.

DIN-ISO-11277 (2002). Soil quality - Determination of particle size distribution in mineral soil material - Method by sieving and sedimentation: Beuth.

Dinnes, D.L., Karlen, D.L., Jaynes, D.B., Kaspar, T.C., Hatfield, J.L., Colvin, T.S. & Cambardella, C.A. (2002). Review and Interpretation: Nitrogen Management Strategies to Reduce Nitrate Leaching in Tile-Drained Midwestern Soils, USDA-ARS/ UNL Faculty.

Dommermuth, H. & Trampf, W. (1991). Die Verdunstung in der Bundesrepublik 1951 bis 1980, Teile 1 - 3 Offenbach, Germany: Deutscher Wetterdienst-Eigenverlag.

DVWK (1994). Auswertung und Bewertung von Grundwasserproben. DVWK.

DVWK (1996). Ermittlung der Verdunstung von Land- und Wasserflächen. DVWK-Merkblätter für die Wasserwirtschaft Hamburg, Germany: Parey.

DWA (2012). Merkblatt DWA-M 905 - Gewinnung von Bodenlösung - Beprobungssysteme und EinflussgrößenGermany: DWA.

Feddes, R.A., Kowalik, P.J. & Zarandny, H. (1978). Simulation of field water use and crop yield. New York: John Wiley & Sons.

Filipovic, V., Coquet, Y., Pot, V., Houot, S. & Benoit, P. (2014). Modelling the effect of soil structure on water flow and isoproturon dynamics in an agricultural field receiving repeated urban waste compost application. *Sci. Total. Environ.*, 499, 546-559.

Finners, H., Grottenthaler, W., Kühn, D. & Eckelmann, W. (2005). Bodenkundliche Kartieranleitung: Schweizerbart'sche Verlagsbuchhandlung.

Flury, F., Yates, M.V. & Jury, W.A. (1999). Numerical analysis of the effect of the lower boundary condition on solute transport in lysimeters. *Soil Sci. Soc. Am. J.*, 63, 1493-1499.

Follett, R.F. (2004). Nitrogen transformation and transport processes. In: Follett, R.F., J.L. Hatfield (Eds.), *Nitrogen in the Environment: Sources, Problems, and Management* (pp. 17-44). Amsterdam: Elsevier.

Gebler, S., Hendricks-Franssen, H.-J., Pütz, T., Post, H. & Schmidt, M.V., H. . (2015). Actual evapotranspiration and precipitation measured by lysimeters: a comparison with eddy covariance and tipping bucket. *Hydrol. Earth Syst. Sc.*, 19, 2145-2161.

Gee, G.W., Newman, B.D., Green, S.R., Meissner, R., Rupp, H., Zhang, Z.F., Keller, J.M., Waugh, W.J., Velde, M.v.d. & Salazar, J. (2009). Passive wick fluxmeters: design considerations and field applications. *Water Resour. Res.*, 45, 1-18.

Godlinski, F. (2005). Abschätzung der Phosphorausträge aus der ungesättigten Bodenzone anhand numerischer Interpretationen von Lysimeterversuchen. PhD Thesis, Universität Rostock, Germany, 168 pp.

Gooday, R., Anthony, S. & Fawcett, L. (2008). A field scale model of soil drainage and nitrate leaching for application in nitrate vulnerable zones. *Environ. Modell. Softw.*, 23, 1045-1055.

Goss, M.J., Howse, K.R., Lange, P.W., Christian, D.G. & Harris, G.L. (1993). Losses of nitrate-nitrogen in water draining from under autumn-sown crops established by direct drilling or mouldboard ploughing. *J. Soil Sci.*, 44, 35-48.

Greco, G. (2006). Mesocosm - technical manual. Centro Regionale die Competenza Universita degli Studi die Napoli Federico II: Napoli Italy.

Groh, J., Vanderborght, J., Pütz, T. & Vereecken, H. (2016). How to controll the lysimeter bottom boundary to investigate the effect of climate change on soil processes? *Vadose Zone J.*, 15(7), 1-15.

Gusman, A.J. & Marino, M.A. (1999). Analytical modeling of nitrogen dynamics in soils and groundwater. *J. Irrig. Drain. E. - ASCE*, 125(6), 330-337.

Haferkorn, U. (2000). Größen des Wasserhaushaltes verschiedener Böden unter landwirtschaftlicher Nutzung im klimatischen Grenzraum des Mitteldeutschen Trockengebietes - Ergebnisse der Lysimterstation Brandis, Georg-August-University, Göttingen.

Hagenau, J., Meissner, R. & Borg, H. (2015). Effect of exposure on the water balance of two identical lysimeters. *J. Hydrol.*, 520, 69-74.

Harmel, R.D. & Smith, P.K. (2007). Consideration of measurement uncertainty in the evaluation of goodness-of-fit in hydrologic and water quality modelling. *J. Hydol.*, 337, 326-336.

Hatfield, J.L., Jaynes, D.B., Burkart, M.R., Cambardella, C.A., Morman, T.B., Brueger, J.H. & Smith, M.A. (1999). Water quality in Walnus Creek watershed: Setting and farming pracices. *J. Environ. Qual.*, 28, 11-24.

Heumann, S., Ringe, H. & Böttcher, J. (2011a). Field-specific simulations of net N mineralization based on digitally available soil and weather data. I. Temperature and soil water dependency. *Nutr Cycl Agroecosyst*, 91, 219-234.

Heumann, S., Ringe, H. & Böttcher, J. (2011b). Field-specific simulations of net N mineralization based on digitally available soil and weather data. II. Pedotransfer functions for the pool sizes. *Nutr Cycl Agroecosyst*, 91, 339-350.

Hoffmann, M., Schwartengräber, R., Wessolek, G. & Peters, A. (2016). Comparison of simple rain gauge measurements with precision lysimeter data. *Atmos. Res.*, 174-175, 120-123.

Johnson, D.W., Walker, R.F. & Ball, J.T. (1995). Lessons from lysimeters: Soil N release from disturbance compromises controlled environmental study. *Ecol. Appl.*, 5, 395-400.

Jury, W.A. & Nielson, D.R. (1989). Nitrate transport and leaching mechanism. In: Follett, R.F. (Ed.), *Nitrogen Management and Ground Water Protection* (pp. 139-157). Amsterdam: Elsevier Sci. Pubs.

Kahle, P. & Mehl, D. (2014). Nitrataustäge über Dränung landwirtschaftlich genutzter Böden in Mecklenburg-Vorpommern-Fallstudien. *Korrespondenz Wasserwirtschaft*, 7, 198-205.

Kersebaum, K.C. & Richter, J. (1991). Modelling nitrogen dynamics in a plant-soil system with a simple model for advisory purposes. *Fert. Res.*, 27, 273-281.

Knoblauch, S. (2009). Langjährige Ergebnisse über das pflanzliche Aneignungsvermögen von Bodenwasser landwirtschaftlicher Kulturen in einem tiefgründigen Braunerde-Tschernosem aus Löß, Proccedings of the 13th Lysimeter Conference. LFZ, Gumpenstein, Austria, pp. 131-136.

Kölle, W., Werner, P., Strebel, O. & Böttcher, J. (1983). Denitrifikation in einem reduzierenden

Grundwasserleiter. *Vom Wasser*, 61, 125-146.

Krause, P., Boyle, D.P. & Bäse, E. (2005). Comparison of different efficiency criteria for hydrological model assessment. *Adv. Geosci.*, 5, 89-97.

Kunkel, R., Hannappel, S., Voigt, H.J. & Wendland, F. (2002). Die natürliche Grundwasserbeschaffenheit ausgewählter hydrostratigraphischer Einheiten Deutschlands. Forschungszentrum Jülich/ HYDOR Consult GmbH/ Brandenburgisch-Technische Universität Cottbus.

LAGB. (1999). Bodenatlas Sachsen-Anhalt.

LAGB. (2003). GK 25 - Geologische Karte 1:25000.

Lanthaler, C. & Fank, J. (2005). Lysimeterstations and soil hydrology measuring sites in Europe - results of a 2004 survey, *11. Gumpensteiner Lysimetertagung* (pp. 19-24). Raumberg-Gumpenstein: LFZ.

Legates, D.R. & McCabe, G.J. (1999). Evaluating the use of "goodness-of-fit" measures in hydrologic and hydroclimatic model validation. *Water Resour. Res.*, 35(1), 233-241.

Leterme, B. & Mallants, D. (2011). Climate and Land Use Change impacts on groundwater recharge, ModelCare.

Marchetti, R., Donatelli, M. & Spallacci, P. (1997). Testing denitrification functions of dynamic crop models. *J. Environ. Qual.*, 26, 394-401.

Meissner, R., Rupp, H., Seeger, J., Ollesch, G. & Gee, G.W. (2010). A comparison of water flux measurements: passive wick-samplers versus drainage lysimeters. *Eur. J. Soil Sci.*, 61, 609-621.

Meissner, R., Rupp, H. & Seyfarth, M. (2014). Advanced Technologies in Lysimetry. In: Mueller, L., A. Saparov, G. Lischeid (Eds.), *Novel Measurement and Assessment Tools for Monitoring and Management of Land and Water Resources in Agricultural Landscapes of Central Asia* (pp. 159-173). Switzerland: Springer.

Meissner, R., Seeger, J., Rupp, H., Seyfarth, M. & Borg, H. (2007). Measurement of dew, fog, and rime with a high precision gravitation lysimeter. *J. Plant Nutr. Soil Sci.*, 170, 335-344.

Meurer, K.H.E., Prasuhn, V., Iden, S.C. & Durner, W. (2013). Inverse Modellierung des Wassertransportes in Großlysimetern der Forschungsanstalt Zürich-Reckenholz, Gumpensteiner Lysimetertagung-Lysimeter als Bestandteil der Entscheidungsfindung, Gumpenstein (Austria), pp. 79-84.

Moriasi, D.N., Arnold, J.G., Van Liew, M.W., Bingner, R.L., Harmel, R.D. & Veith, T.L. (2007). Model evaluation guidelines for systematic quantification of accuracy in watershed simulations. *American Society of Agriculture and Biological Engineers*, 50(3), 885-900.

Nakamura, K., Harter, T., Mathews, M.C., Meyer, R.D. & Gandois, D. (2007). Fate of liquid dairy manure nitrogen in an irrigated double crop corn-grain rotation, California. In: Chang, A., T. Harter, J. Letey, D. Meyer, R.D. Meyer, M.C. Mathews, F. Mitloehner, S. Pettygrove, P. Robinson, R. Zhang (Eds.),

Groundwater Quality Protection: Managing Dairy Manure in the Central Valley of California; Appendix H (pp.: University of California.

Pärn, J., Pinay, G. & Mander, Ü. (2012). Indicators of nutrient transport from agricultural catchments under temperate climate: a review. *Ecol. Indic.*, 22, 4-15.

Peters, A. & Durner, W. (2009). Large zero-tension lysimeters for soil water and solute collection in undisturbed soils. *Hydrol. Earth Syst. Sc.*, 13, 1671-1683.

Randall, G.W. & Goss, M.J. (2008). Nitrate losses to surface water through subsurface, tile drainage. In: Hatfield, N.L., R.F. Follett (Eds.), *Nitrogen in the Environment: Sources, Problems, and Management* (pp. 145-176). Amsterdam, Niederlande: Elsevier.

Randall, G.W. & Iragavarapu, T.K. (1995). Impact of long-term tillage systems for continous corn and nitrate leaching to tile drainage. *J. Environ. Qual.*, 24, 360-366.

Randall, G.W., Iragavarapu, T.K. & Bock, B.R. (1997). Nitrogen application methods and timing for corn after soybean in a ridge-tillage system. *J. Prod. Agric.*, 10, 300-307.

Randall, G.W. & Mulla, D.J. (2001). Nitrate nitrogen in surface waters as influenced by climatic conditions and agricultural practices. *J. Environ. Qual.*, 30, 337-344.

Refsgaard, J.C., Auken, E., Bamberg, C.A., Christensen, B.S.B., Clausen, T., Dalgaard, E., Efferso, F., Ernstsen, V., Gertz, F., Hansen, A.L., He, X., Jacobsen, B.H., Jensen, K.H., Jorgensen, F., Jorgensen, L.F., Koch, J., Nilsson, B., Petersen, C., Schepper, G., Schamper, C., Sorensen, K.I., Therrien, R., Thirup, C. & Viezzoli, A. (2014). Nitrate reduction in geologically heterogeneous catchments - A framework for assessing the scale of predictive capability of hydrological models. *Sci. Total. Environ.*, 468-469, 1278-1288.

Ritchie, J.T. (1972). Model for predicting evaporation from a row with incomplete cover. *Water Resour. Res.*, 8(5), 1204-1213.

Ritter, A. & Munoz-Carpena, R. (2013). Performance evaluation of hydrological models: Statistical significance for reducing subjectivity in goodness-of-fit assessments. *J. Hydrol.*, 480, 33-45.

Robert, P.C. (2002). Precision agriculture: a challenge for crop nutrition management. *Plant and Soil*, 247, 143-149.

Robertson, G.P. & Groffman, P.M. (2007). Nitrogen transformations. In: Paul, E.A. (Ed.), *Soil mocribiology, Biochemistry, and Ecology* (pp. 341-364). New York: Sprimger.

Rubol, S., Silver, W.L. & Bellin, A. (2012). Hydrologic control on redox and nitrogen dynamics in a peatland soil. *Science of the Total Environment*, 432, 37-46.

Salem, H.M., Valero, C., Munoz, M.A., Rodriguez, M.G. & Silva, L.L. (2015). Short-term effects of four tillage practices on soil physical proberties, soil water potential, and maize yield. *Geoderma*, 237-238, 60-70.

Schaap, M.G., Leij, F.J. & Van Genuchten, M.T. (2001). Rosetta: A computer program for estimating soil hydraulic parameters with hierarchical pedo-transfer-functions. *J. Hydrol.*, 251, 163-176.

Schepper, G., Therrien, R., Refsgaard, J.C. & Hansen, A.L. (2015). Simulating coupled surface and subsurface water flow in a tile-drained agricultural catchment. *J. Hydol.*, 521, 374-388.

Shirmohammadi, A., Djodjic, F. & Bergström, L. (2005). Scaling issues in sustainable management of nutrient losses. *Soil Use Manage.*, 21, 160-166.

Silva, R.G., Holub, S.M., Jorgensen, E.E. & Ashanuzzaman, A.N.M. (2005). Indicators of nitrate leaching loss under different land use of clayey and sandy soils in southeastern Oklahoma. *Agr. Ecosyst. Environ.*, 109, 346-459.

Simunek, J., Sejna, M., Saito, H., Sakai, M. & Van Genuchten, M.T. (2013). The HYDRUS-1D Software Package for Simulating the One-Dimensional Movement of Water, Heat, and Multiple Solutes in Variably-Saturated Media Version 4.17.

Simunek, J., Van Genuchten, M.T. & Sejna, M. (2008). Development and Applications of the HYDRUS and STANMOD Software Packages and Related Codes. *Vadose Zone J.*, 7(2), 587-600.

Simunek, J., van Genuchten, M.T. & Sejnas, M. (2012). The HYDRUS Software Package for Simulating the Two- and Three-Dimensional Movement of Water, Heat, and Multiple Solutes in Variably-Saturated Porous Media.

Smith, J.U. (1999). Models and scale - Up- and down-scaling. In: Stein, A., F.W. Penning de Vries (Eds.), *Data and Models in Action: Methodological Issues in Production Ecology* (pp. 81-98). Springer.

Sutanto, S.J., Wenninger, J., Coenders-Gerrits, A.M.J. & Uhlenbrook, S. (2012). Partitioning of evaporation into transpiration, soil evaporation and interception between isotope measurements and a HYDRUS-1D-model. *Hydrol. Earth Syst. Sci.*, 16, 2605-2616.

Troxler, J., Zala, M., Natsch, A., Nievergelt, J., Keel, C. & Defago, G. (1998). Transport of biocontrol pseudomonas fluorescens through 2.5-m deep outdoor lysimeters and survival in the effluent water. *Soil Biol. Biochem.*, 30, 621-631.

Übelhör, A., Gruber, S. & Claupein, W. (2014). Influence of tillage intensity and nitrogen placement on nitrogen uptake and yield in strip-tilled white cabbage (Brassica oleracea convar.capitata var. alba). *Soil & Tillage Research*, 144, 156-163.

Van Genuchten, M.T. (1980). A closed-form equation for predicting the hydraulic conductivity of unsaturated soils. *Soil Sci. Soc. Am. J.*, 44, 892-898.

VDLUFA. (2002). Bestimmung von mineralischem Stickstoff (Nitrat und Ammonium) in Bodenprofilen (Nmin-Labormethode). VDLUFA.

Vereecken, H. & Dust, M. (1998). Modelling water flow and pesticide transport at lysimeter and field scale. *ACS Symp.*, Ser. 699, 189-202.

Vereecken, H., Kasteel, R., Vanderborght, J. & Harter, T. (2007). Upscaling hydraulic properties and soil water flow processes in heterogeneous soils: A review. *Vadose Zone J.*, 6, 1-28.

Vereecken, H. et al. (2016). Modelling soil processes: Review, key challenges, and new perspectives. *Vadose Zone J.*, 1-57.

von Hoyningen-Hüne, J. (1983). Die Interzeption des Niederschlags in landwirtschaftlichen Beständen. *Schriftenreihe des DVWK*, 53, 1-53.

Vos, J.A. (2001). Monitoring nitrate leaching from submerged drains-short communications. *J. Environ. Qual.*, 30, 1092-1096.

Warsta, L., Karvonen, T., Koivusalo, H., Paasonen-Kivekas, M. & Taskinen, A. (2013). Simulation of water balance in a clayey, subsurface drained agricultural field with three-dimensional FLUSH-model. *J. Hydol.*, 476, 395-409.

Weed, D.A.J. & Kanwar., R.S. (1996). Nitrate and water present in and flowing from root-zone soil. *J. Environ. Qual.*, 25, 709-719.

Wegehenkel, M. & Gerke, H.H. (2015). Water table effects on measured and simulated fluxes in weighing lysimeters for differently-textured soils. *J. Hydrol. Hydromech.*, 63, 82-92.

Weihermüller, L., Siemens, J., Deurer, M., Knoblauch, S., Rupp, H., Göttlein, A. & Pütz, T. (2007). In Situ Soil Water Extraction: A Review. *J. Environ. Qual.*, 36, 1735-1748.

Wriedt, G. (2004). Modelling of nitrogen transport and turnover during soil and groundwater passage in a small lowland catchment of Northern Germany, Doctoral Thesis, Germany.

Zacharias, S., Bogena, H., Samaniego, L., Mauder, M., Fuß, R., Pütz, T., Frenzel, M., Schwank, M., Baessler, C., Butterbach-Bahl, K., Bens, O., Borg, E., Brauer, A.,

Dietrich, P., Hajnsek, I., Helle, G., Kiese, R., Kunstmann, H., Klotz, S., Munch, J.C., Papen, H., Priesack, E., Schmid, H.P., Steinbrecher, R., Rosenbaum, U., Teutsch, G. & Vereecken, H. (2011). A network of terrestrial environmental observatories in Germany. *Vadose Zone Journal*, 10, 955-973.

Zhu, J., Young, M.H. & Van Genuchten, M.T. (2007). Upscaling shemes and relationships for the Gardner and van Genuchten hydraulic functions for heterogeneous soils. *Vadose Zone J.*, 6, 186-195.

Zhu, Y., Fox, R.H. & Toth, J.D. (2002). Leachate collection efficiency of zero-tension pan passive capillary fiber wick lysimeters. *Soil Sci. Soc. Am. J.*, 66, 37-43.

Erklärung / Declaration under Oath

Ich erkläre an Eides statt, dass ich, Denise Bednorz, die Arbeit selbstständig und ohne fremde Hilfe verfasst, keine anderen als die von mir angegebenen Quellen und Hilfsmittel benutzt und die den benutzten Werken wörtlich oder inhaltlich entnommenen Stellen als solche kenntlich gemacht habe.

I, Denise Bednorz declare under penalty of perjury that this thesis is my own work entirely and has been written without any help from other people. I used only the sources mentioned and included all the citations correctly both in word or content.

Halle, den 26.10.2017

Datum / Date   Unterschrift des Antragstellers / Signature of the applicant

Erklärung über bestehende Vorstrafen und anhängige Ermittlungsverfahren / Declaration concerning Criminal Record and Pending Investigations

Hiermit erkläre ich, Denise Bednorz, dass ich weder vorbestraft bin noch dass gegen mich Ermittlungsverfahren anhängig sind. / I, Denise Bednorz, hereby declare that I have no criminal record and that no preliminary investigations are pending against me.

Halle, den 26.10.2017

Datum / Date   Unterschrift des Antragstellers / Signature of the applicant

Tabellarischer Lebenslauf/ Curriculum vitae

Name: Denise Bednorz

Geburtsdatum/ Date of birth: 24.06.1986

Geburtsort/ Place of birth: Wolfen

Beruflicher Werdegang/ Professional career

01.01.2017 – aktuell: MDSE – Mitteldeutsche Sanierungs- und Entsorgungsgesellschaft mbH – Datenmanager Altlasten/ Data manager contaminated sites

01.11.2013 – 31.12.2016: Martin-Luther-Universität Halle-Wittenberg – Wissenschaftlicher Mitarbeiter/ Martin-Luther-University Halle-Wittenberg – Scientific researcher

01.07.2011 – 31.10.2013: Helmholtz-Zentrum für Umweltforschung Leipzig – Department Grundwassersanierung – Wissenschaftlicher Mitarbeiter/ Helmholtz Centre for Environmental Research Leipzig – Department Groundwater remediation – Scientific researcher

14.02.2011 – 27.06.2011: Helmholtz-Zentrum für Umweltforschung Leipzig – Department Hydrogeologie – Wissenschaftlicher Mitarbeiter/ Helmholtz Centre for Environmental Research Leipzig – Department Hydrogeology – Scientific researcher

Studium/ Education

2008 – 2011: Martin-Luther-Universität Halle-Wittenberg - MSc - Studium Angewandte Geowissenschaften (Abschluss: sehr gut)/ Martin-Luther-University Halle-Wittenberg MSc-study - Applied Geosciences (final mark: very good)

2005 – 2008: Martin-Luther-Universität Halle-Wittenberg - BSc - Studium Angewandte Geowissenschaften (Abschluss: gut)/ Martin-Luther-University Halle-Wittenberg BSc-study - Applied Geosciences (final mark: good)

Publikationsliste von Denise Bednorz

2016

Bednorz, D., Tauchnitz, N., Christen, O., Rupp, H. & Meissner, R. (2016). Evaluating the transferability of measurements from simple constructed non weighable gravitation lysimeters to predict the water regime on field scale - A case study. *J. Plant Nutr. Soil Sci.*, 179 (6), 809-820.

Bednorz, D., Tauchnitz, N., Christen, O., Rupp, H. & Meissner, R. (2016). The impact of soil heterogeneity on nitrate dynamic and losses in tile-drained arable fields. *Water Air Soil Pol.*, 227(295), 1-18.

Bednorz, D., Tauchnitz, N., Christen, O. & Meissner, R. (2016): Nitrate leaching-measurements and numerical simulations. - ESA-Congress 2016, Edinburgh (UK).

Bednorz, D., Tauchnitz, N., Christen, O., Rupp, H. & Meissner, R. (2016): Field experiments to evaluate nitrate-leaching from drained agriculturally used areas. - EGU General Assembly 2016, Wien (Österreich).

2015

Bednorz, D., Tauchnitz, N., Bischoff, J., Schrödter, M., Koblenz, B., Rücknagel, J., Rupp, H., Christen, O. & Meissner, R. (2015): Der Einfluss der Bodenheterogenität auf Nirataus-träge aus landwirtschaftlich genutzten Flächen.- In: Kage, H., Sieling, K. & Francke-Weltmann, L. (Hrsg): Mitt. Ges. Pflanzenbauwiss.; 27, 161-162, Braunschweig.

Bednorz, D., Tauchnitz, N., Bischoff, J., Schrödter, M., Koblenz, B., Rücknagel, J., Rupp, H., Christen, O. & Meissner, R. (2015): Lysimeter- und Feldversuche als Grundlage zur modellgestützten Bewertung der Stickstoffkinetik in der ungesättigten Zone in Abhängig-keit von Bodenphysik und Bewirtschaftung.- Tagung der Deutschen Bodenkundlichen Ge-sellschaft - Unsere Böden unser Leben, München.

Bednorz, D., Schubert, M. & du Puits, M. (2015): Verfahren und Datenverarbeitungsvor-richtung zum Feststellen einer Kontamination eines Bodenvolumens mit Kohlenwasser-stoff.-Patent DE 102013219559 A1.

Bednorz, D., Tauchnitz, N., Bischoff, J., Schrödter, M., Rücknagel, J., Koblenz, B., Wiese, F., Christen, O. & Meissner, R. (2015): Bewertung der N-Effizienz des Gülle-Strip-Till-Verfahrens – Kombinierte Lysimeter- und Feldversuche als Grundlage zur Modellierung der Stickstoffkinetik in der ungesättigten Zone.- In: Lysimeter: Forschung im System Boden – Pflanze – Atmosphäre; 16. Gumpensteiner Lysimetertagung; S. 131-136, Gumpenstein (Österreich).

2014

Bednorz, D. (2014): Quantifizierung der N-Austräge in Dränage- und Sickerwasser.- Ackerbautagung in Iden (26. Nov. 2014) und Bernburg (27. Nov. 2014), Landesanstalt für Landwirtschaft, Forsten und Gartenbau.

Bednorz, D., Tauchnitz, N., Bischoff, J., Schrödter, M., Rücknagel, J., Koblenz, B., Meissner, R. & Christen, O. (2014): Verringerung von Stickstoffausträgen aus landwirtschaftlichen Nutzflächen durch Verbesserung der Stickstoffeffizienz im Zuge der Anwendung des Gülle-Strip-Till-Verfahrens.- In: Pekrun, C., Wachendorf, M. & Francke-Weltmann, L. (Hrsg): Mitt. Ges. Pflanzenbauwiss.; 26, 274-275, Wien (Österreich).

Tauchnitz, N., Bischoff, J., Schrödter, M., Wiese, F., Meissner, R., Rupp, H. **Bednorz, D**. & Christen, O. (2014): Zur Dynamik der Nährstoffausträge im Dränabfluss von Bodennutzungssystemen.- In: Pekrun, C., Wachendorf, M. & Francke-Weltmann, L. (Hrsg): Mitt. Ges. Pflanzenbauwiss.; 26, 68-69.

2013

Bednorz, D., Schubert, M., du Puits, M., Hüsers, N. und Weiss, H. (2013): Entwicklung eines innovativen, anwenderoptimierten Radonmesssystems zur Detektion von Mineralölkontaminationen im Boden.- Dechema-Symposium- Strategien zur Boden- und Grundwassersanierung; Dechema e.V., Darmstadt.

Bednorz, D., Schubert, M., du Puits, M., Hüsers, N. und Oeser, V. (2013): Development of an innovative, user-optimized radon detection system for localization of subsurface NAPL-contamination. - Aquaconsoil, Barcelona.

2012

Schubert, M., Paschke, A., **Bednorz, D**., Bürkin, W. & Stieglitz, T. (2012): Kinetics of the water/air phase transition of radon and its implication on detection of radon-in-water concentrations: practical assessment of different on-site radon extraction methods. – In: Environ. Sci. Technol.; 46 (16); S. 8945 – 8951.

Bednorz, D., Dilbat, M., Gossel, W., Ihling, H. & Weise, S. M. (2012): Hydrogeologische Modellierung zur Charakterisierung spezifischer Nitratbelastungen in kleinen Einzugsgebieten am Beispiel Diehsa. – In: Liedl, R., Burghardt, D., Simon, E., Reimann, Th. & Kaufmann-Knoke, R. (Hrsg.): Grundwasserschutz und Grundwassernutzung – Modelle, Analysen und Anwendungen, Schriftenreihe der DGG; 78; S. 176.